BEHAVIOR OF STEEL PLATES UNDER AXIAL COMPRESSION AND THEIR EFFECT ON COLUMN STRENGTH

By

Ahmed Hasan Ahmed Al-Wathaf

Supervisor

Professor Yasser Hunaiti

Submitted in Partial Fulfillment of the Requirements for the Degree of Master of Science in Civil Engineering / Structures

Faculty of Graduate Studies

University of Jordan

May 2002

This thesis was successfully defended and approved on: 7th May 2002

Examination Committee	**Signature**
Dr. Yasser Hunaiti, Chairman Prof. of Structures	.....
Dr. Bassam Abu Ghazaleh, Member Prof. of Structures	.....
Dr. Raed Samra, Member Prof. of Structures	.....
Dr. Mohammad Rjoub, Member Assis. Prof. of Structures	.....

To My Family

Acknowledgement

It is a pleasure for me to express my deepest gratitude and appreciation to my supervisor Prof. Yasser Hunaiti for his kind supervision, guidance, and excellent suggestions throughout the study. I appreciate his encouragement and generous support during this work.

I would like to thank Mr. Nader Yousef, Mr. Abdel-Hadi Mohammed, Mr. Daoud Hasan at the Engineering Workshop of the University of Jordan and Eng. Mahmmoud Abu Abed at the Structural Laboratory of Jordan University of Science and Technology.

I would like to express my gratitude to the staff of the Civil Engineering Department and members of the examination committee.

I would like also to express my thanks to Dr. Abbas Al-Shahary for his encouragement and valuable advice.

Finally, I wish to acknowledge Sana'a University for all support during my postgraduate study.

LIST OF CONTENTS

LIST OF TABLES

LIST OF FIGURES

NOTATION

The following is a list of the most important symbols that are used in this thesis. All other symbols and other meanings of the symbols are explained as and where appear in the text.

A	cross sectional area.
A_e	effective cross sectional area.
A_{stiff}	cross sectional area of stiffener.
A_{tube}	cross sectional area of tube.
a	length of plate.
B	width of long side of tube section.
B_e	effective width including thickness of plate.
b	width of plate.
b_e	effective width.
b_s	width of stiffener.
b'	width of plate from stiffener to supported plate on long side of tube.
b_s'	width of stiffener on short side of tube.
C	length of short side of tubes.
C_1, C_2, C_3, C_4	coefficients determined by regression.
c	width of plate on short side of tube.
c'	width of plate from stiffener to supported plate on short side of tube.
D	flexural rigidity of plate.
E	modulus of elasticity in elastic range.
E_s	secant modulus of elasticity.
E_t	tangent modulus of elasticity.

F_{av} average compressive stress.

F_{cr} critical compressive stress.

F_u ultimate compressive stress.

F_y specified yield stress.

f compressive stress.

I moment of inertia.

I_e moment of inertia of effective sectional area.

I_s moment of inertia of stiffener around its centroid.

K effective length coefficient of column.

k buckling stress coefficient of plate with appropriate subscript.

L column length.

l stub column length.

P axial load.

P_{cr} critical load.

P_u ultimate axial load.

P_y crushing load.

Q strength reduction factor.

Q_a form factor for stiffened element.

Q_s form factor for unstiffened element.

r radius of gyration.

r_e radius of gyration of effective cross sectional area.

t thickness of plate.

t_c thickness of short side plate of tube section.

t_s thickness of stiffener.

t_s' thickness of stiffener on short side of tube.

w	deflection of plate.
α	aspect ratio of plate.
δ	cross sectional area of stiffener and plate ratio.
δ_u	maximum deflection of plate at collapse.
ε	strain.
γ	stiffener and plate rigidity ratio.
ξ	coefficient of restraint.
ν	Poisson's ratio.
η	plasticity reduction factor.
λ	slenderness parameter of plate.
λ_c	slenderness parameter of column.
λ_r	width-thickness ratio of noncompact section.
λ_p	width-thickness ratio of compact section.
μ	effective width coefficient.
σ	compressive stress.
σ_{av}	average compressive stress
σ_{cr}	critical compressive stress of plate.
σ_{CR}	critical compressive stress of column.
σ_e	compressive stress on effective section and stress at edges.
σ_p	proportional limit stress.
σ_u	ultimate compressive stress.
σ_y	yield stress.
ω	half wavelength of buckled plate.

Abbreviations

AISC	American Institute of Steel Construction
AISI	American iron and Steel Institute
ASD	Allowable Stress Design
CRC	Column Research Council
LRFD	Load and Resistance Factor Design
SSRC	Structural Stability Research Council

ABSTRACT

Behavior of Steel Plates Under Axial Compression and Their Effect on Column Strength

By
Ahmed Hasan Ahmed Al-Wathaf

Supervisor
Prof. Yasser Hunaiti

An experimental study is conducted to investigate the behavior and postbuckling strength of plate elements in square and rectangular steel hollow sections having width-thickness ratios more than that in common rolled sections and their effect on the strength of columns. Two types of stub columns are tested under axial compression until failure; ordinary tubes and tubes reinforced by longitudinal stiffeners.

Based on the test results, two empirical compact equations for the effective section take into account the interaction between plate elements are formulated to predict the postbuckling strength for both types. The interaction strength of columns having tube sections is predicted using the modified SSRC column strength equations to consider the effect of local buckling of plate elements. All the results are compared with the relevant formulas and the AISC specifications.

The test results show that the used formula in steel practice slightly overestimates the postbuckling strength. It is shown that the discrepancies between the proposed postbuckling strength and the test results are within an acceptable range and, consequently, the proposed effective section equations by this study may be used for the tested sections.

Using longitudinal stiffeners in which some tested sections become entirely effective as rolled sections can attain distinct increasing in the postbuckling strength. The improvement in postbuckling strength is obviously shown in tube sections with

higher slenderness ratios of plate elements. The test results also show that the smaller stiffeners are relatively more efficient in increasing the strength compared to their size.

The interaction column strength curves obviously show that the interaction between local and overall flexural buckling begins at relatively lower stress for sections with higher slenderness ratios of plate elements. Furthermore, the proposed interaction strengths for ordinary tubular columns are relatively closer to the predicted strength by the AISC, ASD and LRFD, for the sections with relatively lower slenderness ratios of plate elements.

Chapter 1

INTRODUCTION

1.1 General

Most structural steel members are composed of flat plate elements, which form flanges and webs of the cross sections. The performance of these members to carry loads depends mainly upon the properties of the members as a whole as well as the properties and the behavior of the plate elements.

Two cases of instability may occur in a steel column; overall (global) column instability and plate element (local) instability. Local buckling of plate elements in a steel column can cause premature failure of the entire section and reduce the overall strength. The mode of failure and load carrying capacity of steel columns are affected by the behavior of plate elements and the interaction between local and overall buckling.

1.2 Plate Elements in Steel Members

Wide varieties of structural steel shapes are manufactured. The cross-sectional shape and the size are governed by the arrangement of the material for optimum structural efficiency, functional requirements, dimensional and weight capacity of rolling mills, and material properties. These four sets of criteria lead, for most cases, to

use steel sections consist of an assembly of flat rectangular plates joined at right angle to form flanges and webs of their cross sections.

Fig.1.1 shows a number of cross-sectional shapes for metal compression or flexural members. Except for the hollow cylinders Fig.1.1*a*, all members are composed of connected elements which, for purposes analysis and design, can be treated as flat plates. When a plate element is subjected to direct compression, bending, shear, or a combination of these stresses in its plane, theoretical critical loads may be evaluated indicating that the plate may buckle locally before the member as a whole becomes unstable or before the yield stress of the material is reached. Such behavior is characterized by distortion of the cross section of the member. The almost inevitable presence of initial out-of-straightness may result in a gradual growth of cross-sectional distortion with no sudden discontinuity in real behavior at the theoretical critical load.

The theoretical critical load for a plate is not necessarily a satisfactory basis for design, since the ultimate strength can be much greater than the critical buckling load. For example, a plate loaded in uniaxial compression, with both longitudinal edges supported, will undergo stress redistribution as well as develop transverse tensile membrane stresses after buckling that provide post-buckling support. Thus additional load may often be applied without structural damage. Initial imperfection in such a plate may cause bending to begin below the buckling load, yet unlike an initially imperfect column, the plate may sustain loads greater than the theoretical buckling load.

1.3 Local and Overall Buckling of Steel Members

The effect of local plate buckling on the strength of the entire member depends upon the location of the buckled element, its buckling and post-buckling strength, and the type of the member.

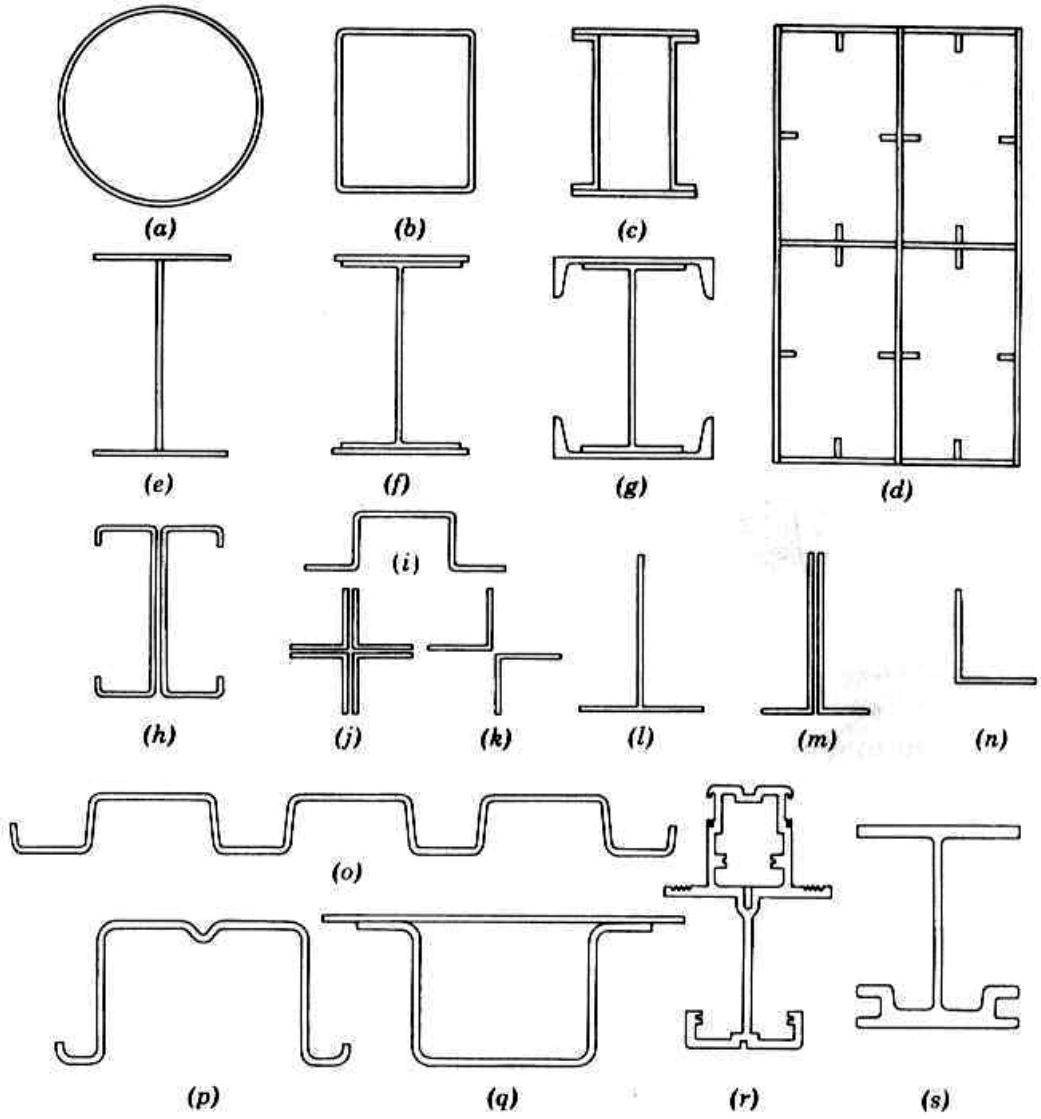

Fig.1.1 Compression or flexural members (Galambos, 1998)

Thin-walled structures are susceptible to local buckling if the in-plane stresses (i.e. stresses in the plane of the plate elements) reach their critical value. If this happens, the geometry of the cross-section of the structure changes. However, if a thin-walled column is made sufficiently long it may suffer overall buckling before it buckles locally. This means that thin-walled structures must be designed against both local and overall buckling. Theory and experiments show that these two phenomena can interact

and when this happens the buckling load can be depressed below the value of the individual buckling loads (Murray, 1986).

Local buckling of thin plate elements of a rectangular hollow strut (stub column) can be investigated to explain this type of behavior. The length of the strut is chosen to avoid overall flexural buckling (such as the stub columns of this experimental study). As the load increases it is observed that ripples, or wavelike deflections, appear along the length of the plates forming the sides of the rectangular tube. The deformations are characterized by the fact that the corners of the tube, the junctions between the flat sides, remain essentially straight. The magnitude of these out-of-plane deflections increases with the load in a nonlinear fashion and is accompanied by a corresponding nonlinear decrease in axial stiffness. The load carried by the strut reaches a maximum when the corners "crumple" or alternatively the plate elements develop a plastic mechanism. The most important feature in this behavior is that, due to this local collapse, the strut fails at a maximum load, which has a lower magnitude than crushing load (Walker, 1975).

Slender compression members that are not susceptible to torsional, or flexural-torsional buckling will lose their stability by flexural buckling. Doubly symmetric sections and closed sections, axially loaded, do not have any tendency to twist if they are of dimensions commonly used in structures.

1.4 Rectangular Plates with Stiffeners

Increasing the thickness of a plate can always increase its stability, but such a design will not be economical in respect to the weight of the materials to be used. An economical solution is obtained by keeping the thickness of the plate as small as possible and increasing the stability by introducing reinforcing stiffeners.

It is obvious that reinforcing the plate by transverse stiffeners will have little effect on the buckling strength of the plate unless these stiffeners are very closely spaced. Therefore introducing one or more longitudinal stiffeners will be more economical. These stiffeners not only carry a portion of the compression load but also subdivide the plate into small panels, thus increasing considerably the critical stress at which the plate will buckle. Figs. 1.1*d* and 1.1*p* shows plates that have intermediate longitudinal stiffness and Figs. 1.1*h* and 1.1*o* shows plates that have edge longitudinal stiffeners.

1.5 Previous Research

The history of the theory of plate stability under edge compression goes back to 1891, when Bryan (Bleich, 1952) presented the analysis for a rectangular plate simply supported on all edges and acted upon on two opposite sides by a uniformly distributed compression in the plane of the plate. Credit for the most extensive treatment of the buckling problems of rectangular plates belongs to Timoshenko (1963). Bleich (1952) made an attempt to extend the theory of flat-plate stability into the inelastic range. Credit for the first extensive analysis of the stability of plate assemblies belong to Lundquist, Stowell, and Schuette, who applied the moment distribution method to the stability of structures composed of plates (Bleich, 1952). Three categories of previous research will be conducted in this section. These categories are:

1. Experimental and analytical studies on the effective section concept and to investigate local and overall buckling of columns.
2. Research concerning the interaction between plate elements and local with overall buckling analytically.
3. Research concerned with rectangular plates stiffened longitudinally.

Many researchers have investigated the concept of effective width and the interaction of local and overall buckling in the postbuckling range. DeWolf, Pekoz, and Winter (1974) presented an analytical approach, which accounts for the combined effects of local buckling, column buckling, and nonuniform material properties in compression members. This research is based on the tangent modulus concept and utilizes the effective width concept. A simplification, based on the CRC (Column Research Council) column curve, was also given as an approximation for use in routine design situations.

In 1979, Kalyanaraman, Pekoz, and Winter (1979) confirmed experimentally two effective width expressions for the postbuckling range of unstiffened elements. Both the tangent modulus and the SSRC (Structural Stability Research Council) methods for calculating the flexural buckling strength of columns, when modified to take into account the reduction in stiffness as a result of local buckling, can be used to calculate the flexural buckling strength of columns with locally buckled elements.

Usami and Fukumoto (1982) presented an empirical formula based on the AISC method and the effective width concept to predict the local and overall interaction-buckling strength of welded built-up box columns made of high strength steel. Furthermore, a discussion of an economical way of proportioning box sections was presented.

Usami (1982) investigated, theoretically, the postbuckling behavior of rectangular plates in combined compression and bending. The theoretical results were utilized to derive effective width formulas for combined compression and bending. A family of postbuckling strength curves, which were calculated from the derived effective width formula, for box sections were presented.

During the few past decades, attention is focused on the local buckling of plate elements and the interaction between plate elements in cross sections, local with overall buckling, and their influence on the column behavior and the ultimate load carrying capacity. Among the earlier references in the interaction of local and overall buckling in the postbuckling range are those by Bijlaard, Fisher, and Graves-Smith (Galambos, 1998).

Little (1979) presented a theoretical method, based on the application of average stress-strain curves to account for the effect of local buckling and residual stresses on the column strength, ultimate strength, and the load-deflection curves for square steel box welded columns obtained by integrating the moment-curvature-thrust relations along the axis of the column.

Hancock (1981) proposed a nonlinear finite strip analysis to produce accurate solutions for the deflections and stresses in imperfect folded plate assemblies under axial compression. The effective flexural rigidity concept of an imperfect thin-walled box column subjected to loads greater than the local buckling load was found to agree with other research.

In 1985, Dawe, Elgabry, and Grondin (1985) used an analytical technique for predicting the local buckling behavior of hollow structural sections to predict elastic and inelastic local bucking capacities of axially loaded hollow structural sections. The technique, similar to finite strip-method, is based on the principal of virtual work and used a Rayleigh-Ritz solution procedure.

An exact solution of longitudinally or transversely stiffened rectangular flat plates acted upon by uniformly distributed stresses on two opposite edges was published by Lokshin. Later, Barbre investigated the effect of longitudinal stiffeners in two particular

cases, namely, one rib in the middle of the plate, and two ribs dividing the width of the plate into equal panels. He gave numerical tables and charts for the design of the stiffeners (Bleich, 1952). Recent researches treat this problem in two approaches, the first is the equivalent column method, which is concerned with the stiffener and adjacent areas of the plate, and the other approach is an extension of the effective width concept.

Desmond, Pekoz, and Winter (1981) investigated experimentally and analytically the behavior of rectangular plates with intermediate stiffeners for thin-walled members. An approach was presented for predicting effective widths of intermediately stiffened compression elements that are either adequately or partially stiffened. In their study, recommendations that provide the minimum required stiffener rigidity to support these elements adequately were also presented.

Bernard, Bridge, and Hancock (1993) showed experimentally that the intermediate stiffener was found to exert a strong influence on the primary mode of buckling in the compressed flanges profiled steel decks loaded in pure flexure. They found that the primary mode of buckling depends on the size of the intermediate stiffener. Moreover, distortional buckling was associated with small stiffeners and local buckling was associated with large stiffeners.

1.6 Objectives and Scope of the Research

The nature of manufacturing process of square and rectangular steel hollow sections requires forming these sections with lower thickness, which may affect their structural performance. Also, variations in structural characteristics introduced during the forming process of these sections may affect their strength and the behavior of their plate elements and, therefore, these matters must be verified.

The purpose of this research is to investigate experimentally the behavior of steel plate elements of square and rectangular hollow sections that are used in practice.

A systematic study of postbuckling behavior of the plate elements of the tube sections, which are considered thin-walled section, will be conducted in order to verify their strength and develop a compact effective section formula takes into account the interaction between plate elements based on the results of axial compression tests of stub columns. This formula will be used to predict the interaction buckling strength for columns affected by local buckling.

In order to improve the buckling and postbuckling strength, stub columns of the same sections will be stiffened by longitudinal stiffeners on their sides. These specimens will also be tested under axial compression to study the effects of stiffeners on the postbuckling strength of the original sections and the efficiency of the stiffeners. Also, effective section formula takes into account the interaction between plate elements for this type of sections will be developed, and used to predict the interaction buckling strength of the columns affected by local buckling.

Furthermore, this study aims at determining whether the American Institute of Steel Construction Specification AISC is adequate regarding the strength of columns composed of sections similar to the test specimens. This will be achieved by a comparison between the strength predicted by the specification and the strength predicted by this research.

Chapter 2

BEHAVIOR OF RECTANGULAR PLATES UNDER UNIAXIAL COMPRESSION

2.1 General

The analysis of column buckling is relatively simple because bending can be assumed to take place in one plane only. By comparison, the buckling of a plate involves bending in two planes and therefore is fairly involved. Another significant difference between columns and plates is also apparent if one compares their buckling characteristics. For a column, buckling terminates the ability of the member to resist axial load, and the critical load is thus the failure load of the member, the same, however, is not true for plates. These structural elements can, subsequent to reaching the critical load, continue to resist increasing axial force, and they do not fail until a load considerably in excess of the critical load is reached. The critical load of a plate is therefore not its failure load. Instead, one must determine the load-carrying capacity of a plate by considering its postbuckling behavior.

2.2 Elastic Stability of Rectangular Plates Under Uniaxial Compression

The following is the solution of the stability problem of rectangular plates compressed in one direction by a uniformly distributed load in the plane of the plate with different boundary conditions at the unloaded edges in the elastic range.

A flat plate loaded on the two edges parallel to the *y*-axis by the uniformly distributed load, $t\sigma_x$, where *t* is the plate thickness and σ_x is the normal compression stress in *x*-direction (Fig. 2.1a) will be considered. We assume these edges to be simply supported so that the plate can rotate freely about them. Clamping the loaded edges has little effect on the critical load for plates with large aspect ratios such as those used in customary column sections. The edges parallel to the *x*-direction, edges *a*, may be supported in various ways (Bleich, 1952):

Case I: the plate is elastically restrained at the unloaded edges, *a*. This case includes, as limiting cases, simply supported or clamped edges.

Case II: One of the unloaded edges, *a*, is elastically restrained and the other is free. This case likewise includes the two limiting conditions in which the supported edge is free to rotate or is clamped.

Fig. 2.1b shows typical longitudinal sections of buckled plates, and Fig. 2.1c shows cross sections for each case of support. In plates supported on both edges, Case *I*, buckling occurs in one or more half waves depending upon the aspect ratio *a/b* in which *a* and *b* are the length and the width of the plate respectively. In Case *II,* where one edge of the plate is free, the plate will buckle in one half wave when it is free to rotate at the supported edge but in one or more half wave if elastically restrained or clamped.

The solution of buckling problem of plates is based upon the fundamental differential equation for the deflection, *w,* of a thin flat plate under the action of forces

in its middle plane. This equation is derived under the assumption that the deflection, *w*, is small compared to the thickness, *t*, of the plate. The equation reads (Bleich, 1952):

$$D\left[\frac{\partial^4 w}{\partial x^4}+2\frac{\partial^4 w}{\partial x^2 \partial y^2}+\frac{\partial^4 w}{\partial y^4}\right]+\sigma_x t\frac{\partial^2 w}{\partial x^2}=0 \qquad (2.1)$$

where:

$$D=\frac{Et^3}{12(1-\nu^2)} \qquad (2.2)$$

in which:

E modulus of elasticity in elastic range.

ν Poisson's ratio, 0.3 for steel.

The solution of Eq. 2.1 can be expressed in a general formula for all cases as follows:

$$\sigma_{cr}=k\frac{\pi^2 E}{12(1-\nu^2)(b/t)^2} \qquad (2.3)$$

Where:

k buckling stress coefficient, which will be determined for each case later.

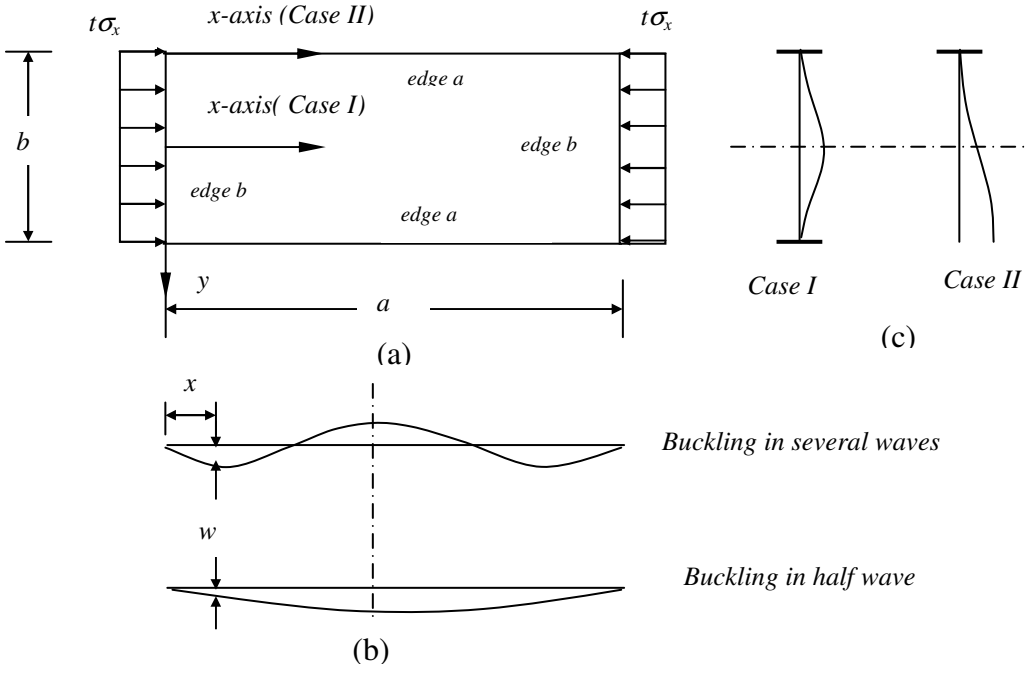

Fig. 2.1 Rectangular plate suffers buckling.

Equal elastic restrained will be assumed on both unloaded edges, Fig. 2.1c, Case *I*. The coefficient of restraint, ξ which will be determined next in the next Chapter, is a function of the dimensions of the buckling and restraining plates. It may be noted that ξ can theoretically be assumed from 0 to ∞. When ξ=0, the plate is completely fixed at the supported edges, and when $\xi=\infty$, it is free to rotate about these edges. The general expression of the coefficient of buckling, *k*, for both cases is given as follows:

$$k=\left(\frac{n}{\alpha}\right)^2+p+q\left(\frac{\alpha}{n}\right)^2 \qquad (2.4)$$

Where:

n number of waves in longitudinal direction.

α aspect ratio *a/b*.

a length of the plate.

b width of the plate.

p and q Factors depending on the coefficient of restraint ξ.

For long plates, buckling coefficient, *k*, approaches the minimum value, which gives the minimum buckling stress as follows:

$$k_{\min}=p+2\sqrt{q} \qquad (2.5)$$

The factors *p* and *q* can be obtained from Fig. 2.2 for Case *I* and Fig. 2.3 for Case *II*, which are plotted against ξ. Eq. 2.5 is valid for elastic and inelastic buckling (Bleich, 1952).

For Case I, if the restraint on the unloaded edges of a plate is unequal, the following approximate method has been recommended:

The method outlined above for equal restraint on both unloaded edges is applied, first using the coefficient of restraint ξ_1 of one side to find a plate coefficient k_1 from Eq. 2.5 and then using the other value ξ_2 to find a plate coefficient k_2. The mean value

$k=(k_1+k_2)/2$ represents a fairly good approximation of the exact value of k and can be introduced into Eq. 2.3 to obtain the critical stress of the plate under consideration.

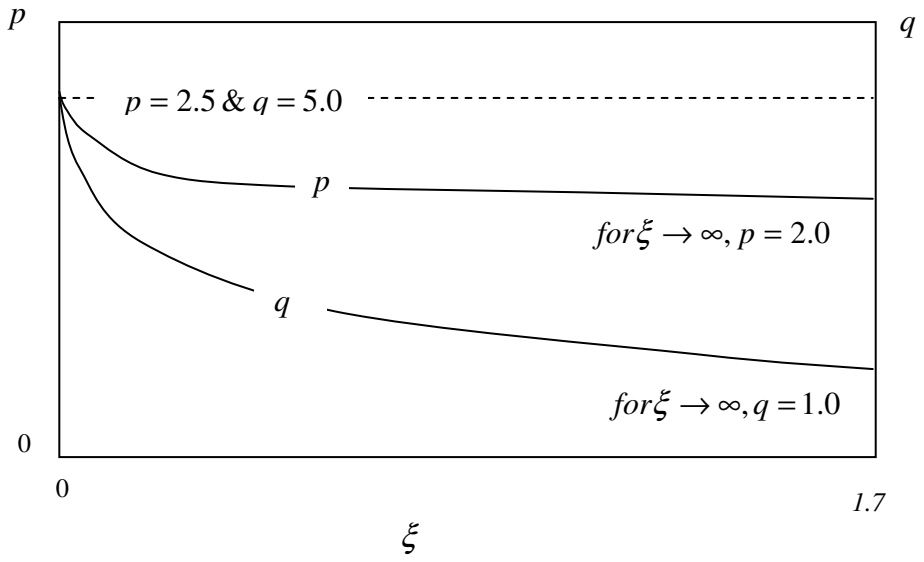

Fig. 2.2 p & q values for Case *I*

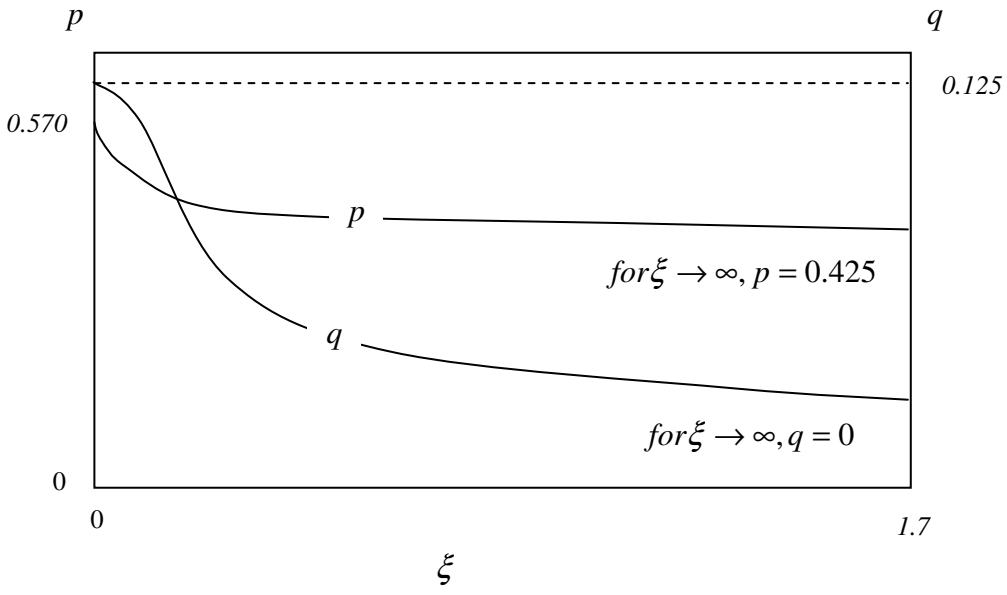

Fig. 2.3 p & q values for Case *II*

Fig. 2.4 shows the limiting cases for coefficient of buckling, k, where the plate is simply supported, $\xi=\infty$, or fixed, $\xi=0$. In this figure two cases of loaded edges are depicted, one is for simply supported, and the other for fixed ends. It is shown that the differences between the two cases are small, particularly for long plates.

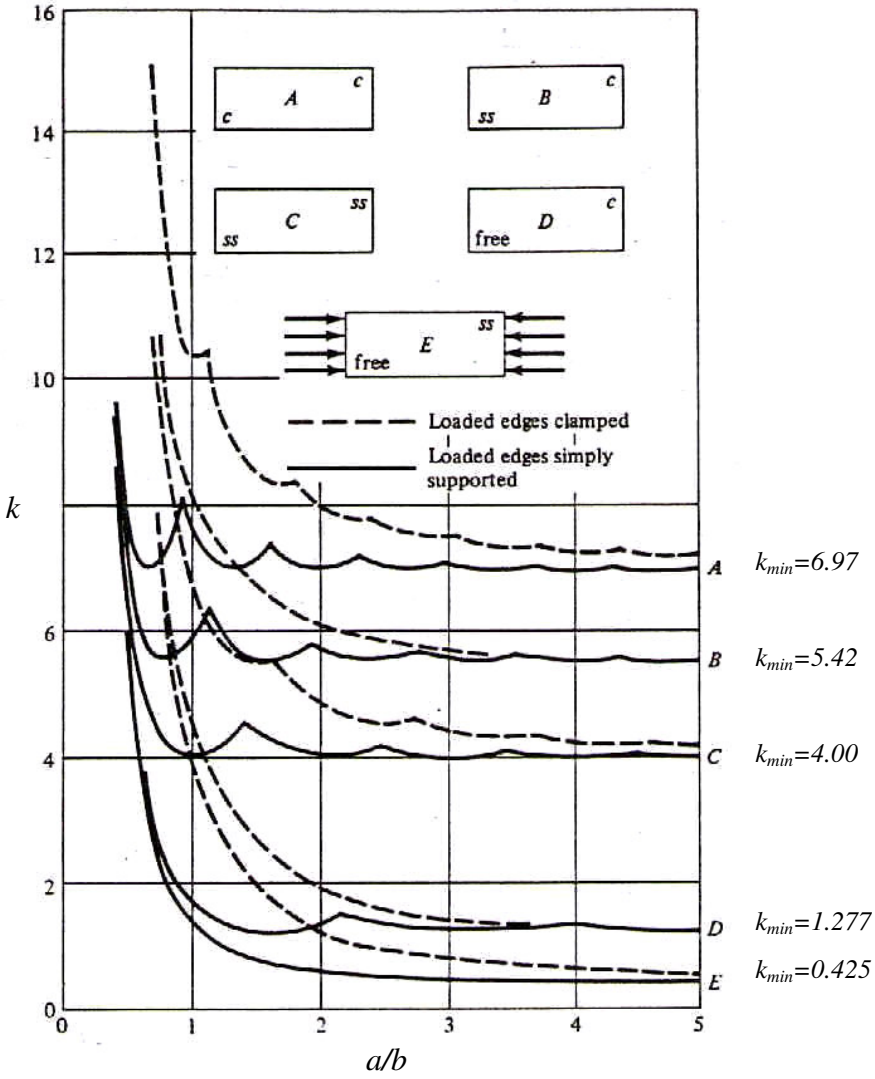

Fig. 2.4 Elastic buckling coefficients for limiting cases (Salmon and Johnson, 1996)

2.3 Inelastic Buckling of Plates

2.3.1 Plasticity Reduction Factor

For plates as well as columns and beams, it is not unusual for the proportional limit of the material to be exceeded prior to reaching the critical stress. If this occurs, the elastic theory presented in the preceding section must be replaced by an analysis capable of dealing with the inelastic behavior.

Investigation of inelastic plate buckling indicate that Eq. 2.3, the elastic buckling relationship, can be extended into the inelastic range, provided that Young's modulus is replaced by a reduced modulus. Thus the inelastic critical stress for plates is usually given in the form

$$\sigma_{cr} = k\frac{\pi^2 E\eta}{12(1-\nu^2)(b/t)^2} \tag{2.6}$$

where η is a plasticity reduction factor, or $E\eta$ is a reduced modulus. Since inelastic behavior always decreases the stiffness of a plate, η<1, the inelastic critical stress given by Eq. 2.6 is always less than the corresponding elastic stress given by Eq. 2.3.

The results obtained from inelastic plate studies indicate that the factor η is a function of the shape of the stress-strain curve, the type of loading, the length to width ratio of the plate, and the boundary conditions. If a long rectangular plate is uniaxially compressed and simply supported along both edges, Gerard shows the plasticity reduction factor is to be as follows (Chajes, 1974):

$$\eta = \frac{E_s}{E}\left[\frac{1}{2}+\frac{1}{2}\sqrt{\frac{1}{4}+\frac{3}{4}\frac{E_t}{E}}\right] \tag{2.7}$$

in which E_s is the secant modulus and E_t is the tangent modulus of the material. For the same plate, if only one edge is simply supported and the other is free, then the factor will be as follows:

$$\eta = \frac{E_s}{E} \tag{2.8}$$

A relation for η considerably more suited for design purpose than the foregoing ones was derived by Bleich (1952). Using an approximate theory based on the assumption of anisotropic behavior of the plate when the critical stress σ_{cr} lies above the elastic limit, he obtained the following simple expression:

$$\eta = \sqrt{\frac{E_t}{E}} \tag{2.9}$$

According to Bleich, for long plates the buckling coefficient, *k*, becomes independent of η. This is important because it permits the use of precalculated values for the coefficient, *k*, which are applicable in the elastic and inelastic ranges of buckling.

2.3.2 Critical Stress in The Inelastic Range

According to Bleich the reduction factor, η, depends on σ_{cr} in the inelastic range, which is an unknown quantity at the outset of the computation, and iterative method would be necessary to determine σ_{cr}. This can be avoided by writing Eq. 2.6 in the form:

$$\frac{\sigma_{cr}}{\eta} = k\frac{\pi^2 E}{12(1-\nu^2)(b/t)^2} \tag{2.10}$$

Determining σ_{cr}/η from this equation the corresponding value of σ_{cr} can be found from a precalculated table of the value σ_{cr} as a function of σ_{cr}/η. Such a table can be computed from the η^2-values for the material under consideration. Bleich suggests a formula for η^2, which depends upon the yield strength σ_y, proportional limit for the material σ_p, and the average compressive stress σ_c (Bleich, 1952). This formula can be expressed as follows:

$$\eta^2 = \frac{(\sigma_y - \sigma_c)\sigma_c}{(\sigma_y - \sigma_p)\sigma_p} \tag{2.11}$$

This equation is applicable beyond the proportional limit of the material, and valid for inelastic buckling of plates and columns. The reduction in the modulus of elasticity in the SSRC formula of strength of short columns is based on Eq.2.11 using $\sigma_p = 0.5\sigma_y$.

2.4 Postbuckling Behavior of Uniaxially Compressed Plates

When the magnitude of the critical stress in a plate is reached, slight buckling waves will appear very gradually, however the plate will not fail. It will continue to carry increasing load, sometimes a large multiple of that which causes the first barely perceptible waving, particularly when the width/thickness, *b/t,* ratio is large. This phenomenon is known as postbuckling strength and is of decisive importance for thin-walled metal structures.

Postbuckling strength can be easily understood physically. Fig. 2.5a shows a compressed square thin plate buckles into slight half waves at the critical stress. These half waves are replaced by a grid model for simplicity. A plate, however, is a two-dimensional body and the crossties roughly represent its action perpendicular to the direction of compression. It is evident that, when the struts start buckling (bending), tension and bending are induced in the crossties, which, thereby, counteract further buckling of the struts. They do so more effectively for those struts closer to the stiffened edges. Consequently, the grid (plate) is enabled to carry additional load, but it will be primarily those portions, which are close to the edges that resist increasing stress. The distribution of compressive stresses is, therefore, nonuniform in this postbuckling range, Fig. 2.5b. The plate will not be able to carry further additional load and begins to fail only when the most highly stressed portions reach the yield strength of the material. It is

thus seen that the stresses in the crossties, representing the membrane stress in the compressed plate, are the reason for postbuckling strength and for the difference between the column and the plate buckling.

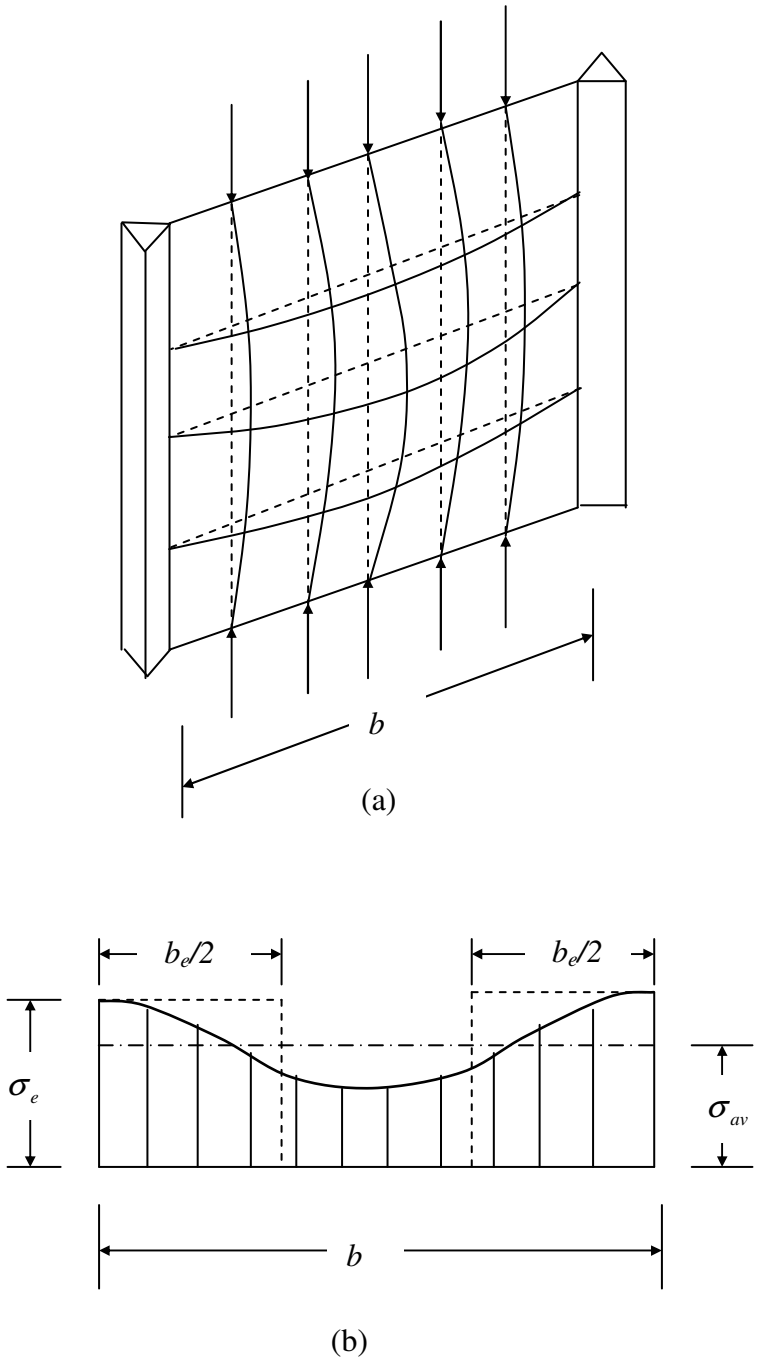

Fig. 2.5 Postbuckling behavior of a plate

2.4.1 Maximum Strength and Effective Width Concept

The value of the load corresponding to the nonuniform compressive stress distribution is more difficult to determine than the buckling strength. Equation of critical buckling, Eq. 2.3, is not applicable because it neglects the effect of membrane stresses in the middle plane of the plate, which become significant for large deflections.

For design purposes, it is convenient to replace the area under the curve of nonuniform stress distribution by two rectangles of the same maximum stress and the same total area, Fig. 2.5b.

A very important semi-empirical method of estimating the maximum strength of plates is the effective width concept. Only a fraction of the width is considered effective in resisting the applied compression. In a plate structure, use of the effective width leads to an effective cross-section consisting of portions meeting along a junction. It is near these junctions that the plates will begin to yield preceding failure. In postbuckling range, a load P that the plate carries can be expressed as:

$$P = \sigma_e b_e t \tag{2.12}$$

where:

σ_e maximum stress at edges, Fig. 2.5b.

b_e effective width.

t thickness of plate.

The edge stress, σ_e, continues to increase with the increase in the strain of the plate until a limiting value is reached. In the case of flat-yield steel, this limit is σ_y for practical purposes or the offset-yielded stress for gradually yielding steel; the ultimate load can be written as:

$$P_u = \sigma_y b_e t \tag{2.13}$$

From Fig. 2.5b and equating $\sigma_e b_e t$ to $\sigma_{av} b\, t$, where σ_{av} is the average stress on entire width *b*, the following expression can be obtained:

$$\frac{\sigma_{av}}{\sigma_e} = \frac{b_e}{b} \tag{2.14}$$

At failure, and by equating $\sigma_y b_e t$ to $\sigma_u b\, t$, in which $\sigma_e = \sigma_y$ and $\sigma_{av} = \sigma_u$, Eq.2.14 becomes:

$$\frac{\sigma_u}{\sigma_y} = \frac{b_e}{b} \tag{2.15}$$

For a plate assembly with unequal dimensions, Eqs.2.14 and 2.15 must be modified to include the total effective area, A_e. Therefore, Eq.2.14 becomes:

$$\frac{\sigma_{av}}{\sigma_e} = \frac{A_e}{A} \tag{2.16}$$

And Eq.2.15 becomes:

$$\frac{\sigma_u}{\sigma_y} = \frac{A_e}{A} \tag{2.17}$$

2.4.2 Effect of Imperfections on Plate Behavior

When testing a plate, it is observed that the magnitude of the out-of-plane deflections grows from the beginning of load application. In other words there is no load that we can identify as the critical load. This lack of agreement between the observed behavior of a real plate and that predicted on the basis of a perfect flat plate is of course due to the fact that real plates are not flat prior to loading. Owing to the process of manufacture some initial deflections will exist, these will be different in magnitude and shape from one plate to another.

In order to analyze the plate precisely we need to be able to specify the initial imperfection but we don't know these until the plate is manufactured. Therefore, to

simplify the analysis, the initial imperfections are chosen to coincide in shape with the deflected shape that would occur in a buckled perfect plate. Based on this assumption, analysis shows that the magnitude of ultimate strength, as a function of initial imperfection of a plate, can be determined from (Walker, 1975):

$$\frac{P_y}{P_{cr}} = \frac{P_u}{P_{cr}} + 2.83\left(\frac{P_u}{P_{cr}} - 1 + \frac{\varepsilon}{\delta_u}\right) + 0.52\left(\frac{P_u}{P_{cr}} - 1 + \frac{\varepsilon}{\delta_u}\right)^2 \qquad (2.18)$$

where:

P_y crushing load $= A\sigma_y$.

A cross sectional area of a plate

P_u ultimate load, load at collapse of plate.

P_{cr} critical buckling load of plate.

ε amplitude of the initial imperfection.

δ_u maximum deflection of plate at collapse.

But values of initial imperfection will vary according to the plate dimension. We can arrange for ε/t to be a parameter of the plate geometry. A suitable description is given as follows:

$$\frac{\varepsilon}{t} = \beta\left(\frac{P_y}{P_{cr}}\right) \qquad (2.19)$$

in which β is a constant that can be adjusted to fit experimental results.

In the next section, it will be seen that the effective width formula resulting from tests can reflect the total effect of various imperfections as well as residual stresses.

2.4.3 Effective Width Formulas

For plates under uniform compression, stiffened along both edges parallel to the direction of the applied compression, a compact form for the effective width formula can be expressed as follows:

$$b_e = \mu t \sqrt{\frac{kE}{\sigma_e}} \tag{2.20}$$

where

μ nondimensional coefficient determined theoretically or from tests.

σ_e maximum stress at edges, at failure $\sigma_e = \sigma_y$.

t thickness of plate.

k buckling stress coefficient.

Karman's formula:

Eq. 2.20 was first developed by Karman (Galambos, 1998), based on Eq.2.3, he proposed theoretically that:

$$b_e = 1.9t \sqrt{\frac{E}{\sigma_e}} \tag{2.21}$$

in which $k=4.0$ and $\nu = 0.3$, and assuming that the two strips along the sides, each on the verge of buckling, carry the entire load.

Combining Eqs. 2.3 and 2.21, the following expression can be obtained:

$$\frac{b_e}{b} = \sqrt{\frac{\sigma_{cr}}{\sigma_e}} \qquad \leq 1 \tag{2.22}$$

Therefore, the effective width at the ultimate load is given by:

$$\frac{b_e}{b} = \sqrt{\frac{\sigma_{cr}}{\sigma_y}} \qquad \leq 1 \tag{2.23}$$

Substituting Eq. 2.22 into Eq. 2.15, Karman's equation gives the theoretical ultimate load that the plate can carry as follows:

$$\sigma_u = \sqrt{\sigma_{cr} \sigma_y} \tag{2.24}$$

Winter's formula

As a result of many tests and studies of postbuckling strength, Winter suggested another formula for the effective width, which includes a correction coefficient from tests and reflecting the total effect of various imperfections (Galambos, 1998). The formula, in a similar form of Eq.2.21 in which *k=4.0*, is:

$$b_e = 1.9t\sqrt{\frac{E}{\sigma_e}}\left(1-0.415\sqrt{\frac{E}{\sigma_e}}\frac{t}{b}\right) \qquad (2.25)$$

or , alternatively, in the form of Eq.2.22,

$$\frac{b_e}{b} = \sqrt{\frac{\sigma_{cr}}{\sigma_e}}\left(1-0.22\sqrt{\frac{\sigma_{cr}}{\sigma_e}}\right) \qquad \leq 1 \qquad (2.26)$$

For the ultimate load, using $\sigma_e = \sigma_y$. Eqs. 2.25 and 2.26 are adopted in the AISI and the AISC specifications (Salmon and Johnson, 1996; Galambos, 1998).

Considering that Eqs. 2.21 and 2.25 are appropriate formulas for determining the effective design width of stiffened compression elements with *k=4.0*, generalized formulas for different stiffened compression elements with various rotational edge restrains which are identical to Eqs. 2.21 and 2.25 can be written as follows (Galambos, 1998):

$$b_e = 0.95t\sqrt{\frac{kE}{\sigma_e}} \qquad (2.27)$$

$$b_e = 0.95t\sqrt{\frac{kE}{\sigma_e}}\left(1-0.209\sqrt{\frac{kE}{\sigma_e}}\frac{t}{b}\right) \qquad (2.28)$$

For a given value of σ_y , the limiting ratio of width/thickness, $(b/t)_{lim}$, in which the plate can be considered entirely effective, will be obtained from Eq.2.28 as follows:

$$\left(\frac{b}{t}\right)_{\lim} \le 0.64\sqrt{\frac{kE}{\sigma_y}} \tag{2.29}$$

Slenderness parameter, λ

Euler formula, Eq.2.3, for critical stress can be written in the following form:

$$\frac{\sigma_{cr}}{\sigma_y} = \frac{1}{\lambda^2} \tag{2.30}$$

where

$$\lambda = \frac{b}{t}\sqrt{\frac{12\sigma_y(1-\nu^2)}{\pi^2 Ek}} \tag{2.31}$$

From Eqs.2.23 and 2.15, Karman's equation for the ultimate load can be written as follows:

$$\frac{\sigma_u}{\sigma_y} = \frac{b_e}{b} = \frac{1}{\lambda} \qquad \le 1 \tag{2.32}$$

Also, Winter's equation, Eq.2.26, can be expressed as:

$$\frac{b_e}{b} = \frac{1}{\lambda}(1-0.22\frac{1}{\lambda}) \quad \le 1 \tag{2.33}$$

Eqs.2.32 and 2.33 as well as Eqs.2.27 and 2.28 can be used for simply supported end condition and for other conditions, because the buckling coefficient, *k*, is taken as a variable (Galambos, 1998; Usami and Fukumoto, 1982).

Furthermore, Eqs. 2.27 and 2.28 can be written for the ultimate load as follows:

$$\frac{b_e}{b} = 0.95\sqrt{k}\,\frac{t}{b}\sqrt{\frac{E}{\sigma_y}} \qquad \le 1 \tag{2.34}$$

$$\frac{b_e}{b} = 0.95\sqrt{k}\,\frac{t}{b}\sqrt{\frac{E}{\sigma_y}}\left(1-0.209\sqrt{k}\sqrt{\frac{E}{\sigma_y}}\frac{t}{b}\right) \le 1 \tag{2.35}$$

If using the following form for the slenderness parameter:

$$\lambda' = \frac{b}{t}\sqrt{\frac{\sigma_y}{E}} \tag{2.36}$$

Eqs. 2.34and 2.35 can be written as follows:

$$\frac{\sigma_u}{\sigma_y} = \frac{b_e}{b} = \frac{0.95\sqrt{k}}{\lambda'} \tag{2.37}$$

$$\frac{\sigma_u}{\sigma_y} = \frac{b_e}{b} = \frac{0.95\sqrt{k}}{\lambda'}\left(1 - \frac{0.209\sqrt{k}}{\lambda'}\right) \tag{2.38}$$

2.5 Stability of Rectangular Plates with Longitudinal Stiffeners

The theory of stiffened plates will be used to obtain simple design rules for the required rigidity of stiffeners in order that the plate and stiffener combinations will develop the specified critical buckling stress. Since the stiffeners carry the same compressive stresses as the plate, they may be considered as columns, and thus, the question of the stability of the stiffeners themselves, which must be designed with due regard to the additional possibility of torsional or local failure should be investigated. In this section, the case of a simply supported plate reinforced by one longitudinal stiffener on centerline will be studied.

Fig. 2.6 shows a rectangular thin plate of length *a*, width *b*, and thickness *t*, which is reinforced by a longitudinal stiffener on the centerline. The cross-sectional area of the stiffener is *A*, and its moment of inertia is *I*. It is assumed that the centerline of the stiffener lies in the middle plane of the plate, and the moment of inertia, *I*, therefore refers to the axis of the stiffener in this plane. Torsional rigidity of the stiffener is regarded as small and will be neglected; only the flexural rigidity of the stiffener perpendicular to the plane of the plate is being considered. The plate is loaded by a uniformly distributed load $t\sigma_x$ acting on the edges $x=0$ and $x=a$. The stiffener is

assumed welded or riveted to the plate and having the same compressive stress σ_x as the plate.

Because of the symmetry of the plate stiffener system, the displacement of the buckled system will be one of the following two types:

1. A symmetric configuration with deflected stiffener, some writers call this mode stiffener buckling mode or distortional buckling, Fig. 2.6b.
2. An antisymmetric configuration or local buckling of plate where the stiffener remains straight and the plate buckles between the stiffener and the edges, Fig. 2.6c.

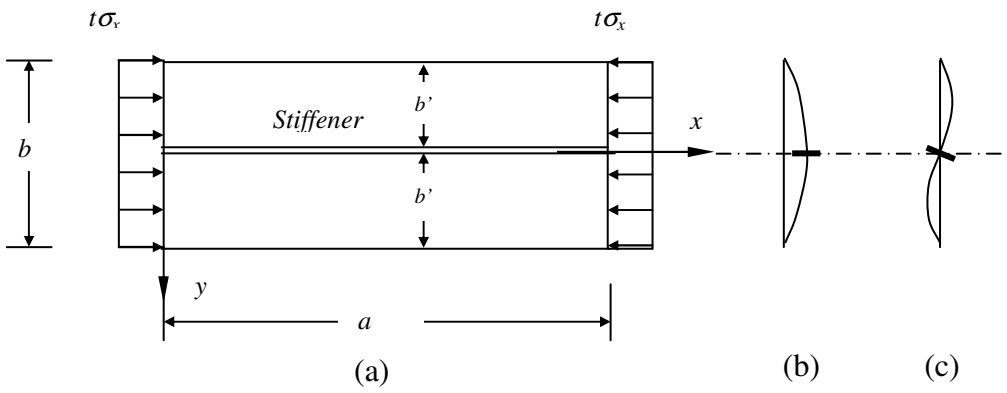

Fig. 2.6 Mode of buckling of thin plate with intermediate stiffener

2.5.1 Requirements of Stiffener Rigidity

The antisymmetric displacement form, Fig.2.6c, will occur when the rigidity ratio of the stiffener and the plate, $\gamma = EI/Db$, is larger than a certain value, γ_o. It is important to note that the critical stress for antisymmetric buckling, Fig.2.6c, does not depend on the rigidity ratio, γ, but on the critical stress for a simply supported plate of width *b/2*. For values of γ below γ_o, the symmetric displacement form, Fig. 2.6b, in which the

stiffener deflects with the plate will occur. At the ratio γ_o both configurations are equally possible.

The theoretical rigidity ratio γ_o, at which the critical buckling of the assembly is initiated by simultaneous symmetric and antisymmetric mode of buckling, can be computed approximately from the following formula (Bleich, 1952):

$$\gamma_o = 11.4\alpha + (1.25 + 16\delta)\alpha^2 - 5.4\sqrt{\alpha} \qquad (2.39)$$

where

α aspect ratio, a/b.

δ A/bt

A area of cross section of stiffener.

The maximum value for γ_o can be obtained from the following expression:

$$\gamma_{o\max} = 24.4 + 112\,\delta\,(1+\delta) \qquad (2.40)$$

If the rigidity ratio γ_o that is obtained from Eq.2.39 is greater than $\gamma_{o\max}$, γ_o must be replaced by $\gamma_{o\max}$. The above formulas are valid for $0 \le \delta \le 0.2$.

It should be noted that for long plates, the rigidity ratio γ_o is independent from the aspect ratio, α. The required moment of inertia of the stiffener is:

$$I_o = \frac{bt^3}{12(1-\nu^2)}\gamma_o = 0.092bt^3\gamma_o \qquad (2.41)$$

Eq. 2.41 is valid for all kinds of metal in elastic and inelastic ranges (Bleich, 1952). If the moment of inertia of the stiffener, I, is larger than the value I_o given by Eq. 2.41, each panel of the plate will buckle as a simply supported plate at a critical stress which is independent of the value of I_o. When the stiffener is frequently welded or riveted to one side of the plate only, adjacent zones of the plate can be included with the stiffener cross section.

The case of rectangular plates clamped at both unloaded edges which having one stiffener at the center was also investigated by Barber (Bleich, 1952). Fig. 2.7 shows, for comparison, the values of $\gamma_{o\max}$ for plates having simply supported edges and plates with two fixed edges. The criteria for stiffener rigidity that will be used in this study will be presented in Sec.3.3.2.

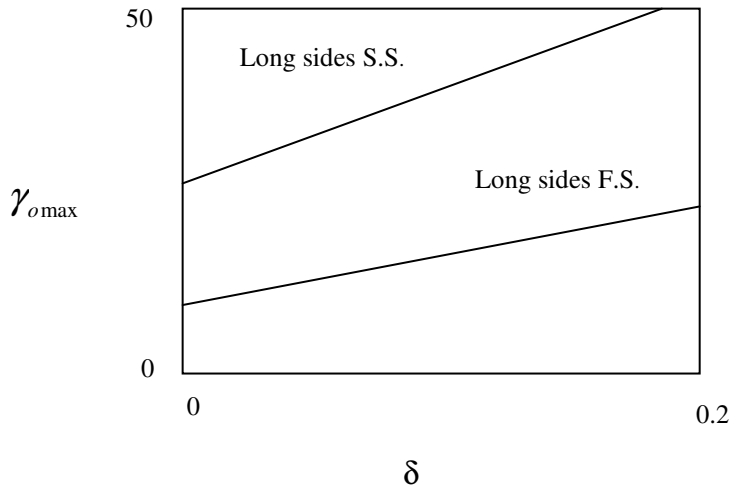

Fig. 2.7 Maximum rigidity ratio versus δ for long sides simply supported and fixed.

2.5.2 Buckling Stress Coefficient

I-Antisymmetric mode of buckling

In this mode, Fig.2.6c, the moment of inertia of the stiffener, *I,* is greater than or equal to I_o which means that the plate is adequately stiffened, and buckles between the stiffener and the edges. the coefficient of buckling for this mode can be determined as follows (Desmond *et al*., 1981):

$$(k_b)_{as.=}(b/b')^2 k_{b'}=4k_{b'} \qquad (2.42)$$

where

$(k_b)_{as.}$ buckling coefficient which is expressed as a function of b.

b' $b/2$, Fig 2.6.

$k_{b'}$ buckling coefficient which is expressed as function of b'.

If we assumed simply supported unloaded edges of the plate, $k_b=16$.

II-Symmetric mode of buckling

In this mode, Fig.2.6b, the moment of inertia of the stiffener, I, is greater than or equal to I_o and the plate is considered partially stiffened. For this case when $0 \le I/I_o \le 1$, Desmond *et al*. (1981) suggested the following expression:

$$(k_b)_{sy} = (I/I_o)^{1/2}\left[(k_b)_{as} - (k_b)_{ns}\right] + (k_b)_{ns} \qquad (2.43)$$

where

$(k_b)_{sy}$ predicted buckling stress coefficient for partially stiffened plates.

$(k_b)_{as}$ buckling stresses coefficient for adequately stiffened=16 for simply supported unloaded edges.

$(k_b)_{ns}$ buckling stress coefficient for plate without stiffeners=4 for simply supported unloaded edges.

Fig. 2.8 shows graphically Eqs.2.42 and 2.43 for symmetric and antisymmetric mode of buckling as a function of (I/I_o) for simply supported thin plates.

2.5.3 Postbuckling Strength

Considering plates with longitudinal stiffeners, the effective width concept can be extended to this type of plates (Galambos, 1998; Bernard *et al*., 1993; Desmond *et al*., 1981). Therefore, the equations outlined in Sec.2.4 can be used to obtain their ultimate strength in the postbuckling range.

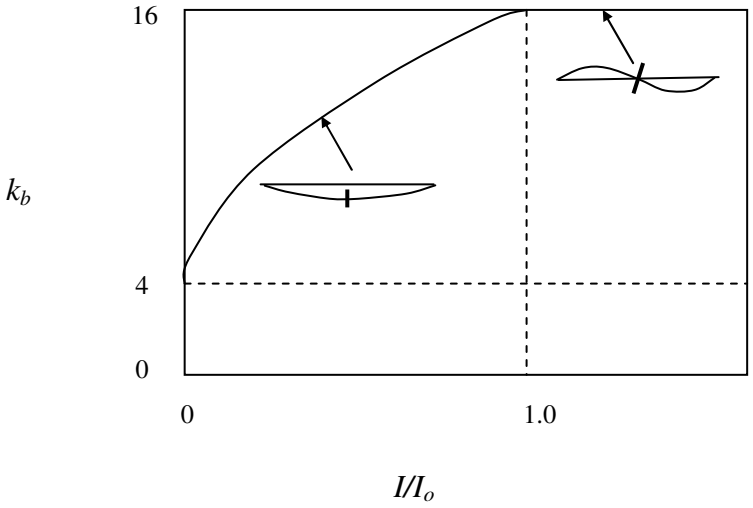

Fig. 2.8 Minimum critical buckling coefficient for long and thin simply supported plate with intermediate stiffener.

Chapter 3

BUCKLING INTERACTION

3.1 Interaction Between Plate Elements

In the preceding chapter, attention has been confined to the behavior of a single plate element supported along one or both of its longitudinal edges. The structural steel sections employed in practice, Fig. 1.1, are composed of plate elements arranged in a variety of configurations. It is clear that the behavior of an assembly of plates would be governed by an interaction between the plate components. In this section the mechanics of such an interaction is discussed briefly.

3.1.1 Buckling of a Plate Assembly

A prismatic plate structure is often viewed simply as a group of stiffened and unstiffened plate elements. The former are plate elements supported on both longitudinal edges by virtue of their connection to adjacent elements, Case *I*, while the later are those supported only along one of their longitudinal edges, Case *II* (Fig. 2.2). Thus the critical local buckling stress of plate elements depends upon the rotational restrains at the unloaded edges of the plate assembly.

3.1.1.1 Buckling Modes of a Plate Assembly

Unlike a single plate element supported along the unloaded edges, a plate assembly can buckle in one of several possible modes. For the case of axial compression, the buckling mode can take one of the following forms (Galambos, 1998):

- ***Mode I***. This is the purely local buckling mode discussed earlier in Sec. 2.2. The mode involves out-of-plane deformation of the component plates with the junction remaining essentially straight and it has a wavelength of the same order of magnitude as the width of the plate elements.
- ***Mode II***. The buckling process may involve in-plane bending of one or more of the constituent plates as well as out-of-plane bending of all the elements, as in a purely local mode. Such buckling mode is referred to as a stiffener buckling mode, local torsional mode, or orthotropic mode, depending on the context, Sec. 2.5. The associated wavelength is considerably greater than that of mode *I*, but there is a half-wavelength at which the critical stress is a minimum.
- ***Mode III***. The plate structure may buckle as a column in flexural or flexural-torsional mode with or without interaction of local buckling. Flexural buckling mode will be discussed in this chapter.

3.1.1.2 Restraint Coefficient, ξ, of Plate Elements of Box Section

In the study of rectangular plates in Section 2.2, a coefficient of restraint, ξ, was introduced, and it is now the time to show how this coefficient can be determined in the case of plate assembly in rectangular hollow sections. Bending and twisting of the restraining plates, thicker plates, in Fig. 3.1 is determined not only by the effect of the elastic interaction between the web plates and the restraining elements but also by the longitudinal compressive forces acting on the restraining plates. The heavier the

restraining plates, the smaller will be the effect of the compressive stresses. This effect takes on a practical significance when the width to thickness ratios, b/t and c/t_c, approach the same value (Fig. 3.1c). In the limiting case, when both plates buckle simultaneously, there is no restraint effect and each element behaves as a plate having simply supported unloaded edges.

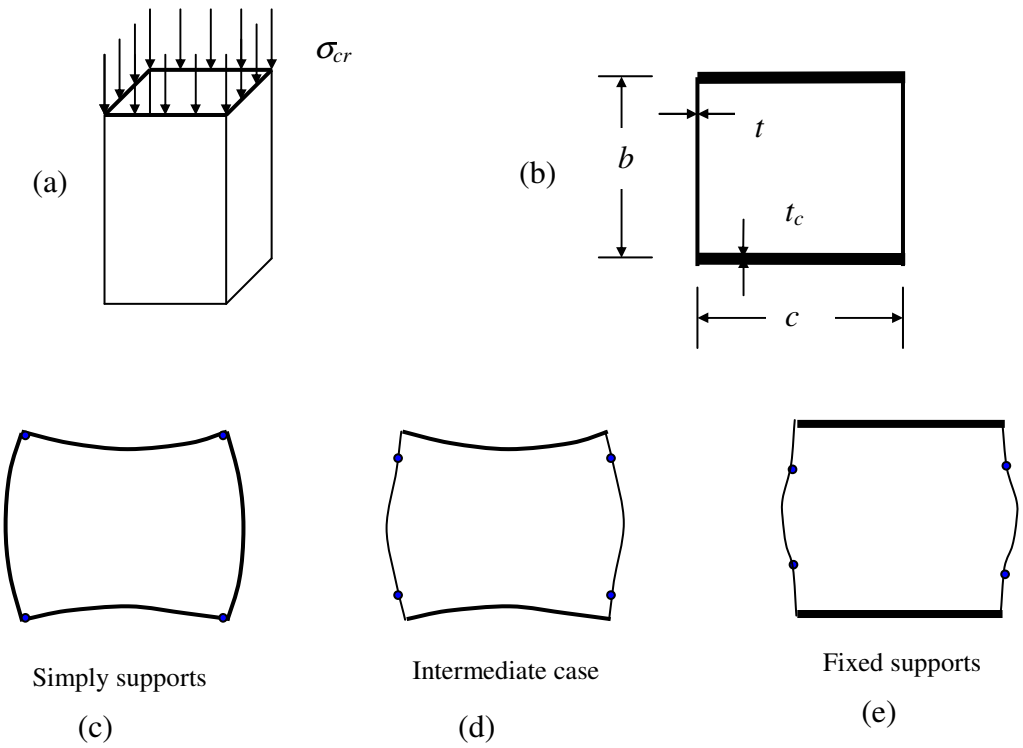

Fig. 3.1 Interaction of plate elements of box section.

The following solution for the restrained coefficient is based upon these assumptions (Bleich, 1952):

1. No overall buckling of entire plate assembly takes place prior to local instability in the plates.
2. The edges where the plates join remain straight and do not distort before local failure takes place.

The coefficient of restraint of box section can be expressed as:

$$\xi = \frac{t^3}{t_c^3} \frac{\rho_1 (c/b)}{1-(t^2c^2/t_c^2b^2)} \tag{3.1}$$

where:

t thickness of considered plate.

b width of considered plate

t_c thickness of thicker plate.

c width of thicker plate.

ρ_1 factor determined from Fig. 3.2.

This equation applies when $(tc/t_cb) \leq 1$. All terms of Eq. 3.1 are shown in Fig. 3.1, except ρ_1 which can be determined from Fig. 3.2 as a function of $c\sqrt{\eta}/\omega$ in which ω is the half wavelength which is determined from:

$$\omega = \psi b\sqrt{\eta} \tag{3.2}$$

where:

ψ coefficient determined from Table 3.1.

η plasticity reduction factor, $\sqrt{E_t/E}$.

Table 3.1 shows the numerical limiting values of factor ψ for the computation of the half wavelength, ω, for elastic and inelastic buckling of plates. To obtain ω, for intermediate cases, trail and error method can be used together with Table 3.1 as a guide. The numerical values in Table 3.1 apply to long plates only.

Computing, in any given case, the value of ξ with the aid of the diagram for ρ_1 in Fig. 3.2, the values of the parameters *p* and *q* can be evaluated from Figs. 2.2 and 2.3. This permits computation of the buckling coefficient, *k*, from Eq. 2.5, which is required to determine σ_{cr} from Eq. 2.3. For inelastic buckling, $\eta^2 = E_t/E$ <1.0,this procedure must be repeated and needs more than one iteration.

In the case of box section with longitudinal stiffeners on all sides, Eq. 2.42 can be used to determine the buckling coefficient of the section for a plate adequately stiffened, because the variation in restraint coefficient is small and will be neglected.

Fig. 3.3 shows results of the application of the method outlined above for buckling coefficient of box-section for various dimensions. Buckling coefficients for the interacted plate elements are utilized for obtaining the entire effective section in postbuckling range (Batista, 1987). To obtain the critical buckling for a tube section from Eq. 2.3, the largest width/thickness ratio for the side that induces the minimum σ_{cr} must be used.

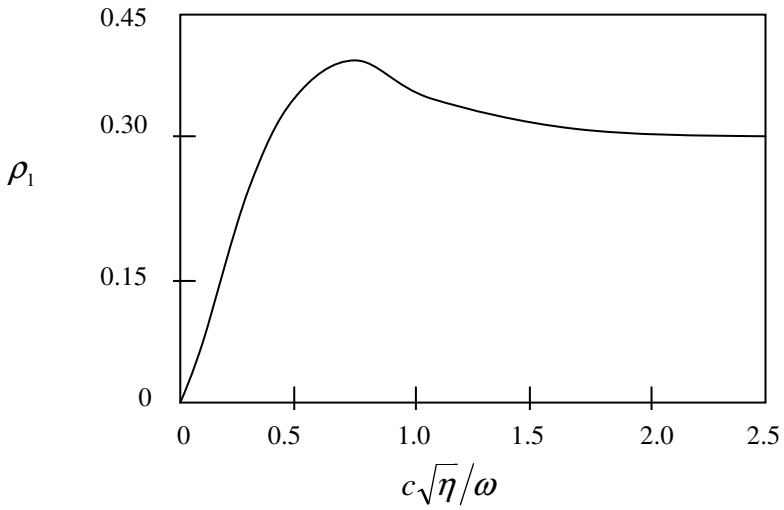

Fig. 3.2 Values of ρ_1

Table 3.1 Values of coefficient ψ of Eq. 3.2 (Bleich, 1952):

Supports Conditions	Both edges simply supported	One edge simply supported, the other fixed	Both edges fixed	One edge simply supported, the other free	One edges fixed, the other free
ψ	1.000	0.800	0.688	*	1.680

* ω is always equal to the length, a, of the plate.

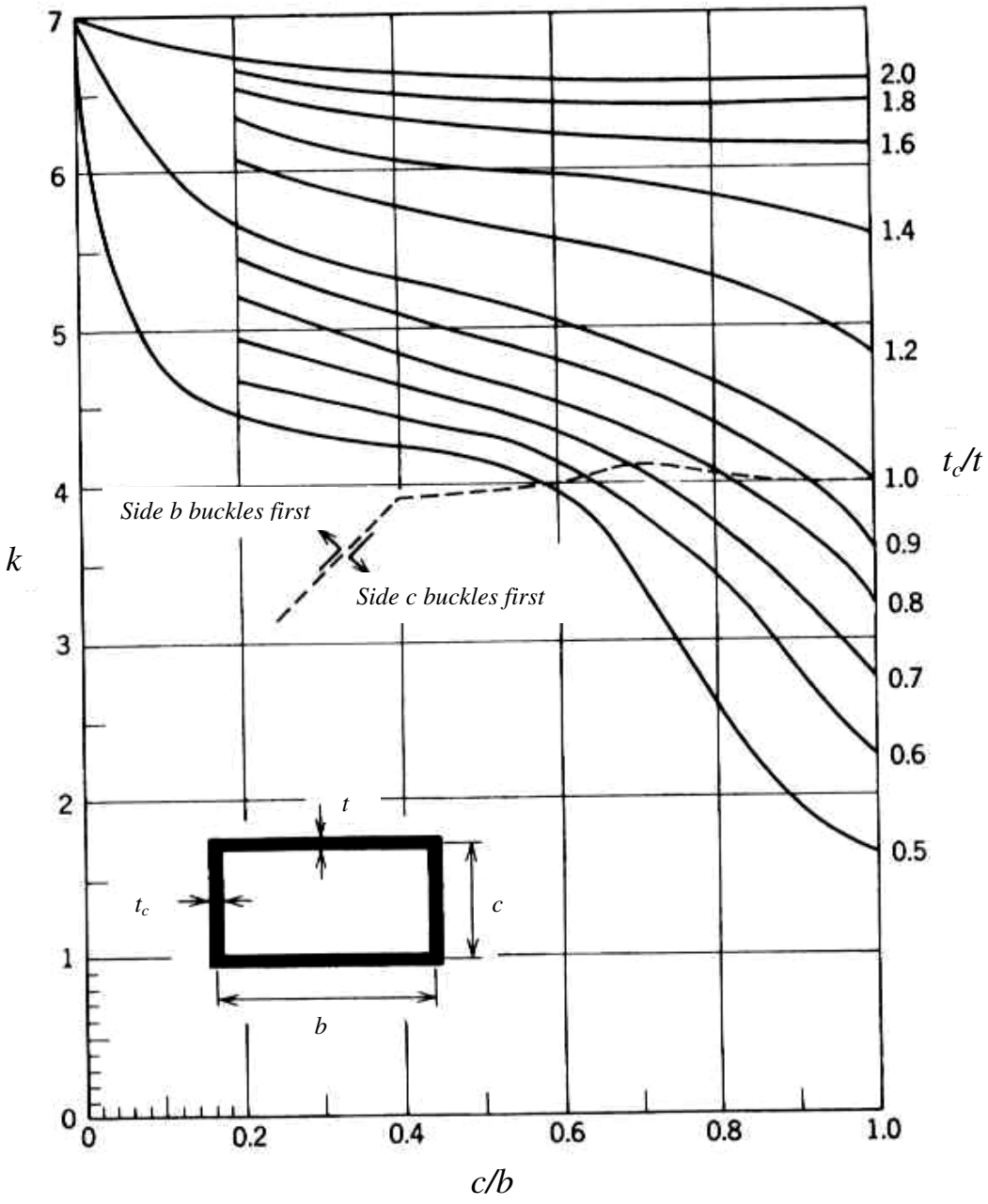

Fig. 3.3 Buckling coefficient, *k*, for box section (Galambos, 1998)

3.2 Interaction Between Local and Overall Buckling

The behavior of a column that exhibited local and overall buckling is very complex. The main difficulty lies in the non-linear behavior of thin-walled column, which results from the interaction of several instability modes; column flexural buckling, plate buckling, and flexural-torsional buckling.

There are two methods for analyzing compressed thin-walled members. One is the effective section method (DeWolf *et al*., 1974, and Kalyanaraman *et al.*, 1977) in which the local instability of a column is treated approximately by reducing the whole section to an effective section. The other is a numerical method, such as the finite element method and the finite strip method (Hancock, 1981). To design compressed columns, the effective width method is the basis of the prevailing specifications, the AISC and AISI (AISC, 1993; AISI, 1980), in which the strength of a thin-walled member is calculated by combining the effective area and the overall stability equations of the member.

3.2.1 Failure Modes of Steel Columns

A concentrically thin-walled compressed section, such as box section, which is subjected neither to torsional-flexural nor to torsional buckling and for which local plate buckling occurs prior to material yielding, fails in one of the following patterns:

1. For small slenderness ratios, such as the stub columns of this study, local plate bucking occurs followed by the development of postbuckling strength as the load is increased with failure occurring when the compressive strength of the component plates is reached.
2. For moderate slenderness ratios, local plate buckling occurs followed by the development of postbuckling strength, with failure precipitated by overall

flexural column buckling. In this pattern, interaction between local and overall buckling occurs and causes a reduction in the strength of the column.

3. For large slenderness ratios, failure occurs by overall buckling without local plate buckling.

3.2.2 Prediction of Column Strength by Effective Section Concept

3.2.2.1 Modified Tangent Modulus Method

This concept is a semi-empirical approach and is applied to a wide variety of column shapes, with a broad range of postbuckling and overall column buckling strength and to account for elastic and inelastic effects in the plates and columns (DeWolf *et al*., 1974).

The bifurcation stress of a column is given by the generally accepted Engesser-Shanley tangent modulus equation:

$$\sigma_{CR} = \frac{\pi^2 E_t}{(KL/r)^2} \tag{3.3}$$

in which:

E_t tangent modulus of elasticity.

L column length.

r radius of gyration.

K effective length factor.

Eq. 3.3 is used as the basis for determining the stress at which overall buckling and thus column failure occurs. Eq. 3.3 can be written as:

$$\sigma_{CR} = \frac{\pi^2 E_t I}{K^2 L^2 A} \tag{3.4}$$

If the cross section is divided into separated components to allow for the inclusion of cold-formed effects at corners, Eq.3.4 can be written as:

$$\sigma_{CR} = \frac{\pi^2 \sum_{i=1}^{j} E_{ti} I_i}{K^2 L^2 A} \tag{3.5}$$

in which

σ_{CR} the average stress on the column cross section at buckling.

j the total number of components the cross section is divided into.

E_{ti} the tangent modulus of the i^{th} component.

I_i moment of inertia of i^{th} component about the axis of overall buckling.

Provided that local buckling does not occur, the full cross section resists overall flexural buckling. However, if local buckling occurs in any of the plate elements, the longitudinal stiffness of those elements is reduced. This effect may be expressed by reducing the full column cross section to a smaller effective cross section.

Fig. 3.4 shows the compressive stress distribution on box section, with and without stiffeners, and the effective sections.

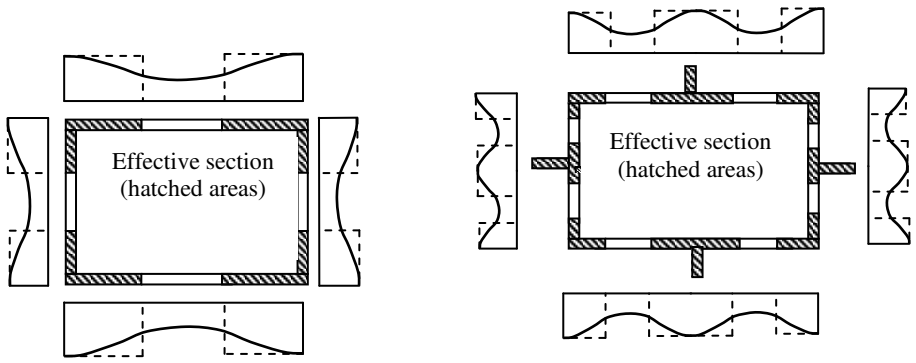

(a) Unstiffened box-section (b) Box section with stiffeners

Fig. 3.4 Compression stress distribution and effective section

The effective areas and the effective moments of inertia will be used in Eq. 3.5 to account for local buckling in determining the ultimate column strength. Eq. 3.5, written in terms of the effective section properties, gives the stress at which overall buckling, and thus column failure, occurs. Thus;

$$\sigma_e = \frac{\pi^2 \sum_{i=1}^{j} E_{ti} I_{i,e}}{K^2 L^2 A_e} \tag{3.6}$$

in which:

σ_e average stress on the effective section.

$I_{i,e}$ moment of inertia of the effective portion of the i^{th} element about the axis of overall buckling.

A_e the sum of the effective areas of those elements.

If the material stress-strain properties are uniform throughout the section, the assumed stress distribution on the effective section is uniform and equal to the edge stress for the flat plate elements. Otherwise, the stress for each element is obtained from the material stress-strain curve for that element using the strain obtained from the average stress-strain curve of a stub column for a particular value of σ_e.

Having determined, in this manner, σ_e from Eq. 3.6 the total column load is:

$$P = \sigma_e A_e \tag{3.7}$$

This procedure gives the maximum strength of a column subjected to combined overall and local buckling with additional consideration of nonuniform material properties.

The solution of Eq. 3.6 when the cross section is not entirely elastic or not fully effective requires iteration, because the tangent modulus and the effective areas are dependent on the stress, which in turn, is dependent on the tangent modulus and the effective areas.

To facilitate the solution, Eq. 3.6 is written in terms of the length rather than the stress, i.e.:

$$L = \sqrt{\frac{\pi^2 \sum_{i=1}^{j} E_{ti} I_{i,e}}{\sigma_e K^2 A_e}} \tag{3.8}$$

3.2.2.2 Modified Structural Stability Research Council Method

The SSRC-Column Strength equations are adopted in the AISC-ASD Specifications. The equations are based on the tangent modulus theory. However, the AISC-LRFD Specifications equations are based on the maximum strength of the column and are identical to SSRC Curve 2P (Galambos, 1998). The procedure and the equations presented in this section will be used to predict the interaction buckling strength of columns.

ASD equations:

The average stress on the total section is:

$$\sigma_{av} = \frac{P}{A} = \frac{A_e}{A}\sigma_e = Q\sigma_e \tag{3.9}$$

where

Q strength reduction factor.

The stress on the effective section of a column, σ_e, at failure can be written as follows:

$$\sigma_e = \left(\sigma_y - \frac{\sigma_y^2}{4\pi^2 E}\left(\frac{L}{r_e}\right)^2 \right) \quad \text{when} \quad \left(\frac{L}{r}\right)_e \le \sqrt{\frac{2\pi^2 E}{\sigma_y}} \tag{3.10}$$

and

$$\sigma_e = \frac{\pi^2 E}{(L/r_e)^2} \quad \text{when} \quad \left(\frac{L}{r}\right)_e \ge \sqrt{\frac{2\pi^2 E}{\sigma_y}} \tag{3.11}$$

where

$$\left(\frac{L}{r}\right)_e = \sqrt{\frac{\pi^2 E}{\sigma_e}}$$

and

$$r_e = \sqrt{I_e / A_e}$$

To obtain the column strength, Eqs. 3.10 and 3.11 will be written in terms of the column length, *L*, and will be given as:

$$L = \frac{2\pi r_e}{\sigma_y}\sqrt{E(\sigma_y - \sigma_e)} \quad \text{when} \quad \left(\frac{L}{r}\right)_e \le \sqrt{\frac{2\pi^2 E}{\sigma_y}} \qquad (3.12)$$

$$L = \sqrt{\frac{\pi^2 E r_e^2}{\sigma_e}} \quad \text{when} \quad \left(\frac{L}{r}\right)_e \ge \sqrt{\frac{2\pi^2 E}{\sigma_y}} \qquad (3.13)$$

LRFD equations:

The previous procedure in ASD can be used for LRFD as follows:

$$\sigma_e = \left(0.658^{(\lambda_c^2)_e}\right)\sigma_y \quad \text{when} \quad (\lambda_c)_e \le 1.5 \qquad (3.14)$$

and

$$\sigma_e = \left(\frac{0.877}{(\lambda_c^2)_e}\right)\sigma_y \quad \text{when} \quad (\lambda_c)_e > 1.5 \qquad (3.15)$$

where

$$(\lambda_c)_e = \left(\frac{L}{r}\right)_e \sqrt{\frac{\sigma_y}{\pi^2 E}}$$

To obtain the column strength, Eqs. 3.14 and 3.15 will be written in terms of the column length, *L*, and will be given as:

$$L = \sqrt{\left(\frac{\pi^2 E r_e^2}{\sigma_y}\frac{(\ln\sigma_e - \ln\sigma_y)}{\ln 0.658}\right)} \qquad (3.16)$$

$$L = \sqrt{\left(\frac{0.877\pi^2 E r_e^2}{\sigma_e}\right)} \qquad (3.17)$$

3.2.2.3 Effective Area, A_e, and Effective Moment of Inertia, I_e:

Expressions presented in this section for effective area and effective moment of inertia are applicable for tube with and without stiffeners because only the tube section is involved for both cases.

I-Square section

Fig. 3.5 shows description for the effective cross section. The effective area and the effective moment of inertia can be expressed as:

$$A_e=2B_et+2(B_e-2t)\,t \tag{3.18}$$

$$I_e = 2\left[\frac{B_e t^3}{12} + B_e t\left(\frac{B}{2}-\frac{t}{2}\right)^2 + 2\left(\frac{t(B_e/2-t)^3}{12} + t(B_e/2-t)\left(\frac{B}{2}-\frac{B_e}{4}-\frac{t}{2}\right)^2\right)\right] \tag{3.19}$$

where

B_e the effective width including the thickness of plate, $B_e = b_e + t$.

II-Rectangular section

The case that will be considered herein is when the ratio of *C/t* of the short sides is less than the limiting value in which short sides will be effective until failure, because the tested rectangular section within this limit (Fig.3.6). Based on the above assumption the effective width can be obtained using the effective area, A_e, as follows:

$$A_e=2B_et+2(C-2t)\,t \tag{3.20}$$

$$B_e=[A_e-2\,(C-2t)\,t]/2t \tag{3.21}$$

The moment of inertia is taken about the minor axis and can be obtained as follows:

$$I_e = 2\left[\frac{B_e t^3}{12} + B_e t\left(\frac{C}{2}-\frac{t}{2}\right)^2 + \frac{t(C-2t)^3}{12}\right] \tag{3.22}$$

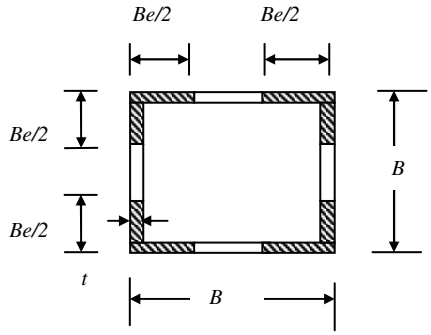

Fig. 3.5 Effective area of square section.

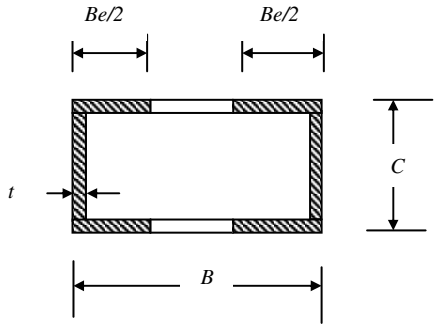

Fig. 3.6 Effective area of rectangular section.

3.3 Specifications Requirements

Two schemes for dealing with local buckling are generally used. The first, which is more common in Europe, aims at preventing plate buckling at any stress less than the computed critical stress of entire column. The second, prevailing in other countries such as U.S.A. (the AISC specifications), has the purpose of preventing local plate buckling at any stress less than the yield point, regardless of the computed critical stress of the entire column. Nevertheless, these specifications allow using thin plate elements in compression members with additional provisions.

The practice in light-gage specifications, for example the AISI, is to use thin plates in structural elements. To use them to advantage, it is necessary to permit local plate buckling before failure, in which event postbuckling strength may be recognized, provided that it is accompanied by a suitable reduction in the effective section.

3.3.1 AISC Provisions for Plate Elements

In the AISC specifications, (AISC, 1980; AISC, 1993), plates supported on both unloaded edges are called stiffened element, such as flanges of box-section. Also, for

plates supported on only one unloaded edge are called unstiffened elements, such as flanges of I-section.

3.3.1.1 Width/Thickness Limits, λ_r

Design limits are generally simplified to insure reaching the yield strength, F_y, in compression elements without local buckling, even though the slenderness ratio of a column may prevent the element from reaching this stress.

ASD Specifications

The width/thickness, *b/t*, ratios to prevent local buckling until the yield stress is reached are the noncompact limits in the AISC (AISC, 1980). Stiffened or unstiffened elements subjected to axial compression, or to uniform compression due to bending as in the case of the flange in a flexural member, shall be considered as fully effective when the ratio of width to thickness is not greater than that given in Section 1-9 (AISC, 1980). The following cases are of special concern:

- Flanges of square and rectangular box-section, stiffened element, of uniform thickness:

$$\frac{625}{\sqrt{F_y}} \tag{3.23}$$

- Plates projecting, unstiffened element, from compression members:

$$\frac{250}{\sqrt{F_y}} \tag{3.24}$$

where F_y is the yield stress in MPa.

LRFD Specifications

Steel sections are classified as compact, noncompact, or slender-element sections (AISC, 1993). For a section to be qualified as compact; its flanges must be continuously

connected to the web or webs and the width/thickness ratios of its compression elements must not exceed the limiting width/thickness ratio, λ_p, from Table B5.1 (AISC, 1993). If the width/thickness ratio of one or more compression elements exceeds λ_p, but dose not exceed λ_r, the section is noncompact. If the width/thickness ratio of any element exceeds λ_r from Table B5.1, the section is referred to as slender-element compression section. The limiting width/thickness ratio, λ_r, for noncompact compression elements in the LRFD specifications (AISC, 1993), for the previous cases are similar to the ASD specifications.

3.3.1.2 Provisions to Account for Buckling and Postbuckling Strength of Plate Elements

For many years the AISC specifications have permitted that the limiting values, which are presented in the previous section, to be exceeded, provided that stress computations were based on specified effective width and specified stress. The specifications require the effective width to be determined for plates supported on both unloaded edges because of the high postbuckling strength of stiffened plate. For a plate supported only along one unloaded edge, the postbuckling strength is smaller and its value is not much above the incipient buckling load as well as it is accompanied by relatively large wave(s) distortions. Thus, the specifications use a reduced stress for unstiffened plates.

a) Effect on Overall Column Strength

For design, it is desired to use gross section properties; thus for stiffened elements (AISC, 1980; AISC, 1993):

$$P_n = Q_a f_{\max} A \tag{3.25}$$

where

Q_a strength reduction factor, A_e/A

P_n nominal strength.

A_e effective area.

A gross area.

f_{max} maximum stress at unloaded edges.

And for unstiffened elements

$$P_n = Q_s f_{max} A \tag{3.26}$$

where

$$Q_s = f_{av}/f_{max}$$

in which

f_{av} average stress

Factors Q_a and Q_s may be thought of as shape factors, or form factors. For a compression system composed of both stiffened and unstiffened elements:

$$P_n = Q\ f_{\max} A \tag{3.27}$$

where $Q=Q_aQ_s$.

ASD Specifications

For the basic SSRC parabola used in AISC, section C5 (AISC, 1980). The following formulas are adopted without a factor of safety. For short columns, the strength of the column, F_{cr} , becomes:

For $\frac{KL}{r} \le C_c'$

$$F_{cr} = QF_y\left[1 - \frac{QF_y}{4\pi^2 E}\left(\frac{KL}{r}\right)^2\right] \tag{3.28}$$

where

$$C_c' = \sqrt{\frac{2\pi^2 E}{QF_y}} \tag{3.29}$$

LRFD specifications

For the equations used in the LRFD Appendix E3, the slenderness parameter for a column, λ_c, will become $\lambda_c\sqrt{Q}$ and the short column equation becomes as follows:

For $\lambda_c\sqrt{Q} \le 1.5$

$$F_{cr} = \left(0.658^{Q\lambda_c^2}\right)QF_y \tag{3.30}$$

where

$$\lambda_c = \frac{KL}{r}\sqrt{\frac{F_y}{\pi^2 E}} \tag{3.31}$$

Whenever $\lambda_c\sqrt{Q} > 1.5$ in the LRFD and $\frac{KL}{r} > C_c'$ in the ASD, the effect of local buckling on overall column strength is negligible; thus, for slender columns the Euler equation is the basis of strength.

b) Form Factor Q_s for Unstiffened Elements

Local buckling of an unstiffened element will reduce the efficiency of the cross-section only when $F_{cr.plate}$ for the plate element is less than $F_{cr\cdot column}$. A full advantage is not taken of the serviceability equation regarding waviness. Instead, the stresses taken at a value between the critical stress and the postbuckling strength.

ASD-Section C2 and LRFD-Appendix B5.3a give similar stress reduction equations for unstiffened flanges, in which width/thickness ratios exceed the applicable limit given in Sec.3.3.1.1. The design strength of axially loaded compression members shall be modified by the appropriate reduction factor Q, as provided in the previous section.

- For plates projecting from compression members:

$$Q_s = 1.415 - 0.00166(b/t)\sqrt{F_y} \tag{3.32}$$

when

$$\frac{249}{\sqrt{F_y}} < \frac{b}{t} < \frac{462}{\sqrt{F_y}} \tag{3.33}$$

or

$$Q_s = \frac{137800}{F_y (b/t)^2} \tag{3.34}$$

when

$$\frac{b}{t} \geq \frac{462}{\sqrt{F_y}} \tag{3.35}$$

where F_y in MPa , b and t in mm.

c) Form Factor Q_a for Stiffened Elements

The concept of effective width is used to account for the strength of stiffened elements under compressive stress. The AISC specifications (AISC, 1980; AISC, 1993) use the effective width formula developed by Winter, Eq. 2.25 in Sec.2.4.3. When the width/thickness ratio of uniformly compressed stiffened elements exceeds the limit values given in Sec.3.3.1.1, reduced effective width shall be used in computing the design properties of the section containing the element.

The ASD-Section C3 and LRFD-Appendix B5.3b give similar effective width equations. The following formulas are presented (without factor of safety) as follows:

- For flanges of square and rectangular box-sections:

$$b_e = \frac{856t}{\sqrt{f}}\left[1 - \frac{170}{(b/t)\sqrt{f}}\right] \tag{3.36}$$

when

$$\frac{b}{t} \geq \frac{625}{\sqrt{f}} \tag{3.37}$$

- For other uniformly compressed elements:

$$b_e = \frac{856t}{\sqrt{f}}\left[1 - \frac{150}{(b/t)\sqrt{f}}\right] \tag{3.38}$$

when

$$\frac{b}{t} \geq \frac{664}{\sqrt{f}} \tag{3.39}$$

where

b actual width of a stiffened compression element.

b_e reduced effective width.

t element thickness.

and F_y in MPa , b and t in mm.

In the previous equations, f is the computed elastic compressive stress in the stiffened elements, based on the design properties. If unstiffened elements are included in the total cross section, f for the stiffened element must be taken such that the maximum compressive stress in the unstiffened element does not exceed F_{cr}. For stiffened element, $Q_a = A_e/A$ as defined previously in Sec.3.3.1.2 (a).

As mentioned before, Eq.3.36 is adopted from Winter's equation using a value of 4.0 for the buckling coefficient and thus the effective cross-sectional area, A_e, is determined by the sum of the computed effective widths of all the plate components of the section using Eq.3.36 independently. Although this procedure may be true for square sections, it is unreasonable for rectangular sections, which means no interaction between plate elements in rectangular sections. In contrast, the proposed equation of effective section in this study (Sec.5.4) is concerned with the interaction between the plate elements for rectangular sections and yields the entire effective section directly.

3.3.2 AISI Recommendation for Stiffeners Rigidity

There are no provisions in the AISC specifications concerning the minimum dimensions of longitudinal stiffeners. The formula that is adopted in the AISI specifications, which is originally developed by Timoshenko, can be used to obtain the limiting moment of inertia for intermediate stiffener, $I_{so,}$ to insure adequate stiffening and to obtain the buckling coefficient in Eq. 2.43. This formula can be expressed as follows (AISI, 1980):

$$I_{so} = 2\left(1.83t^4\sqrt{(b'/t)^2 - (27600/F_y)}\right) \qquad mm^4 \qquad (3.40)$$

where

I_{so} minimum moment of inertia of stiffener about its own centrodial axis parallel to the stiffened element and not less than $9.2t^4$.

b' sub-plate width $=b/2$ when the stiffener at the centerline of plate.

t thickness of plate.

Eq. 3.40 gives the necessary dimensions to equate the critical buckling stress of plates stiffened by intermediate stiffeners to that of identical plates stiffened by webs along both edges (Winter, 1980). However, Desmond (1981) reported that stiffeners provided according to Eq. 3.40 are capable of supporting loads even in the postbuckling range. The value of I_{so} from Eq. 3.40 will be used in this study instead of I_o presented in Sec.2.5.1 to obtain coefficient of buckling for sections with longitudinal stiffeners.

Chapter 4

DETAILS OF TESTS

This chapter describes the test program of this study. Thirty-six stub columns of square and rectangular hollow section were tested to failure under uniaxial compression. All details of the testing program will be presented.

4.1Test Specimens

The structural hollow steel tubes tested in this investigation are classified as cold-formed sections. More details on the fabricating process of this type of sections can be found in a study presented by Hancock *et al*. (1987). Two different sections were prepared and tested, ordinary tubes (unstiffened tubes), and tubes reinforced by longitudinal stiffeners on all sides (stiffened tubes).

The lengths of specimens were chosen to be sufficiently short to prevent overall buckling but long enough to permit local bucking of the individual component plates. The corners radii of sections were considerably small, therefore, their effects were neglected and the corners of the sections were treated as right-angle corners. Dimensions of the specimens are shown in Figs. 4.1 and 4.2 as well as in Tables 4.1 and

4.2. In these Tables, “S”, “R”, and “ST” refer to square tube, rectangular tube, and stiffener respectively.

4.1.1 Unstiffened Tubes

The total number of this type is 12 specimens. Two specimens, A and B, for each cross section were tested to assure the precision of test results. The range of slenderness ratio, *b/t*, for plate elements was from 65.67 to 31.26 as shown in Fig. 4.1 and Table 4.1.

4.1.2 Stiffened Tubes

The total number of this type is 24 specimens divided into two groups. In group I, small stiffeners were used compared to the sectional area of the specimens whereas in group II, relatively large stiffeners were used. Two specimens, A and B, for each cross section were tested to assure the precision of test results. The description of these specimens is shown in Fig. 4.2 and Table 4.2.

Stiffeners

The dimensions of stiffeners were chosen such that local buckling of stiffeners themselves is prevented. The reason for such choice is that; if local buckling of the stiffener is allowed, the problem will be more complicated and other interaction between local buckling of the stiffener and local buckling of the tube flange must be considered. Furthermore, the stiffeners dimensions were chosen so that their moments of inertia about their center are above and below values given by AISI specifications, in order to allow for distortions of all modes. Three types of stiffeners were used (ST1, ST2, and ST3); dimensions of these stiffeners are shown in Fig. 4.2 and Table 4.2 as well as in Table 4.3. The largest stiffener ST3 was placed on the long side of rectangular tubes of group II.

Stiffeners were attached to the tubes by welds on all sides. Since the sections are considered as thin-walled, welding process may cause considerable distortion in the cross section due to shrinkage. In order to minimize such undesired distortions, intermittent weld with minimum size and small length (about 70mm) was used on opposite side of the stiffeners.

Stiffeners were used on short sides of rectangular tubes to assure that failure will first occurs at the long sides, and also to keep the restraint at corners as in the corner of the unstiffened tube sections.

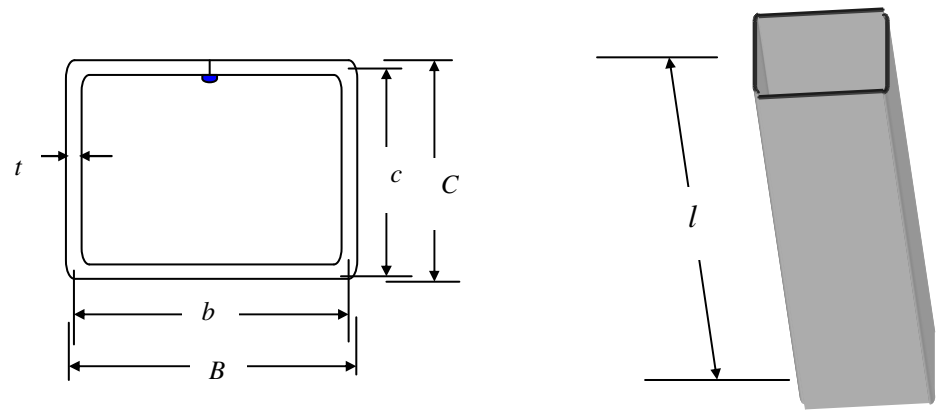

Fig.4.1 Description of unstiffened tube.

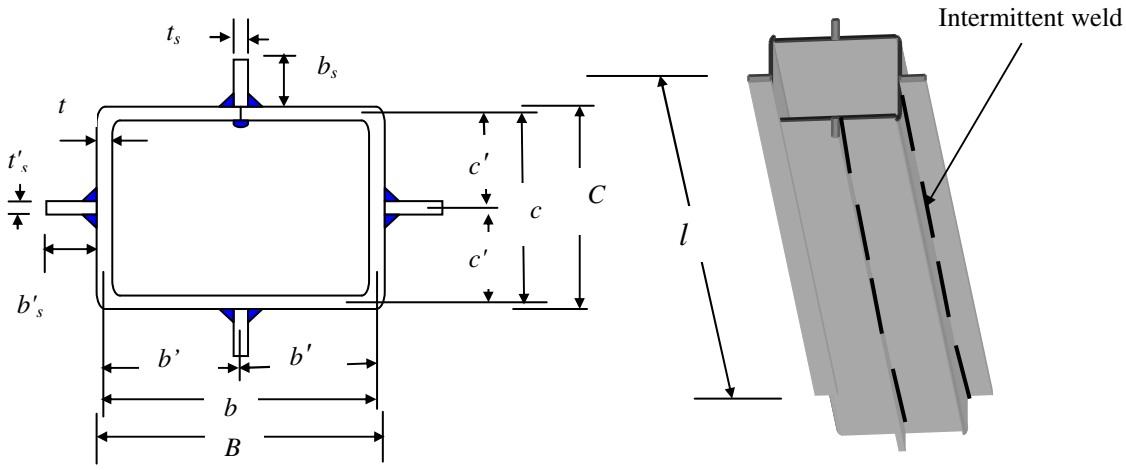

Fig. 4.2 Description of stiffened tube.

Table 4.1 Sectional properties of unstiffened tube Sections

Specimen	***B*** mm	***C*** mm	***t*** mm	***b*** mm	***c*** mm	***l*** mm	***A*** mm^2	***I*** mm^4	***r*** mm	***l/r***	***b/t***	***c/b***	***l/b***
S1	100	100	1.5	98.5	98.5	500	591	955893	40.22	12.43	65.67	1	5.08
S2	100	100	2.1	97.9	97.9	500	822.36	1314244	39.98	12.51	46.62	1	5.11
S3	100	100	2.5	97.5	97.5	500	975	1545781	39.82	12.56	39.00	1	5.13
S4	100	100	3.1	96.9	96.9	500	1201.56	1882288	39.58	12.63	31.26	1	5.16
R1	150	90	2.9	147.1	87.1	550	1358.36	1939179	37.78	14.56	50.72	0.59	3.74
R2	200	100	4.9	195.1	95.1	600	2843.96	5034814	42.08	14.26	39.82	0.49	3.08

Table 4.2 Sectional properties of stiffened tube Sections

Group	**Specimens**	***B*** mm	***C*** mm	***t*** mm	***b*** mm	***c*** mm	b_s mm	t_s mm	b'_s mm	t'_s mm	***l*** mm	A_{stiff}/A_{tube}	I_s/I_{so}
Group I	S1-ST1	100	100	1.5	98.5	98.5	11.8	3.7	11.8	3.7	500	0.30	0.87
	S2-ST1	100	100	2.1	97.9	97.9	11.8	3.7	11.8	3.7	500	0.21	0.33
	S3-ST1	100	100	2.5	97.5	97.5	11.8	3.7	11.8	3.7	500	0.18	0.20
	S4-ST1	100	100	3.1	96.9	96.9	11.8	3.7	11.8	3.7	500	0.15	0.11
	R1-ST2	150	90	2.9	147.1	87.1	30	3.2	30	3.2	550	0.28	1.16
	R2-ST2	200	100	4.9	195.1	95.1	30	3.2	30	3.2	600	0.14	0.19
Group II	S1-ST2	100	100	1.5	98.5	98.5	30	3.2	30	3.2	500	0.65	12.41
	S2-ST2	100	100	2.1	97.9	97.9	30	3.2	30	3.2	500	0.47	4.68
	S3-ST2	100	100	2.5	97.5	97.5	30	3.2	30	3.2	500	0.39	2.87
	S4-ST2	100	100	3.1	96.9	96.9	30	3.2	30	3.2	500	0.32	1.63
	R1-ST2,3	150	90	2.9	147.1	87.1	40	5.2	30	3.2	550	0.45	4.47
	R2-ST2,3	200	100	4.9	195.1	95.1	40	5.2	30	3.2	600	0.21	0.72

"S", "R", and "ST" refer to square tube, rectangular tube, and stiffener respectively.

4.1.3 Mechanical Properties of Steel

Tensile test specimens were cut by electrical saw from the original members. Two tensile specimens for each type were tested and the average yield strength was used. For gradually yielding steel, yield strength at an offset strain of 0.2% was used. The length of these specimens was 600mm and the width was nearly 50mm. The average value of the modulus of elasticity in the elastic range for steel, E (estimated from test) is *200* GPa. Table 4.3 shows the result of tensile tests.

Table 4.3 Yield Stress of tested specimens.

Specimen	**Dimension of Section** mm	**Yield Stress** σ_y MPa
S1	100x100x1.5	281
S2	100x100x2.1	364
S3	100x100x2.5	376
S4	100x100x3.1	381
R1	150x90x2.9	404
R2	200x100x4.9	453
ST1	11.8x3.7	333
ST2	30x3.2	330
ST3	40x5.2	325

4.2 Test Rig

All tests were carried out in the Laboratory of Structures at Jordan University of Science and Technology. The stub columns were tested by incremental monotonic loading in a 2000 kN capacity M1000/RD universal testing machine from DARTIC Limited. A control and measurement cell attached to the testing machine capable of providing data about load, displacement, and control mode was used to collect the experimental data. Computer software was incorporated to read and store all measurements including strain gauges and LVDTs (Linear Variable Displacement

Transducers) readings. General view of the testing machine and the control cell is shown in Fig.4.3.

The yield stress of tensile test specimens was obtained by using 1200 kN capacity M2501 servo-hydraulic universal testing machine.

Fig.4.3 General view for the Testing Machine.

4.3 Instrumentation

The stub column specimens were instrumented to measure loads, vertical displacement, deflections, and strains.

4.3.1 Load and Vertical Displacement Measurements

The applied load and the corresponding vertical displacement were given directly by the data recorder of the control cell. Moreover, the applied load was also given as an output of the computer program together with other measurements.

4.3.2 Strain Measurements

Six specimens from group I were chosen and tested with strain measurements. The strains were measured by electrical strain gauges, PLS-10-11, with 10mm gauge length, 2.01 gauge factor, and 120±0.3Ω gauge resistance. Specimens S3-ST1 (A) and R2-ST2 (B) were tested with 4 strain gauges, whereas specimens S1-ST1 (A), S2-ST1 (B), S4-ST1 (A), and R1-ST2 (B) were tested with 3 strain gauges. All strain gauges were placed at midheight of the specimens and distributed at corners and at the stiffener-plate junctions. Two strain gauges were also placed on stiffeners.

4.4 Experimental Procedure

The stub column specimens were tested under a fixed condition. The load was applied to the specimens by rigid end plates, and increased gradually throughout the test until failure.

In order to obtain reliable results and obvious loading history, two control modes were used. Up to about 80% of the estimated ultimate load of each specimen, load control mode was used. For the remaining period of the test, displacement control mode was used.

Two rates of loading were used in the load control mode, 1.0 kN/sec and 0.5 kN/sec, depending upon the predicted strength of the specimen. The rate of

displacement in the displacement control mode was 0.01mm/sec for all specimens. Fig.4.4 shows test set-up and Figs.4.5 and 4.6 show specimens under test.

Fig.4.4 Test set-up

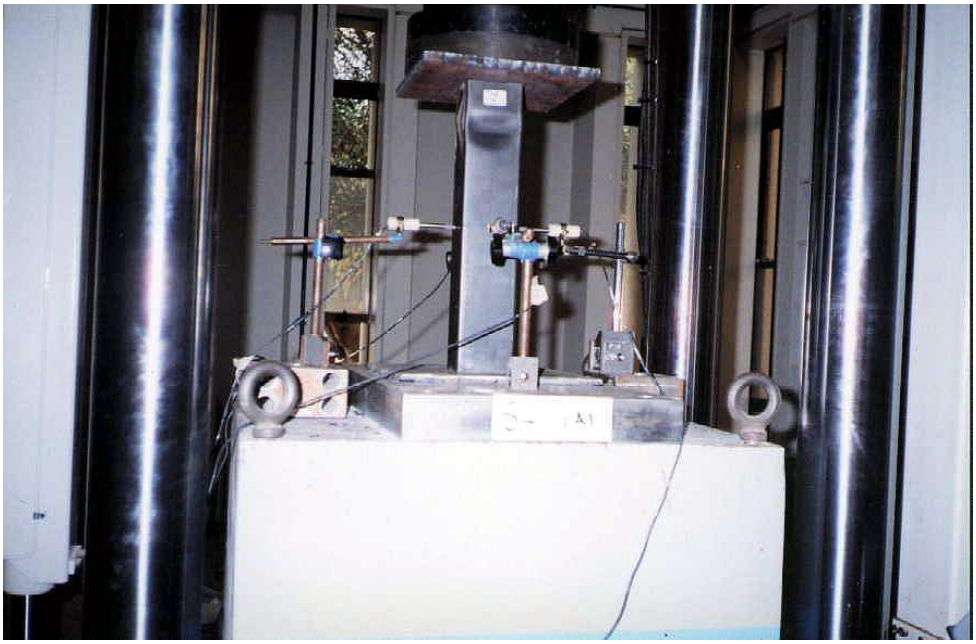

Fig.4.5 Specimen without stiffeners under test

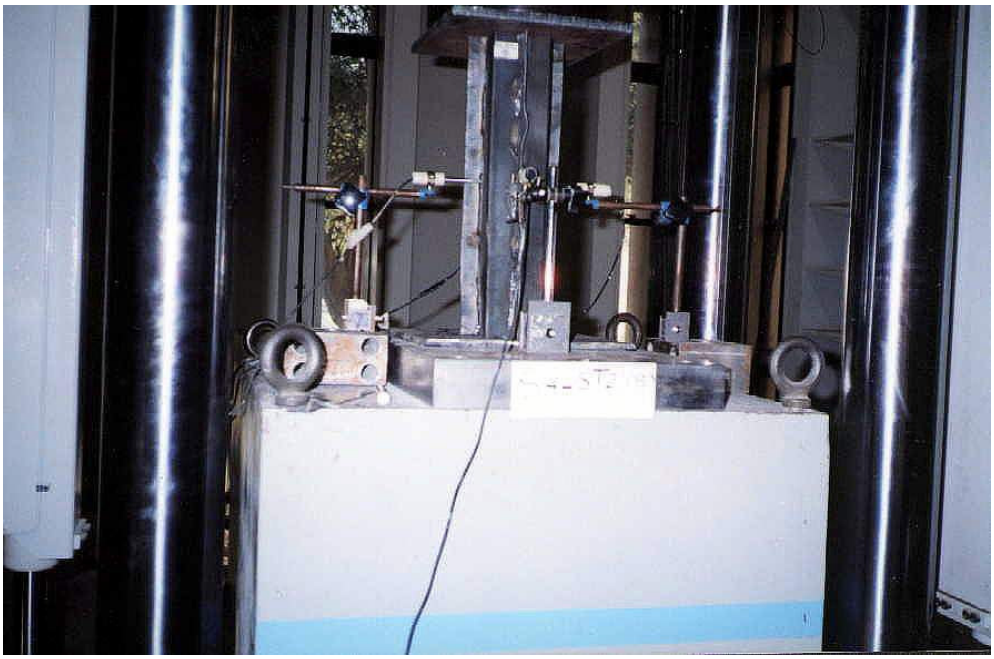

Fig.4.6 Specimen with stiffeners under test

Chapter 5

RESULTS AND DISCUSSION

In this chapter the behavior, the deformations, and the postbuckling strength of the tested stub columns will be presented and discussed. Furthermore, analytical manipulation of the experimental data will be conducted in order to formulate expressions for unstiffened and stiffened tubes, which predict the postbuckling strength as effective section formulas. These formulas will then be used to predict the interaction buckling of columns.

5.1 Behavior of tested stub columns

5.1.1 Unstiffened Square and Rectangular Tubes

In general, the stub columns exhibited a crippling failure. A plastic mechanism developed in the plate elements and the corners tended to crumple. The plastic zones were observed at the middle part for some stub columns and at the ends for other specimens.

The location of failure zones (severe distortions) depends on the location of weak points, initial imperfections, and the elastic buckles formed during the elastic loading range. Cutting the specimen from the original member may cause some initial

imperfection, which may be responsible for developing some plastic mechanism zones at the ends of the specimens. The main characteristic of failure was the shape of distortion in which two opposite sides deflected outward and the other two sides deflected inward. Figs.5.1 and 5.2 show the specimens after failure.

5.1.2 Stiffened Square and Rectangular Tubes

The stiffened specimens behaved as the tubes without stiffeners (described in the previous section). However, for most stub columns of this type, the plastic mechanism zones were observed between the junction of the stiffener and the corners and their size became limited. These failure zones were concentrated at the ends for most specimens and excessive waves in the stiffeners were also observed. Such behavior was resulting from stress concentration at the ends and the initial imperfections arising from the weld and was affected by the size of stiffeners. Figures 5.3 to 5.6 show the specimens after failure.

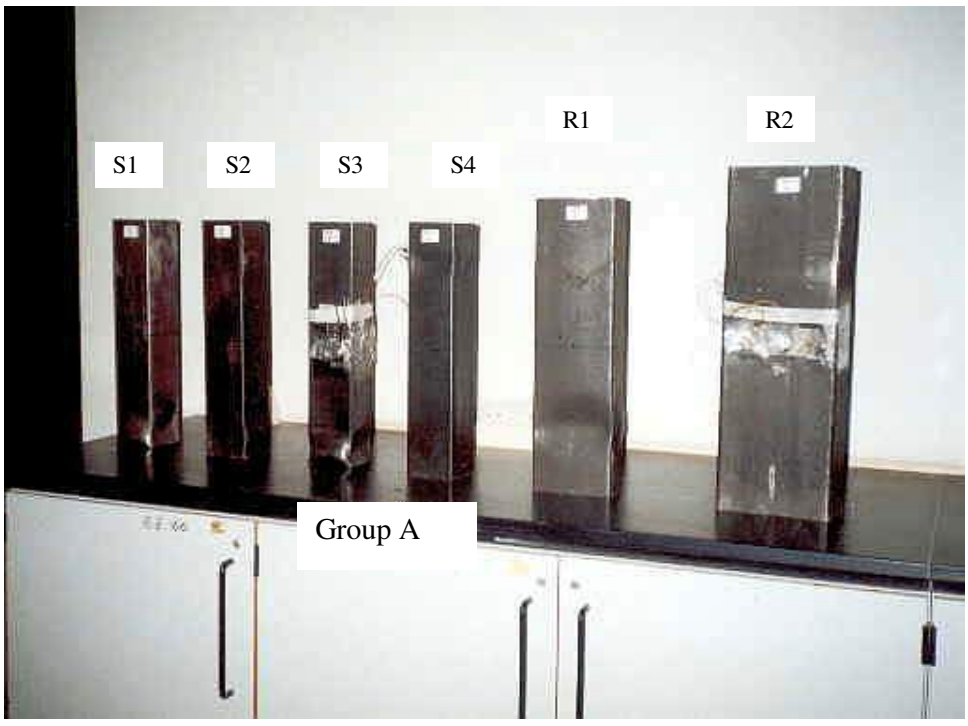

Fig.5.1 Unstiffened tubes after failure, Group A.

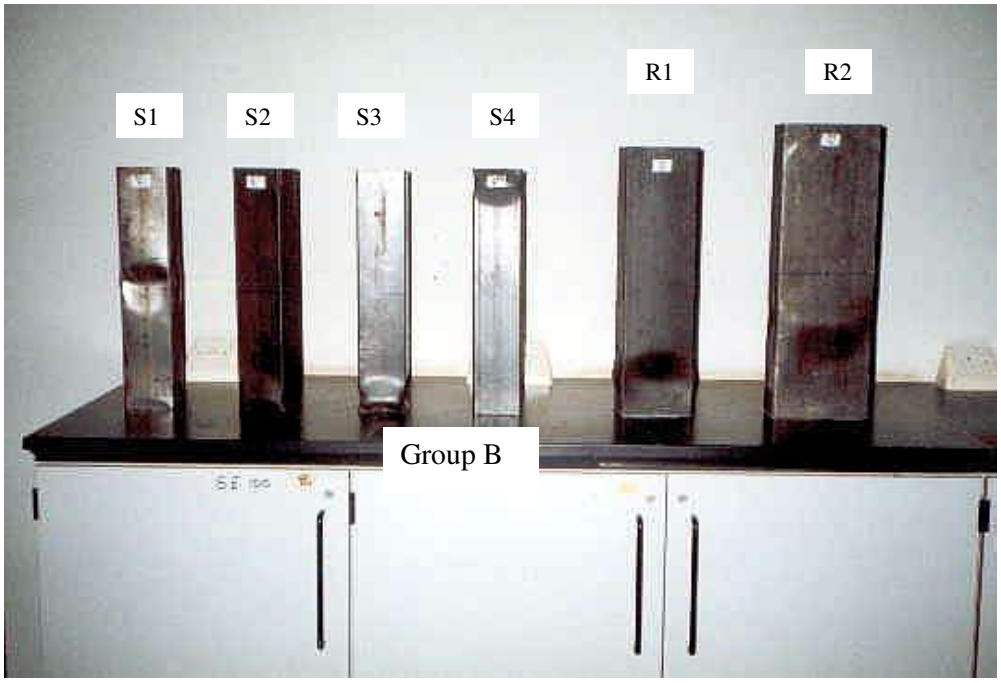

Fig.5.2 Unstiffened tubes after failure, Group B.

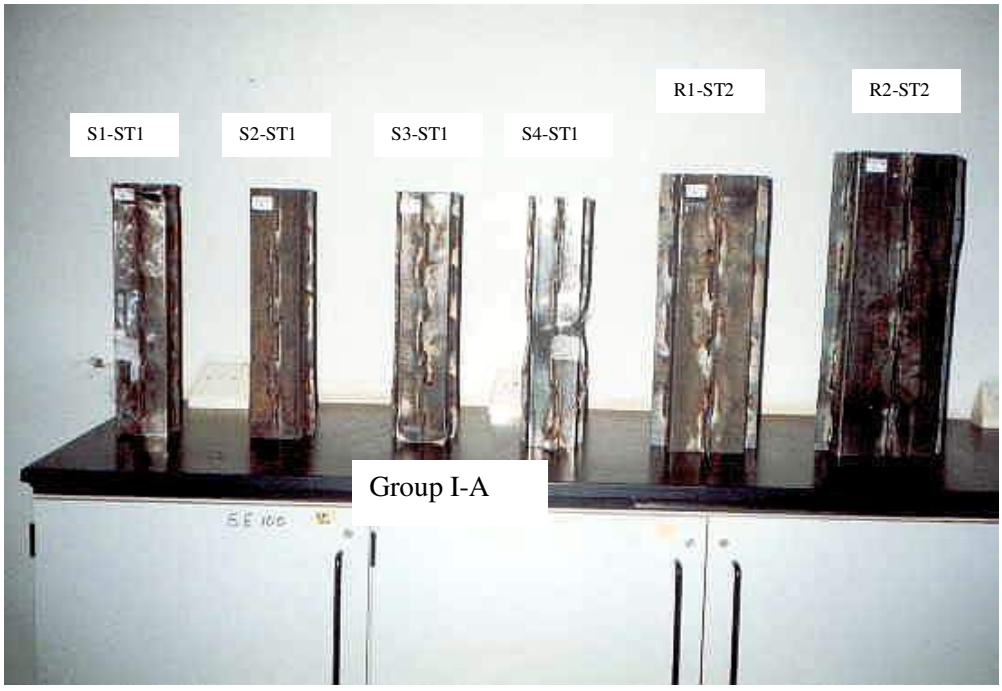

Fig.5.3 Stiffened tubes after failure, Group I-A.

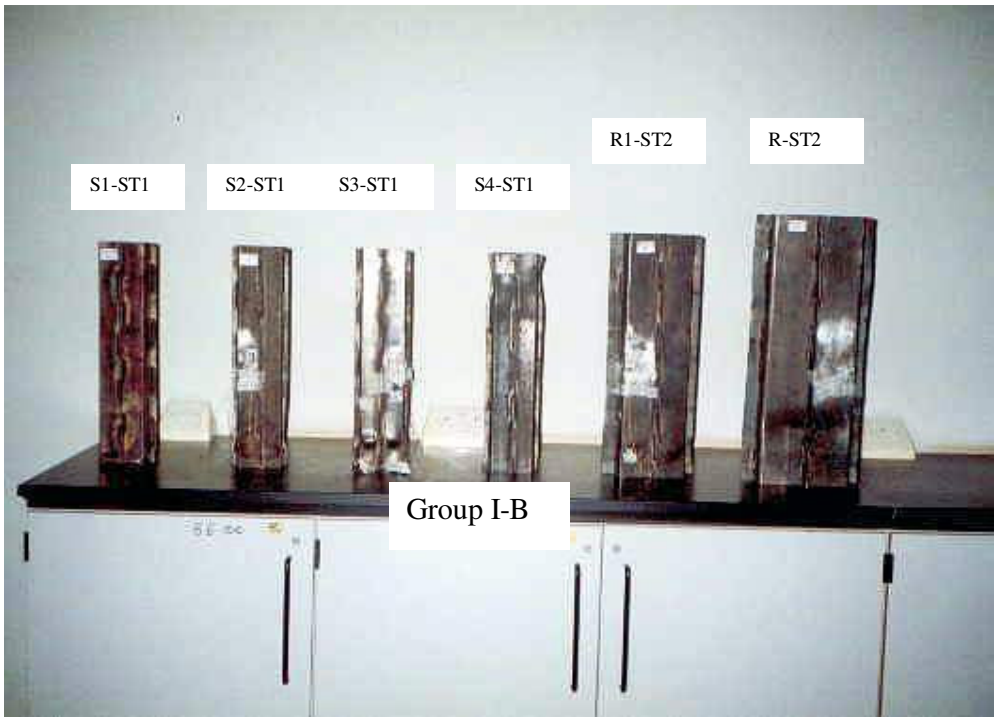

Fig.5.4 Stiffened tubes after failure, Group I-B.

Fig.5.5 Stiffened tubes after failure, Group II-A.

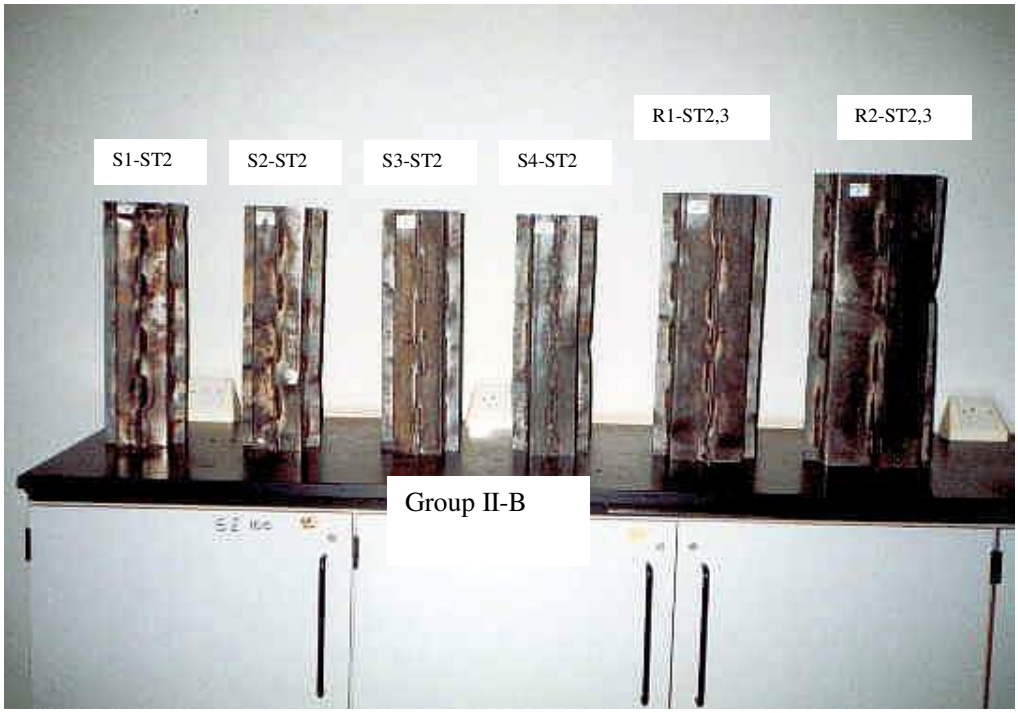

Fig.5.6 Stiffened tubes after failure, Group II-B.

5.2 Strains

Strain results for the six stub columns from Group I are shown in Figures 5.7 to 5.12 which represent the load in kN versus the μ–strain, ε ($x10^{-6}$). The yield strain was varied from 0.0015 to 0.0035.

The objective from using strain gauges in Group I is to check if the stiffeners of this group, which their sectional area is considered smaller compared to the section area of tubes than Group II, can carry stress effectively up to failure. In other words strain gauges were used to check if the stiffeners could be considered as a stiff support for the plate elements of the stub columns. Figures 5.7 to 5.12 show that the strains at the corners, stiffeners, and stiffener-plate junctions reach the yield strain, which means that the stiffeners were fully effective until failure as the corners. This result is very important in the derivation of the effective section for tubes with longitudinal stiffeners, Sec.5.4.

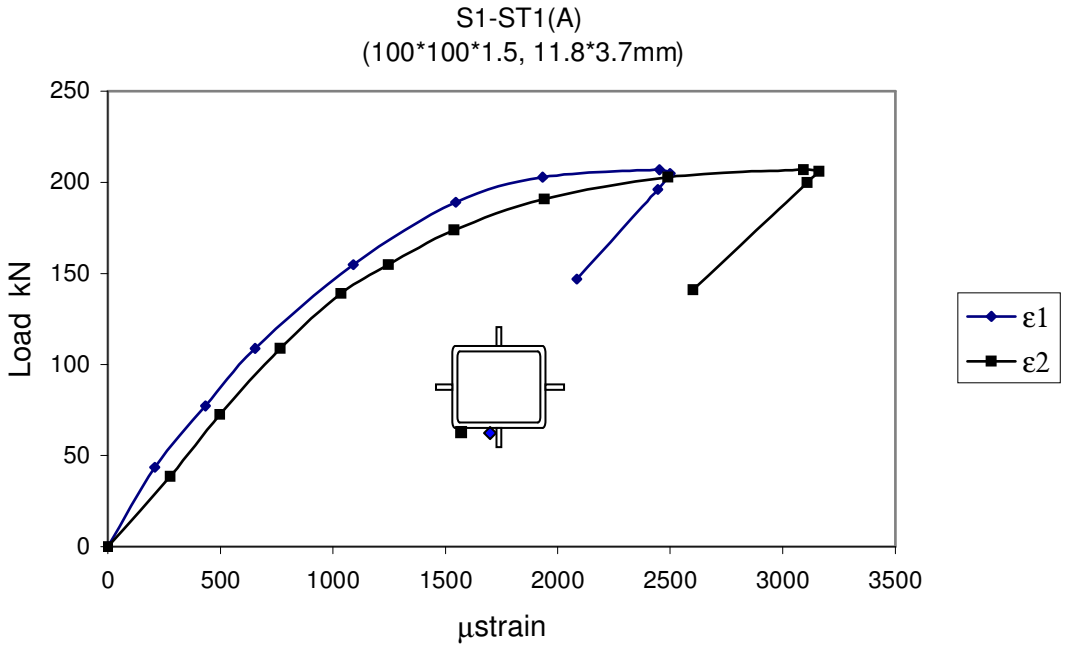

Fig.5.7 Strains in square stiffened tube S1-ST1 (A)

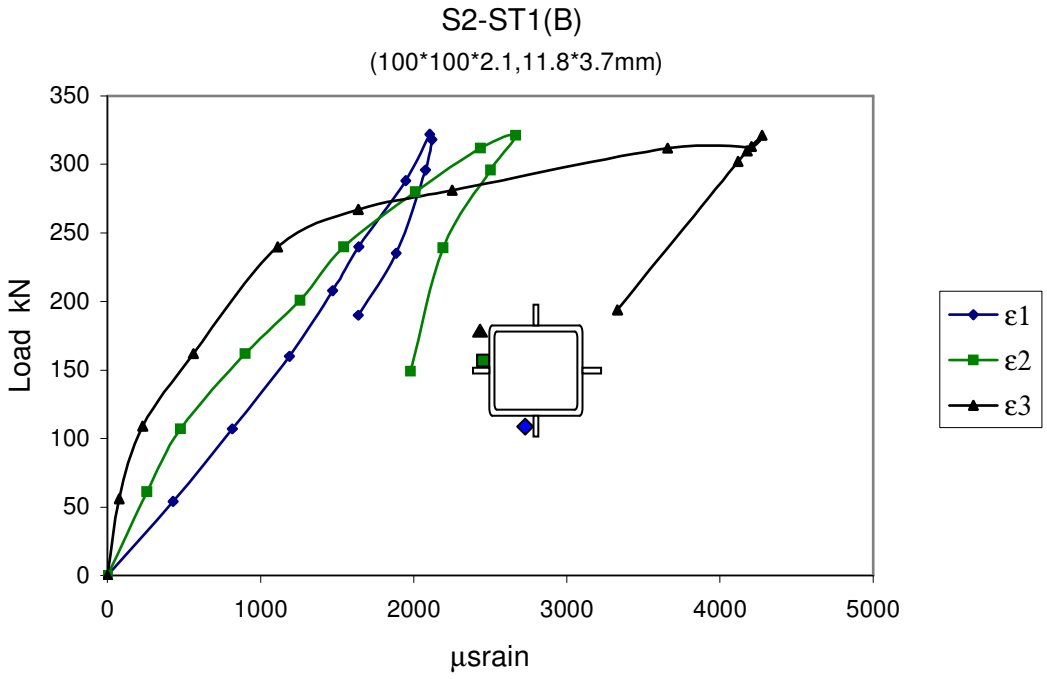

Fig.5.8 Strains in square stiffened tube S2-ST1 (B)

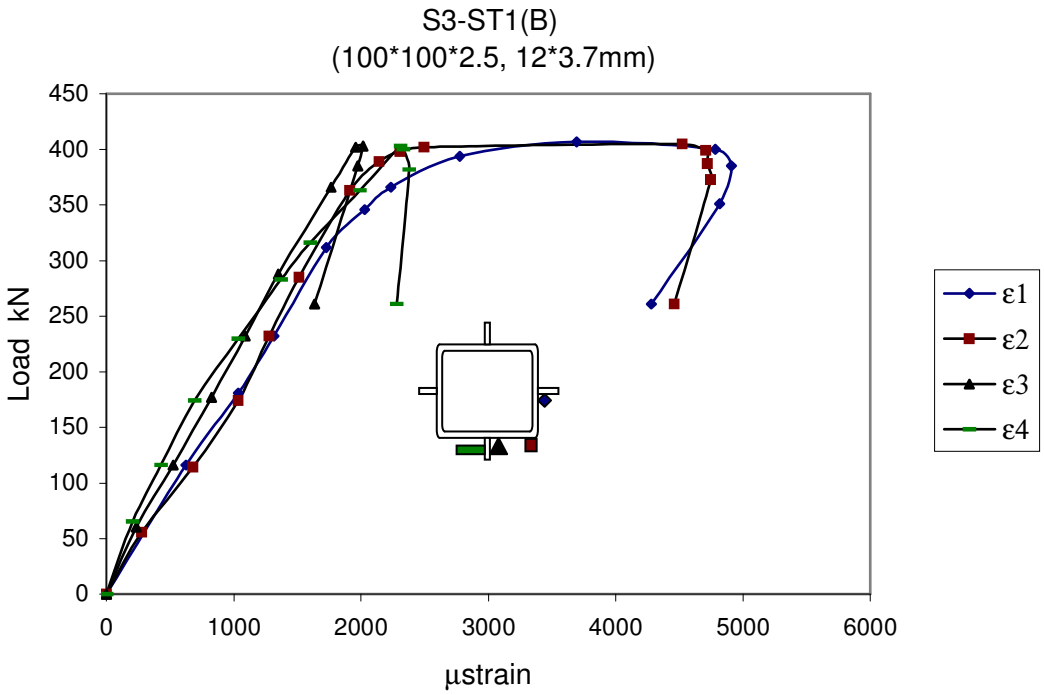

Fig.5.9 Strains in square stiffened tube S3-ST1 (B)

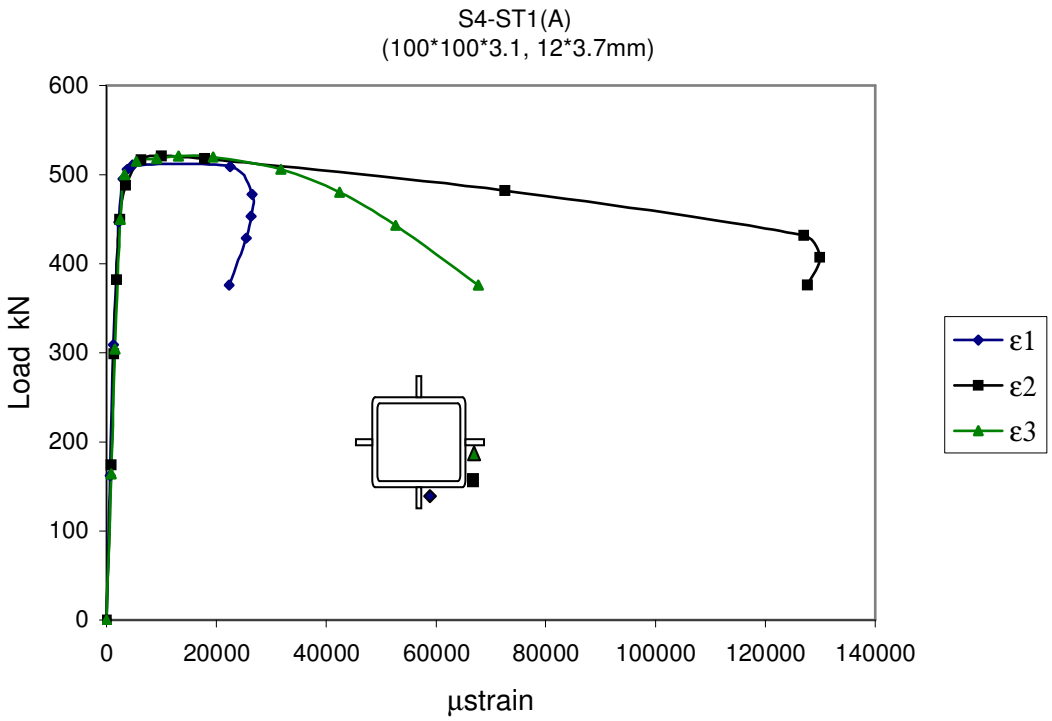

Fig.5.10 Strains in square stiffened tube S4-ST1 (A)

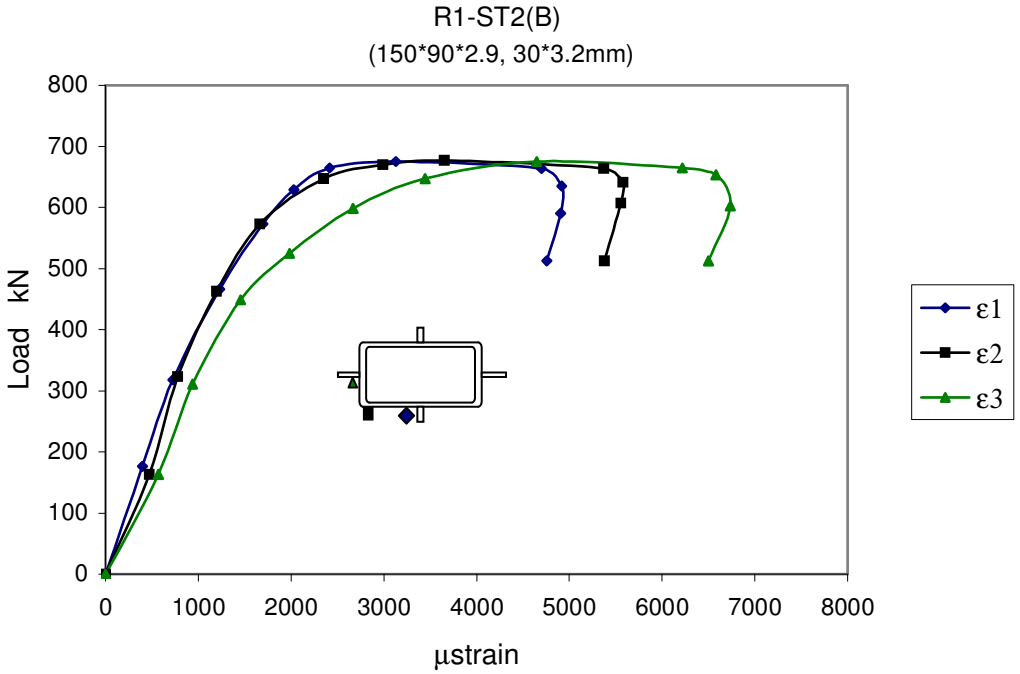

Fig.5.11 Strains in rectangular stiffened tube R1-ST2 (B)

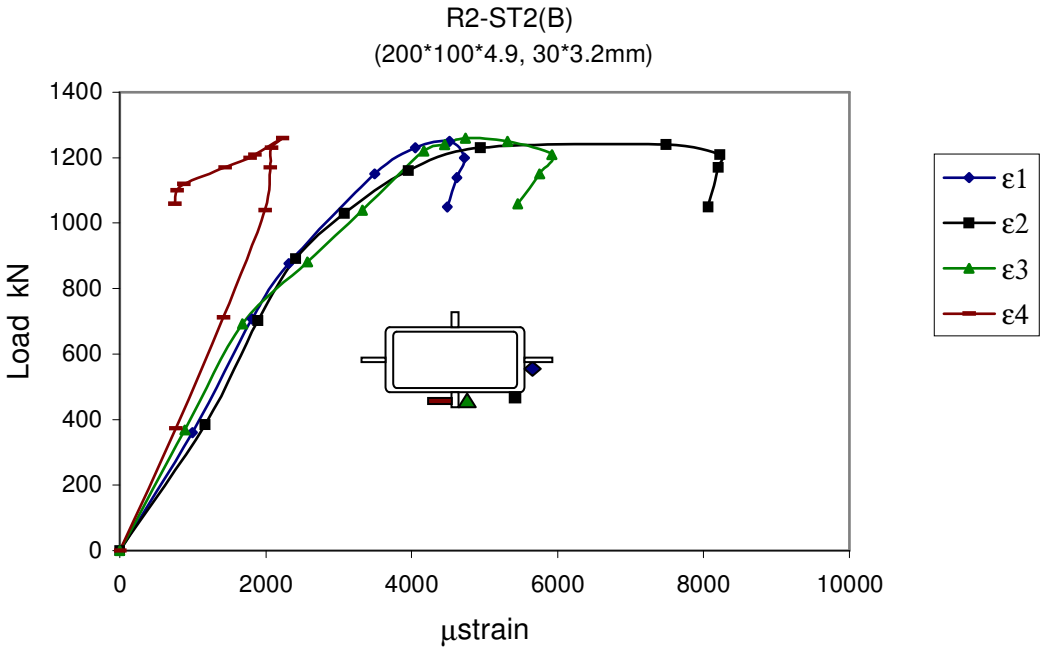

Fig.5.12 Strains in rectangular stiffened tube R2-ST2 (B)

5.3 Postbuckling Strength

5.3.1 Unstiffened Square and Rectangular Tubes

Failure loads of the tested stub columns together with loads predicted by Karman's and Winter's formulas, for a comparison, are shown in Table5.1. Buckling coefficients for the sections, obtained from Fig.3.3 for all formulas, were 4.0 for square sections and 5.0 and 5.2 for R1 and R2 respectively. It should be mentioned that buckling coefficients for rectangular sections are higher than those for square sections, which reflects the interaction between the plate elements of the sides of the rectangular sections. This mean that the short sides restrict the long sides to buckle freely and make some restraint at the corners which allow the plate elements of rectangular section to carry higher stress than square section even though they may have the same *b/t* ratio. Fig.5.13 represents the ratio of the ultimate stress on the total area and the yield stress, F_u/F_y, against the slenderness parameter, λ. This slenderness parameter, λ, was varied between 0.72 and 1.29 for the test specimens.

From Table 5.1 and Fig.5.13, it is obvious that Karman's equation (Eq.2.32), which is a theoretical equation, overestimates the postbuckling strength for plate elements with relatively higher differences from the test results. The ratio between the experimental postbuckling strength to that predicted by Karman's formula varies between 70% and 95%. Winter's equation (Eq.2.33) also slightly overestimates the postbuckling strength for most specimens, except R1, but with relatively lower differences. The ratio between the experimental postbuckling strength to that predicted by Winter's formula varies between 83% and 105%.

In fact, the differences between the test results and Winter's equation may be attributed to the manner of experimental testing (experimental procedure) and the sectional and the material properties. The effect of the experimental procedure can be explained by

reviewing other experimental studies, which investigate the behavior of plates through flexural tests.

5.3.2 Stiffened Square and Rectangular Tubes

Table 5.2 shows the experimental failure loads for the stub columns together with failure loads predicted by Karman's and Winter's formulas for Groups I and II. The load carried by the tube section alone was computed by subtracting the load carried by the four stiffeners, based on the assumption that the stiffeners were fully effective and carried their crushing load, from the total experimental failure load. Strain results verified that all stiffeners were fully effective until failure. Also Fig.5.14 shows the ratio of the ultimate stress on the total area and the yield stress, F_u/F_y, against the slenderness parameter, λ. This slenderness parameter, λ, was varied from 0.36 to 0.66 and buckling coefficients, k_b, were obtained from Eq. 2.43.

Comparisons given in Table5.2 and Fig.5.14 between the experimental failure loads with Karman's and Winter's equations show obviously that the later equations well predict the crushing loads for all specimens, which means that the plate elements were fully effective at failure. However, it is evident that some stub column plates were still not fully effective at failure. The ratio between the experimental postbuckling strength and that predicted by Karman's and Winter's formulas varies between 80% and 100%. Although some specimens, especially in Group I, did not achieve the ultimate strength, their postbuckling strength well improved with different ratios.

Initial imperfections and residual stresses resulted from welding and stress concentration at the specimens' ends may be responsible for the lower strengths for this type of stub columns.

Other comparisons for the postbuckling strength of sections for all cases of side stiffening (no stiffeners, stiffeners in Group I, and stiffeners in Group II) are shown in Table 5.3 and Fig. 5.15. The results given in Table 5.3 and Fig. 5.15 clearly indicate the change in the postbuckling strength of tubes. Fig.5.15 represents the ratio of the load carried by tube sections alone for all cases using the average load of specimens A and B to the crushing load, $(P_u)_{tube}/P_y$, against the ratio of moment of inertia of the stiffeners to the forth order power of the tube thickness, I_s/t^4. It is observed from Fig.5.15 that the higher improvement in the postbuckling strengths occurs for tubes having higher width/thickness ratios.

5.3.3 Stiffener Efficiency

Postbuckling strengths of the stiffened tubes, the section of the tube alone, are also compared with the unstiffened tubes to observe the improvement in the strength. Table 5.4 shows the ratio of the maximum load carried by the stiffened tubes, $(P_u)_{st}$, to the maximum load carried by the unstiffened tubes, $(P_u)_{unst}$. The loads in the table are the average of loads of specimen A and B for each section. From the comparison, it can be seen that stiffened tubes were capable of supporting between 161% and 108% of the loads carried by unstiffened tubes.

The ratio of $(P_u)_{st}/(P_u)_{unst}$,as a percentage, is drawn versus the ratio of the sectional area of stiffeners and tubes in Fig.5.16 as well as the linear trend lines for Groups I and II. It is obviously observed from the slops of the two lines (Fig.5.16) that the strengths of specimens of Group I reach higher value even though the stiffeners were lighter. Moreover, no improvement in stiffening effect was obtained through the heavier stiffeners and the lighter stiffeners were sufficient to produce optimum effect and, therefore, the lighter stiffeners are more efficient. All the previous observations also can be shown in Table 5.3 and Fig. 5.15.

Table5.1 Test results of stub columns of unstiffened tube sections.

Specimen	Section dimensions mm	Buckling coefficient k	Yield strength F_y MPa	Slenderness parameter λ	From test		Karman's Eq.		Winter's Eq.	
					Max. Load kN	F_u/F_y	Max. Load kN	F_u/F_y	Max. Load kN	F_u/F_y
S1-A	100x100x1.5	4	281	1.29	92	0.55	128	0.77	107	0.64
S1-B	100x100x1.5	4	281	1.29	93	0.56	128	0.77	107	0.64
S2-A	100x100x2.1	4	364	1.05	189	0.63	286	0.96	226	0.75
S2-B	100x100x2.1	4	364	1.05	187	0.62	286	0.96	226	0.75
S3-A	100x100x2.5	4	376	0.89	300	0.82	367	1.00	310	0.85
S3-B	100x100x2.5	4	376	0.89	298	0.81	367	1.00	310	0.85
S4-A	100x100x3.1	4	381	0.72	434	0.95	458	1.00	442	0.97
S4-B	100x100x3.1	4	381	0.72	431	0.94	458	1.00	442	0.97
R1-A	150x90x2.9	5	404	1.07	427	0.78	512	0.93	407	0.74
R1-B	150x90x2.9	5	404	1.07	419	0.76	512	0.93	407	0.74
R2-A	200x100x4.9	5.2	453	0.87	1056	0.82	1288	1.00	1103	0.86
R2-B	200x100x4.9	5.2	453	0.87	1072	0.83	1288	1.00	1103	0.86

Table5.2 Test results of stub columns of stiffened tube sections, Group I and II.

Specimens	Section dimensions		Buckling coefficient k_b	Yield stress for tube F_y MPa	Slenderness parameter λ	Yield stress for stiff. F_{ystif} MPa	From Test				Karman's Eq.		Winter's Eq.	
	Tube mm	Stiffeners mm					Max. Load, *Pu* kN	Max. Load for stiff. *Pu(stiff)* kN	Max. Load for tube *Pu(tube)* kN	Fu/Fy (tube)	Max. Load for tube *Pu(tube)* kN	*Fu/Fy* (tube)	Max. Load for tube *Pu(tube)* kN	*Fu/Fy* (tube)
S1-ST1A	100x100x1.5	11.8x3.7	15.2	281	0.66	333	209	58	151	0.91	166	1.0	166	1.0
S1-ST1B	100x100x1.5	11.8x3.7	15.2	281	0.66	333	206	58	148	0.89	166	1.0	166	1.0
S2-ST1A	100x100x2.1	11.8x3.7	10.9	364	0.63	333	321	58	263	0.88	299	1.0	299	1.0
S2-ST1B	100x100x2.1	11.8x3.7	10.9	364	0.63	333	325	58	267	0.89	299	1.0	299	1.0
S3-ST1A	100x100x2.5	11.8x3.7	9.4	376	0.58	333	417	58	359	0.98	367	1.0	367	1.0
S3-ST1B	100x100x2.5	11.8x3.7	9.4	376	0.58	333	410	58	352	0.96	367	1.0	367	1.0
S4-ST1A	100x100x3.1	11.8x3.7	8.1	381	0.51	333	526	58	468	1.02	458	1.0	458	1.0
S4-ST1B	100x100x3.1	11.8x3.7	8.1	381	0.51	333	525	58	467	1.02	458	1.0	458	1.0
R1-ST2A	150x90x2.9	30x3.2	20	404	0.54	330	691	127	564	1.03	549	1.0	549	1.0
R1-ST2B	150x90x2.9	30x3.2	20	404	0.54	330	628	127	501	0.91	549	1.0	549	1.0
R2-ST2A	200x100x4.9	30x3.2	11.9	453	0.58	330	1280	127	1153	0.90	1288	1.0	1288	1.0
R2-ST2B	200x100x4.9	30x3.2	11.9	453	0.58	330	1274	127	1147	0.89	1288	1.0	1288	1.0
S1-ST2A	100x100x1.5	30x3.2	16	281	0.65	330	259	127	132	0.80	166	1.0	166	1.0
S1-ST2B	100x100x1.5	30x3.2	16	281	0.65	330	277	127	150	0.90	166	1.0	166	1.0
S2-ST2A	100x100x2.1	30x3.2	16	364	0.52	330	398	127	271	0.91	299	1.0	299	1.0
S2-ST2B	100x100x2.1	30x3.2	16	364	0.52	330	402	127	275	0.92	299	1.0	299	1.0
S3-ST2A	100x100x2.5	30x3.2	16	376	0.44	330	501	127	374	1.02	367	1.0	367	1.0
S3-ST2B	100x100x2.5	30x3.2	16	376	0.44	330	500	127	373	1.02	367	1.0	367	1.0
S4-ST2A	100x100x3.1	30x3.2	16	381	0.36	330	604	127	477	1.04	458	1.0	458	1.0
S4-ST2B	100x100x3.1	30x3.2	16	381	0.36	330	604	127	477	1.04	458	1.0	458	1.0
R1-ST2,3A	150x90x2.9	40x5.2, 30x3.2	20	404	0.54	325	747	198	549	1.00	549	1.0	549	1.0
R1-ST2,3B	150x90x2.9	40x5.2, 30x3.2	20	404	0.54	325	757	198	559	1.02	549	1.0	549	1.0
R2-ST2,3A	200x100x4.9	40x5.2, 30x3.2	18.4	453	0.46	325	1357	198	1159	0.90	1288	1.0	1288	1.0
R2-ST2,3B	200x100x4.9	40x5.2, 30x3.2	18.4	453	0.46	325	1458	198	1260	0.98	1288	1.0	1288	1.0

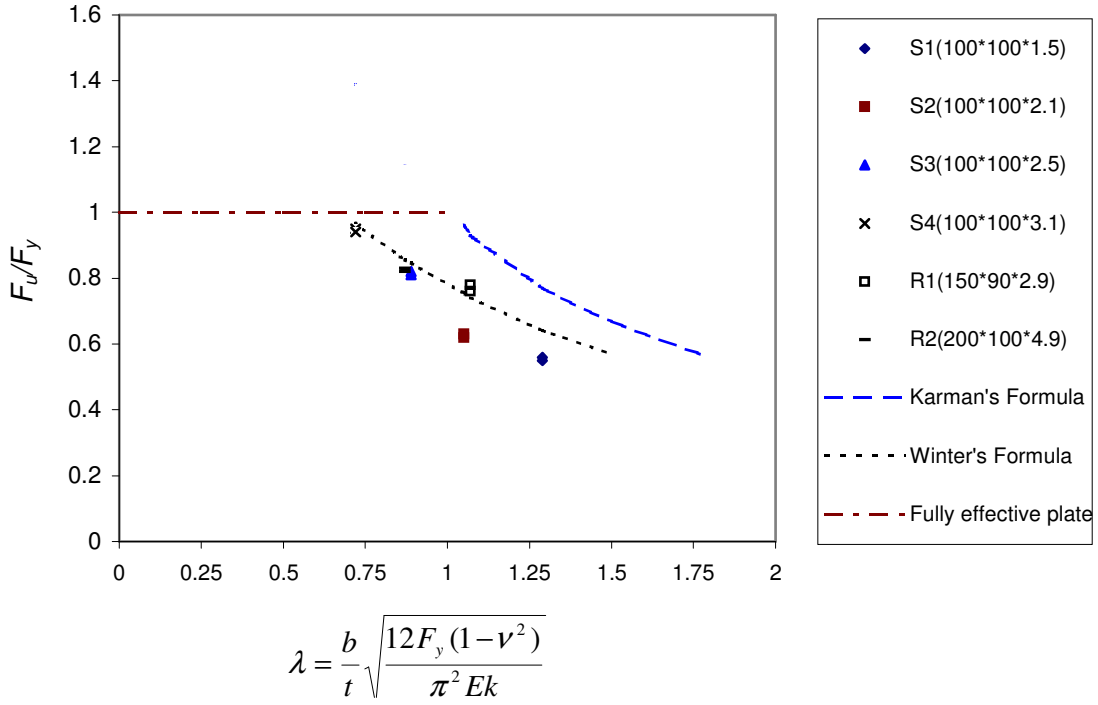

Fig.5.13 Test results of postbuckling strength of plate elements of unstiffened tubes.

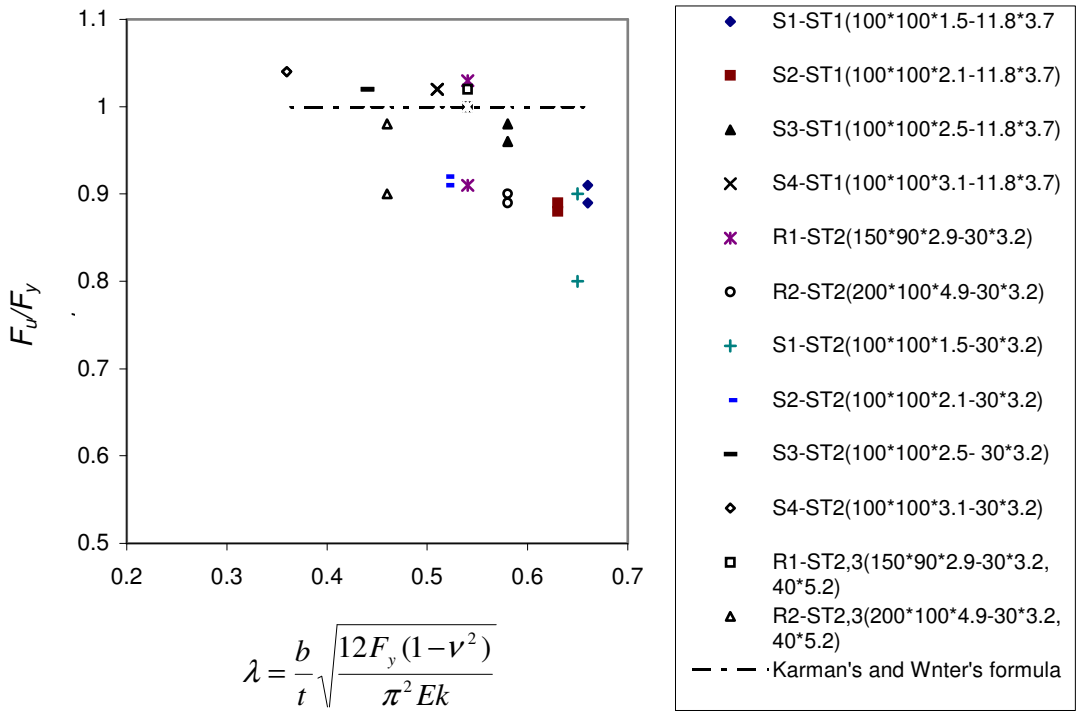

Fig.5.14 Test results of postbuckling strength of plate elements of stiffened tubes.

Table 5.3 Postbuckling strength of tube sections for all cases of stiffening.

Group	Specimens	Section dimensions		$(P_u)_{tube}$ kN	F_y MPa	A_{tube} mm^2	P_y kN	$(P_u)_{tube}/P_y$	I_s/t^4
		Tube mm	Stiffeners mm						
No stiffener	S1	100x100x1.5	-	92.5	281	591	166.1	0.56	0
	S2	100x100x2.1	-	188	364	822.36	299.3	0.63	0
	S3	100x100x2.5	-	299	376	975	366.6	0.82	0
	S4	100x100x3.1	-	432.5	381	1201.56	457.8	0.94	0
	R1	150x90x2.9	-	423	404	1358.36	548.8	0.77	0
	R2	200x100x4.9	-	1064	453	2843.96	1288.3	0.83	0
Group I	S1-ST1	100x100x1.5	11.8x3.7	149.3	281	591	166.1	0.90	100
	S2-ST1	100x100x2.1	11.8x3.7	264.8	364	822.36	299.3	0.88	26
	S3-ST1	100x100x2.5	11.8x3.7	355.3	376	975	366.6	0.97	13
	S4-ST1	100x100x3.1	11.8x3.7	467.3	381	1201.56	457.8	1.02	5
	R1-ST2	150x90x2.9	30x3.2	532.8	404	1358.36	548.8	0.97	102
	R2-ST2	200x100x4.9	30x3.2	1150.3	453	2843.96	1288.3	0.89	12
Group II	S1-ST2	100x100x1.5	30x3.2	141.3	281	591	166.1	0.85	1422
	S2-ST2	100x100x2.1	30x3.2	273.3	364	822.36	299.3	0.91	370
	S3-ST2	100x100x2.5	30x3.2	373.8	376	975	366.6	1.02	184
	S4-ST2	100x100x3.1	30x3.2	477.3	381	1201.56	457.8	1.04	78
	R1-ST2,3	150x90x2.9	40x5.2, 30x3.2	554.4	404	1358.36	548.8	1.01	392
	R2-ST2,3	200x100x4.9	40x5.2, 30x3.2	1209.9	453	2843.96	1288.3	0.94	48

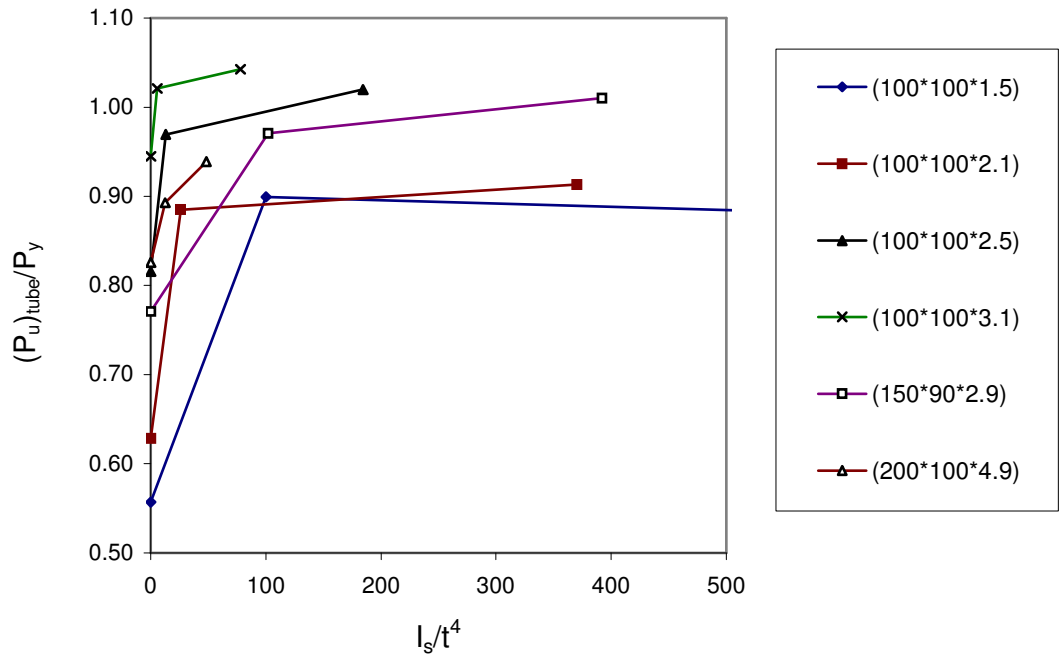

Fig.5.15 Postbuckling strength of tube sections for all cases of stiffening.

Table5.4 Comparison of postbuckling strength of unstiffened and stiffened stub column tube sections.

Group	Specimens	Max load carried by unstiff. tube $(P_u)_{unst}$ kN	Max load carried by stiff. tube $(P_u)_{st}$ kN	$(P_u)_{st}/(P_u)_{unst}$ %	A_{stiff}/A_{tube} %	I_s/I_{so}
Group I	S1-ST1	92.5	149.3	161	30	0.87
	S2-ST1	188	264.8	141	21	0.33
	S3-ST1	299	355.3	119	18	0.20
	S4-ST1	432.5	467.3	108	15	0.11
	R1-ST2	423	532.8	126	28	1.16
	R2-ST2	1064	1150.3	108	14	0.19
Group II	S1-ST2	92.5	141.3	153	65	12.41
	S2-ST2	188	273.3	145	47	4.68
	S3-ST2	299	373.8	125	39	2.87
	S4-ST2	432.5	477.3	110	32	1.63
	R1-ST2,3	423	554.4	131	45	4.47
	R2-ST2,3	1064	1209.9	114	21	0.72

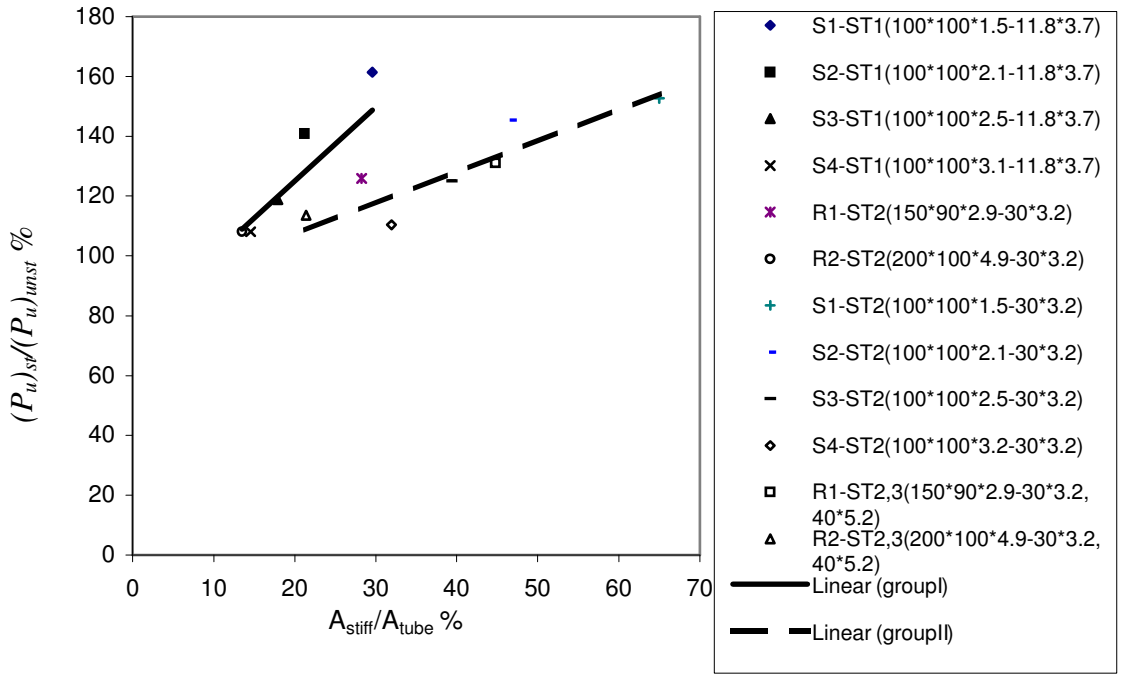

Fig.5.16 Efficiency of stiffeners in Groups I and II of stiffened tubes.

5.4 Proposed Effective Width Equations

It was observed from the test results that Winter's equation slightly overestimates the postbuckling strength for most stiffened and unstiffened tested stub columns tubes which may yield incorrect estimates for the strength of columns having the same cross sections. Therefore compact effective section formulas, for both types, based on the test results will be derived which take into account the interaction between plate elements of the sections and yield the entire effective section directly.

Regressions analysis for the data obtained from tests was conducted using the SPSS-10 Program, which proved to be a powerful tool in data analysis.

5.4.1 Unstiffened Square and Rectangular Tubes

For regression analysis purpose, the compact form for effective section, which is similar to Eq. 2.20, can be expressed as follows:

$$\frac{F_u}{F_y} = \frac{A_e}{A} = \frac{C_1}{\lambda} \tag{5.1}$$

where

C_1 nondimensional constant obtained by regression analysis.

A_e effective area.

A total area of section.

λ slenderness parameter of plate.

F_u ultimate stress on total area.

F_y yield stress.

Non-linear regression analysis was conducted to determine C_1 from the data presented in Table 5.1 for λ and F_u/F_y. The result is C_1=0.714 with 84% for the coefficient of determination, R^2. Substituting C_1 into Eq.5.1 to obtain:

$$\frac{A_e}{A} = \frac{0.714}{\lambda} \tag{5.2}$$

Substituting λ into Eq.5.2, using $\nu=0.3$, the proposed equation can be expressed as follows:

$$\frac{A_e}{A} = \frac{0.68}{(b/t)}\sqrt{\frac{kE}{\sigma_y}} \qquad \leq 1 \tag{5.3}$$

Prior to failure, the yield stress at the edges is replaced by σ_e and Eq.5.3 can be written as:

$$A_e = A\left(\frac{0.68}{(b/t)}\sqrt{\frac{kE}{\sigma_e}}\right) \tag{5.4}$$

where

b/t maximum width/thickness ratio of the plate in the cross section.

k buckling stress coefficient determined from Fig.3.3.

A special case can be considered when the tube is square and the widths of all plate elements are equal with $k=4.0$. For this case Eqs. 5.3 and 5.4 can be written as:

$$\frac{b_e}{b} = \frac{1.36}{(b/t)}\sqrt{\frac{E}{\sigma_y}} \qquad \leq 1 \tag{5.5}$$

$$b_e = 1.36t\sqrt{\frac{E}{\sigma_e}} \tag{5.6}$$

For a given yield stress the plate element remains fully effective up to failure, if the ratio *b/t* is below a limiting value. This limiting value, $(b/t)_{lim}$, can be obtained by setting ,in Eq.5.3, the ratio of A_e/A equal to 1.0. Therefore Eq. 5.3 yields:

$$\left(\frac{b}{t}\right)_{\lim} = 0.68\sqrt{\frac{kE}{\sigma_y}} \tag{5.7}$$

The corresponding limiting slenderness parameter is λ_{lim} =0.714 (from Eq.5.2).

Table5.5 shows the postbuckling strength as predicted by Eq.5.3 and the discrepancy from test results, which varied between –9.5% and 14.3%. Fig.5.17 also represents the postbuckling strength curve predicted by Eq. 5.3 and other curves plotted by Karman's and Winter's formulas as well as the test results.

It is observed from the curve that for the range of slenderness parameter, λ, from 1.29 to 0.769, the postbuckling strength predicted by Eq.5.3 is relatively lower than that predicted by Winter's formula. Moreover, for the range of slenderness parameter, λ, from 0.769 to 0.72 the postbuckling strength predicted Eq.5.3 is relatively higher than that predicted by Winter's formula.

Another comparison between the experimental data and Winter's formula was conducted using non-linear regression analysis for Winter's equation form, Eq.2.33, as follows:

$$\frac{F_u}{F_y} = \frac{A_e}{A} = \frac{1}{\lambda}\left(1 - \frac{C_2}{\lambda}\right) \tag{5.8}$$

where

C_2 nondimensional constant obtained by regression analysis.

Using the data presented in Table 5.1 for λ and F_u/F_y, the result of the regression analysis is: $C_2=0.25$ with 81% for the coefficient of determination, R^2, whereas the value of C_2 in Winter's equation is 0.22. It is worth mentioning that the value of C_2 in the oldest version of winter's Equation before 1968 was 0.25 (Galambos, 1998), which is the same value of the coefficient of C_2 that obtained in this study.

5.4.2 Stiffened Square and Rectangular Tubes

The postbuckling strength measured by testing this type of stub columns, for the tube section alone, were relatively scattered (Fig.5.14). The best fit for the test results was obtained by adding a constant coefficient to Eq.5.1. Therefore Non-linear regression analysis was conducted for the following form:

$$\frac{F_u}{F_y} = \frac{A_e}{A} = \frac{C_3}{\lambda} + C_4 \qquad (5.9)$$

where

C_3 and C_4 nondimensional constants obtained by regression analysis.

Using the data presented in Table 5.2 for λ and F_u/F_y, the result is: C_3=0.128 and C_4=0.706 with 46% for the coefficient of determination, R^2. Substituting C_3 and C_4 into Eq.5.9 to obtain:

$$\frac{A_e}{A} = \frac{0.128}{\lambda} + 0.706 \qquad (5.10)$$

Substituting λ into Eq.5.10, using ν=*0.3,* the proposed equation can be expressed as follows:

$$\frac{A_e}{A} = \frac{0.122}{(b/t)}\sqrt{\frac{k_b E}{\sigma_y}} + 0.706 \qquad \leq 1 \qquad (5.11)$$

Prior failure, the yield stress at the edges is replaced by σ_e and Eq.5.11 can be written as

$$A_e = A\left(\frac{0.122}{(b/t)}\sqrt{\frac{k_b E}{\sigma_e}} + 0.706\right) \qquad (5.12)$$

where

b/t maximum width/thickness ratio of the total plate width, *b*, in cross-section.

k_b buckling stress coefficient of the total plate width, *b*, determined from Eqs.2.42 and 2.43.

The limiting value of fully effective plate can be obtain from Eq. 5.11 which yields:

$$\left(\frac{b}{t}\right)_{\lim} = 0.415\sqrt{\frac{k_b E}{\sigma_y}} \qquad (5.13)$$

The corresponding limiting slenderness parameter is λ_{lim} =0.435 (from Eq.5.10).

Table5.6 shows the postbuckling strength load predicted by Eq.5.11 and the discrepancy from the test results, which varied between -13.4% and 8.3%. Fig.5.18 also shows the postbuckling strength curve predicted by Eq. 5.11 together with the test results.

5.4.3 Characteristics of the Proposed Equations

Unstiffened square and rectangular tube sections

The characteristics of Eqs.5.3 and 5.4 can be summarized as follows:

- Their form is shorter than Winter's formula.
- Utilizing the interaction between the plate elements in rectangular sections where buckling coefficient will be more than 4.0 (for uniform section thickness), whereas the AISC equation (Eq.3.36) uses 4.0 for all cases.
- Computing the entire effective section directly, whereas in the AISC equation it needs to add the effective width for each side independently.

Stiffened square and rectangular tube sections

Eqs.5.11 and 5.12 have the same characteristics as the previous equations (5.3 and 5.4) and additional advantageous can be summarized as follows:

- They allow the designer to predict the postbuckling strength for tube sections having stiffeners that are not stipulated in the AISC specification.
- They allow the designer to predict the postbuckling strength for tube sections having lighter stiffeners less than that are recommended in the AISI specification.

Table5.5 Postbuckling strength according to the proposed equation for unstiffened tubes, Eq.5.3.

Specimen	Dimensions mm	From Test		Eq.5.3		Discrepancy %
		Max. load P_u kN	F_u/F_y	Max. load P_u kN	F_u/F_y	
S1-A	100x100x1.5	92	0.55	91.8	0.55	0.3
S1-B	100x100x1.5	93	0.56	91.8	0.55	1.3
S2-A	100x100x2.1	189	0.63	204.7	0.68	-8.3
S2-B	100x100x2.1	187	0.62	204.7	0.68	-9.5
S3-A	100x100x2.5	300	0.82	294.8	0.80	1.7
S3-B	100x100x2.5	298	0.81	294.8	0.80	1.1
S4-A	100x100x3.1	434	0.95	456.4	1.00	-5.2
S4-B	100x100x3.1	431	0.94	456.4	1.00	-5.9
R1-A	150x90x2.9	427	0.78	366.0	0.67	14.3
R1-B	150x90x2.9	419	0.76	366.0	0.67	12.6
R2-A	200x100x4.9	1056	0.82	1054.2	0.82	0.2
R2-B	200x100x4.9	1072	0.83	1054.2	0.82	1.7

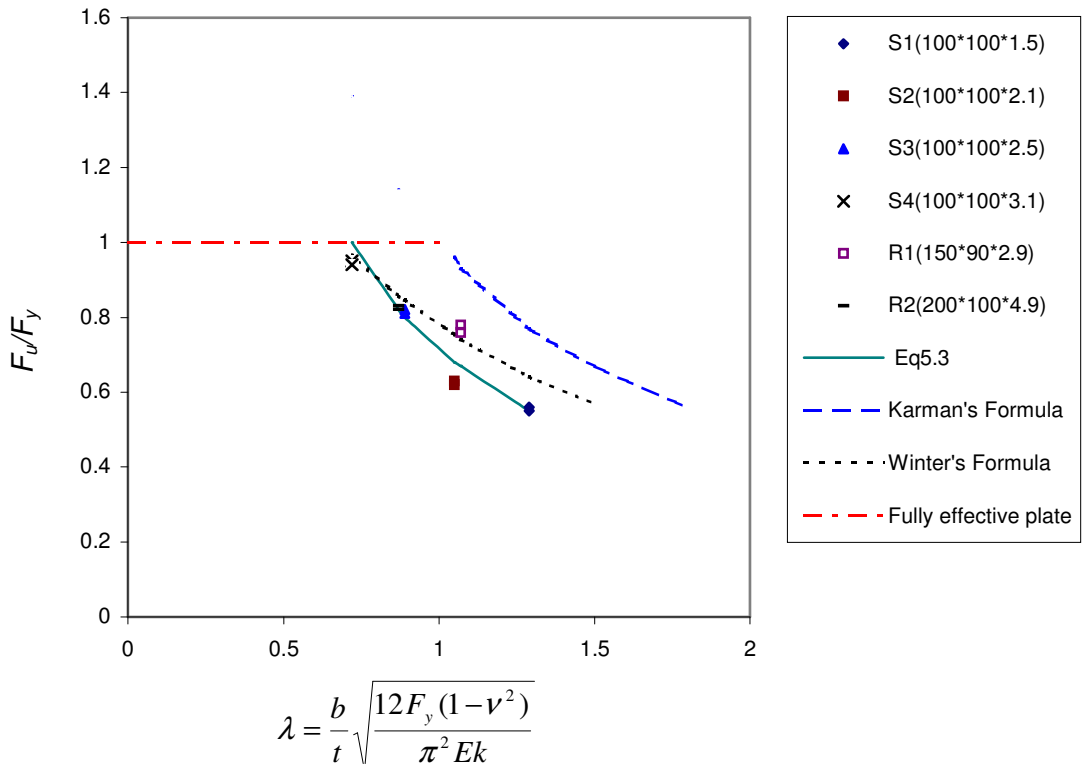

Fig5.17 Postbuckling strength according to the proposed equation for unstiffened tubes.

Table5.6 Postbuckling strength according to the proposed equation for stiffened tubes, Eq.5.11.

Specimen	Section dimensions		From Test		Eq.5.11		Discrepancy %
	Tube mm	stiffeners mm	Max. load, $P_{u,}$ kN	F_u/F_y	Max. load P_u kN	F_u/F_y	
S1-ST1A	100x100x1.5	11.8x3.7	150.8	0.91	149.5	0.900	0.9
S1-ST1B	100x100x1.5	11.8x3.7	147.8	0.89	149.5	0.900	-1.1
S2-ST1A	100x100x2.1	11.8x3.7	262.8	0.88	272.2	0.909	-3.5
S2-ST1B	100x100x2.1	11.8x3.7	266.8	0.89	272.2	0.909	-2.0
S3-ST1A	100x100x2.5	11.8x3.7	358.8	0.98	339.7	0.927	5.3
S3-ST1B	100x100x2.5	11.8x3.7	351.8	0.96	339.7	0.927	3.4
S4-ST1A	100x100x3.1	11.8x3.7	467.8	1.02	438.1	0.957	6.4
S4-ST1B	100x100x3.1	11.8x3.7	466.8	1.02	438.1	0.957	6.2
R1-ST2A	150x90x2.9	30x3.2	564.3	1.03	517.5	0.943	8.3
R1-ST2B	150x90x2.9	30x3.2	501.3	0.91	517.5	0.943	-3.2
R2-ST2A	200x100x4.9	30x3.2	1153.3	0.90	1193.9	0.927	-3.5
R2-ST2B	200x100x4.9	30x3.2	1147.3	0.89	1193.9	0.927	-4.1
S1-ST2A	100x100x1.5	30x3.2	132.3	0.80	149.9	0.903	-13.4
S1-ST2B	100x100x1.5	30x3.2	150.3	0.90	149.9	0.903	0.2
S2-ST2A	100x100x2.1	30x3.2	271.3	0.91	285.0	0.952	-5.1
S2-ST2B	100x100x2.1	30x3.2	275.3	0.92	285.0	0.952	-3.5
S3-ST2A	100x100x2.5	30x3.2	374.3	1.02	365.5	0.997	2.4
S3-ST2B	100x100x2.5	30x3.2	373.3	1.02	365.5	0.997	2.1
S4-ST2A	100x100x3.1	30x3.2	477.3	1.04	486.0	1.062	-1.8
S4-ST2B	100x100x3.1	30x3.2	477.3	1.04	486.0	1.062	-1.8
R1-ST2,3A	150x90x2.9	40x5.2, 30x3.2	549.4	1.00	517.5	0.943	5.8
R1-ST2,3B	150x90x2.9	40x5.2, 30x3.2	559.4	1.02	517.5	0.943	7.5
R2-ST2,3A	200x100x4.9	40x5.2, 30x3.2	1159.4	0.90	1268.0	0.984	-9.4
R2-ST2,3B	200x100x4.9	40x5.2, 30x3.2	1260.4	0.98	1268.0	0.984	-0.6

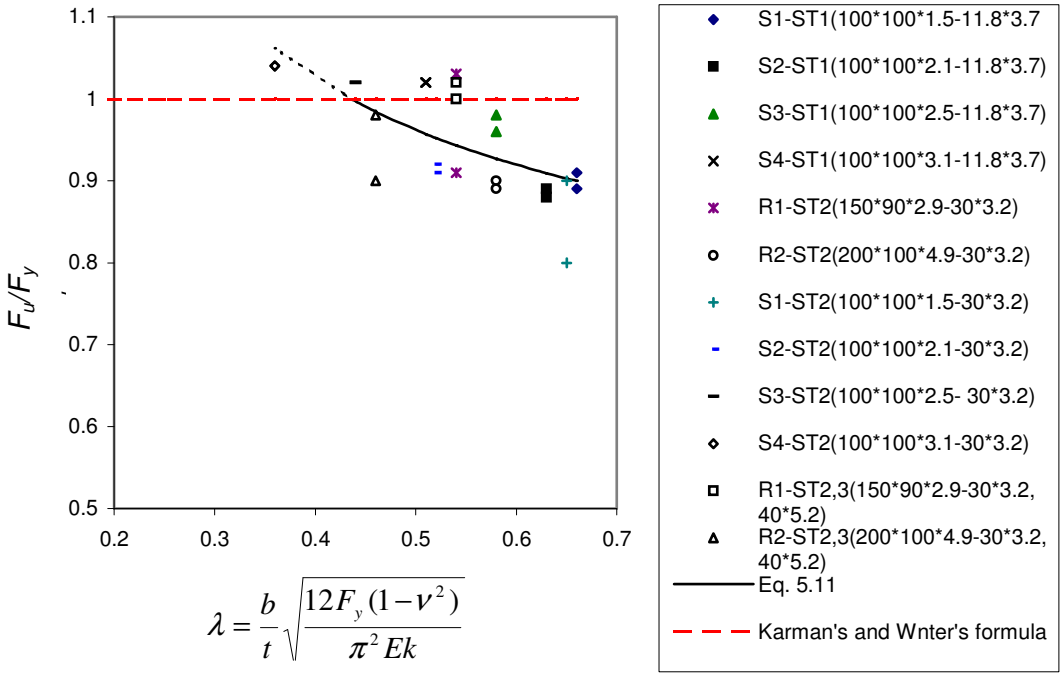

Fig5.18 Postbuckling strength according to the proposed equation for stiffened tubes.

5.5 Interaction of Local and Overall Flexural Buckling

The column strength equations presented by the ASIC specifications, the ASD and the LRFD, were adjusted to take into account the reduction of stiffness due to local buckling. In order to predict the interaction strength for columns having the same sections, Eqs.5.4 and 5.12, which give the effective section when the stress at the edges of plate elements is less than or equal to the yield stress, were used. The procedure and equations outlined in Sec.3.2.2 will be used to construct the column strength curves.

5.5.1 Strength of Unstiffened Tubular Columns

The column strength equations presented by the ASD specification were adjusted twice to take into account the local buckling of the plate elements. The first modification was using the proposed effective section equation (Eq.5.4) and the second one was using the effective width equation presented in the AISC specification (Eq.5.36). This was done also for the column strength equations presented by the LRFD specification. For comparison, the strength of columns, in which no local buckling will occur, was computed by the ASD and the LRFD equations.

Figures 5.19 to 5.23 represent the ratio of the average stress to the yield stress, F_{av}/F_y, versus the slenderness parameter of columns, λ_c, for the sections S1, S2, S3, R1, and R2. The strength curve of section S4 is not shown because the section is not affected by local buckling, and thus it is considered fully effective until failure. It is observed from the figures that for sections having plate elements with relatively higher width/thickness ratio, b/t, the interaction begins at a relatively lower stress. When the width/thickness ratio, b/t, decreases and approaches $(b/t)_{lim}$, the interaction begins at relatively higher stress and the ratio F_{av}/F_y approaches 1.0.

It is also observed that for column sections with plate elements with relatively lower slenderness parameter, λ, the differences between the proposed interaction strength and that proposed by the AISC specifications become smaller. This is because the AISC effective width expression was essentially adjusted from Winter's formula, which yields postbuckling strength close to that obtained by Eq.5.3 at relatively lower λ ratios. This observation is clearly shown from the ratio of $Q_{AISC}/Q_{Eq.5.3}$ in Table 5.7.

5.5.2 Strength of Stiffened Tubular Columns

Most of the stub column sections of Group II were fully effective up to failure while the sections of Group I were partially effective at failure and local buckling occurred at relatively higher stresses. Therefore, the procedure presented in the previous section was followed to account for the interaction buckling for columns having the sections of Group I using the proposed effective section equation for stiffened tube sections (Eq.5.12).

Figures 5.24 to 5.28 show the interaction strength curves for columns having sections S1-ST1, S2-ST1, S3-ST1, R1-ST2, and R2-ST2. The strength obtained from the curves is assigned for the tubes alone. The total strength can be obtained by adding the strength of the stiffeners.

In fact, no reference in the AISC specifications for compressed plate elements supported laterally by stiffeners. The effective width equations presented in the specifications (Eq.3.36) is applicable for thin plate element supported laterally by stiff supports. Therefore, no comparison is made for interaction strengths, and only the interaction strength for columns using Eq.5.12 is presented together with the strength curve in which no local buckling take place. Furthermore, the moments of inertia of the

stiffeners, I_s, for Group I are below values recommended by AISI specification. Thus the strength of the columns cannot even be compared with the AISI specification.

5.5.3 Strength Reduction Factor, *Q*

The reduction coefficient, $Q=A_e/A=F_{av}/F_y$, for the cross sectional area at zero length of column in which $F_{av}=F_u$ for the proposed strength (Eqs.5.3 and 5.11) is shown in Tables 5.7 and 5.8 for unstiffened and stiffened tubes respectively. Only the sections that are shown in the strength column curves are presented in these tables. For rectangular sections, the proposed equations yield the factor Q directly, whereas in the AISC it needs to compute this factor for each side independently from Eq.3.36 and add these together to get Q. The short sides of rectangular sections shown in the curves are fully effective because their width/thickness ratios are less than the limiting values and their sectional properties were computed based on this assumption. For comparison, the strength reduction factor, Q, predicted by the AISC specifications for unstiffened tubes is presented in Table 5.7. It is important to note that the strength reduction factor Q for the ASD is equal to the LRFD because they use the same effective width equation.

5.5.4 Single Column Strength Curve

A single column strength curve for all sections can be developed using a fictitious yield stress, QF_y, instead of the real material yield stress, F_y. The strength reduction factor, Q, proposed in this study or that computed according to the AISC specifications may be used to obtain the strength of tubular columns. Fig.5.29 represents the reduced strength ratio, F_{av}/QF_y, versus the modified slenderness parameter, $\sqrt{Q}\,\lambda_c$, for the column. The ASD and LRFD equations are used in this figure. It is observed from all column strength curves that the ASD equations yield higher strength (17% increase) than the LRFD equations.

Table 5.7 Reduction factor, Q, for unstiffened tubes.

Section	Dimensions mm	Yield stress F_y MPa	b/t	Slenderness parameter of plate λ	Reduction factor, Q		$Q_{AISC}/Q_{Eq.5.3}$
					Eq.5.3	AISC	
S1	100x100x1.5	281	65.7	1.29	0.55	0.66	1.20
S2	100x100x2.1	364	46.6	1.05	0.68	0.78	1.15
S3	100x100x2.5	376	39.0	0.89	0.80	0.88	1.10
R1	150x90x2.9	404	50.7	1.07	0.67	0.81	1.21
R2	200x100x4.9	453	39.8	0.87	0.82	0.87	1.06

Table 5.8 Reduction factor, Q, for stiffened tubes.

Section	Dimensions mm	Yield stress F_y MPa	b/t	Slenderness parameter of plate λ	Reduction factor, Q Eq.5.11
S1-ST1	100x100x1.5-11.8x3.7	281	65.7	0.66	0.90
S2-ST1	100x100x2.1-11.8x3.7	364	46.6	0.63	0.91
S3-ST1	100x100x2.5-11.8x3.7	376	39.0	0.58	0.93
R1-ST2	150x90x2.9-30x3.2	404	50.7	0.54	0.94
R2-ST2	200x100x4.9-30x3.2	453	39.8	0.58	0.93

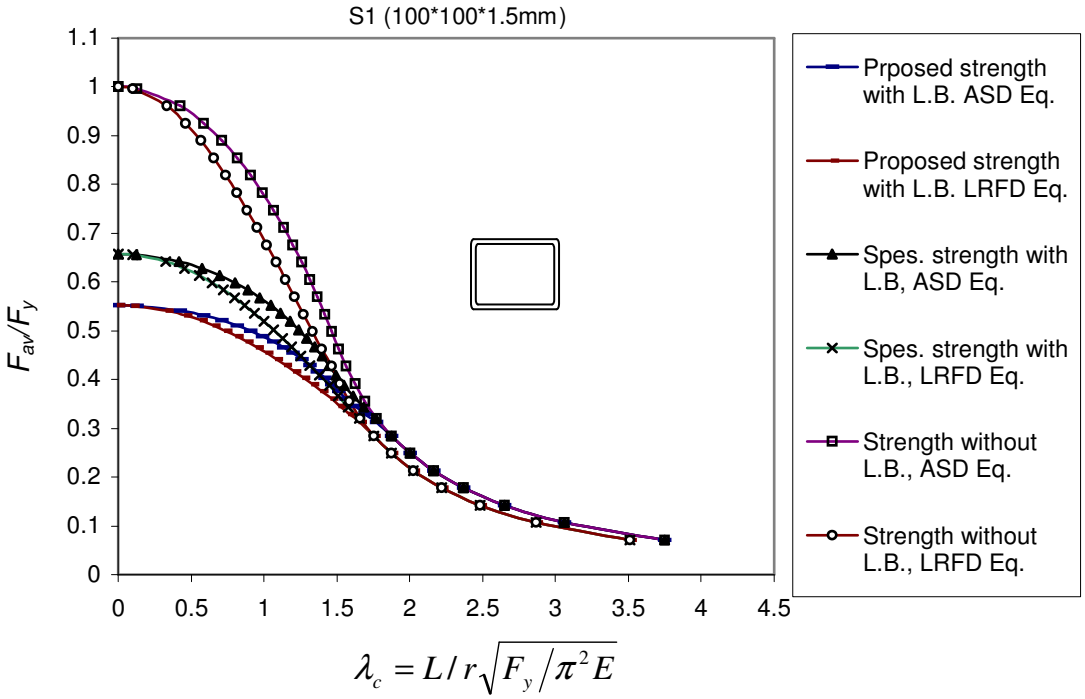

Fig.5.19 Column strength curve of section S1 (100x100x1.5mm)

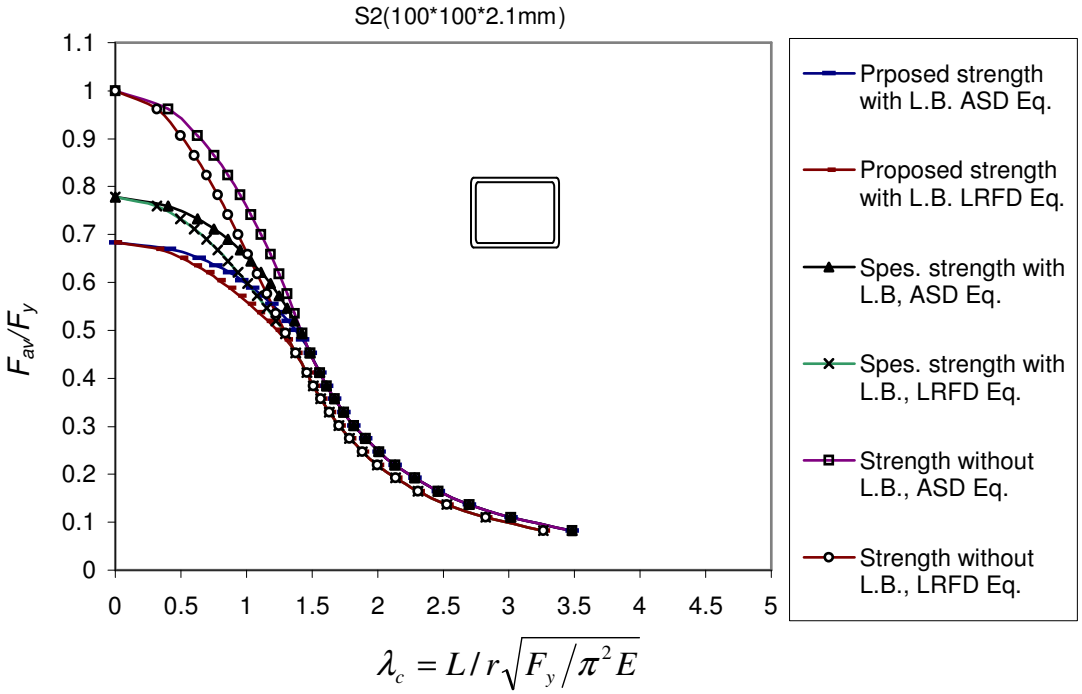

Fig.5.20 Column strength curve of section S2 (100x100x2.1mm)

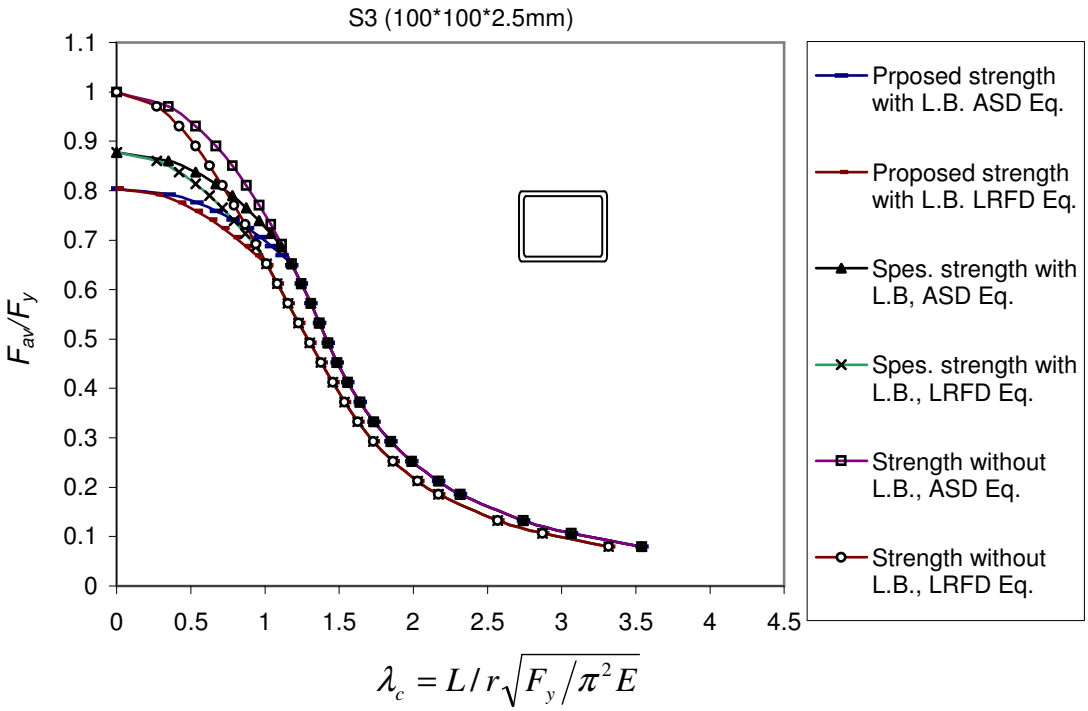

Fig.5.21 Column strength curve of section S3 (100x100x2.5mm)

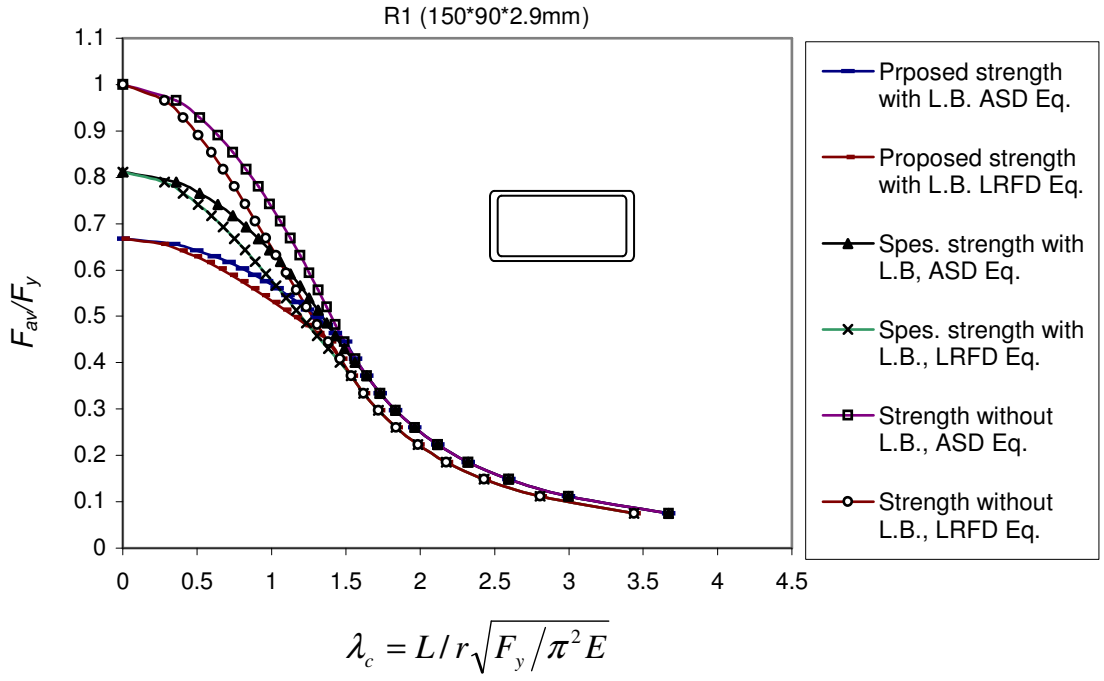

Fig.5.22 Column strength curve of section R1 (150x90x2.9mm)

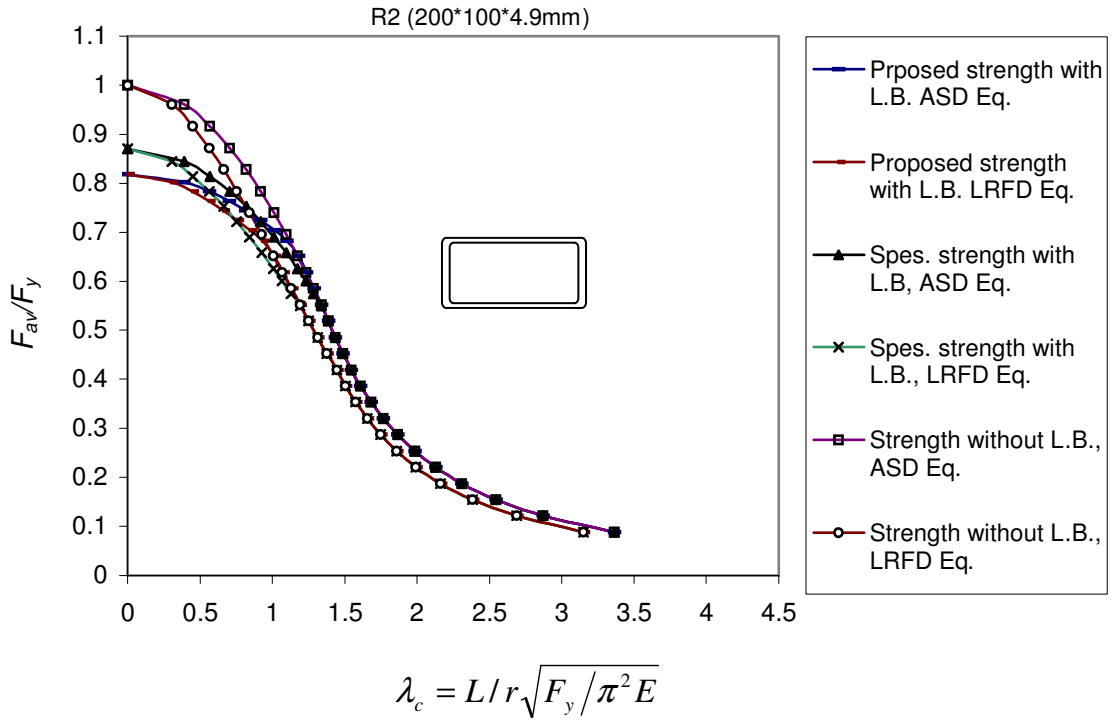

Fig.5.23 Column strength curve of section R2 (200x100x4.9mm)

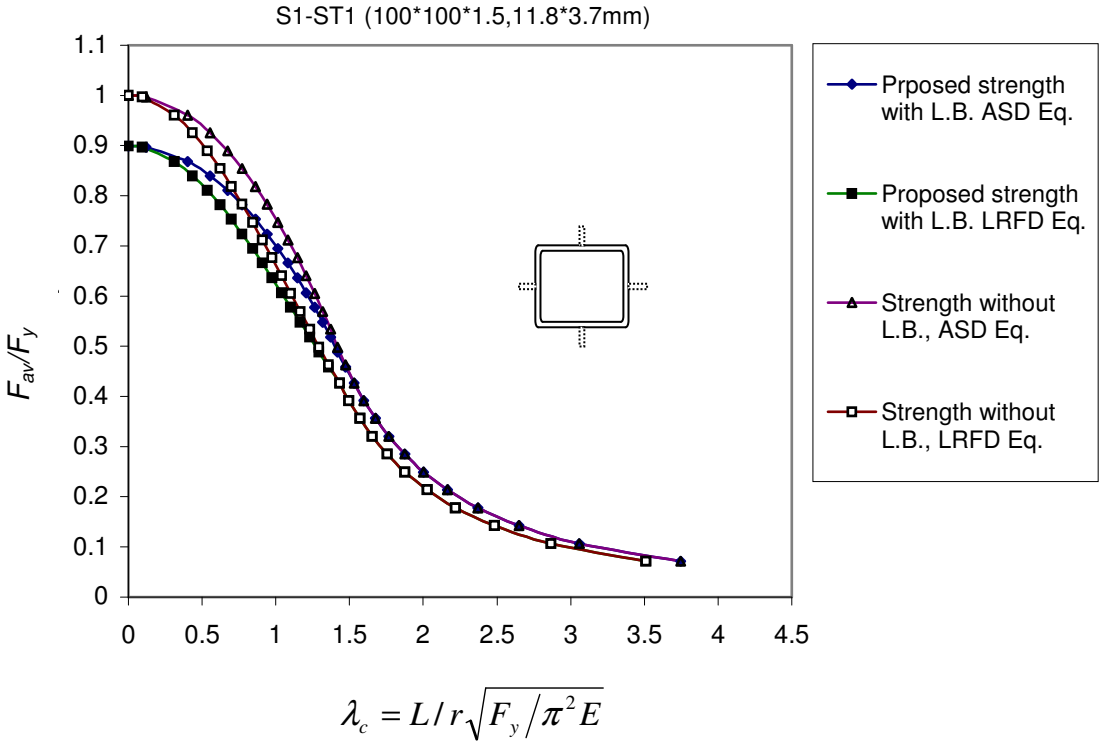

Fig.5.24 Column strength curve of section S1-ST1 (100x100x1.5, 11.8x3.7 mm)

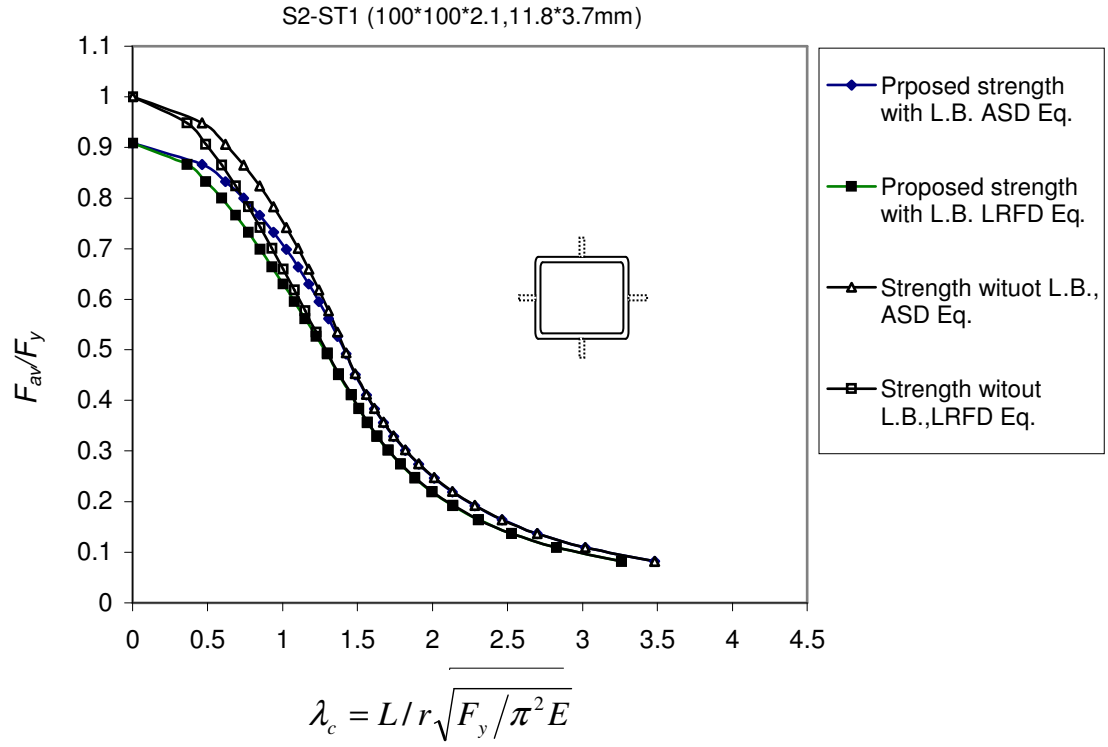

Fig.5.25 Column strength curve of section S2-ST1 (100x100x2.1, 11.8x3.7 mm)

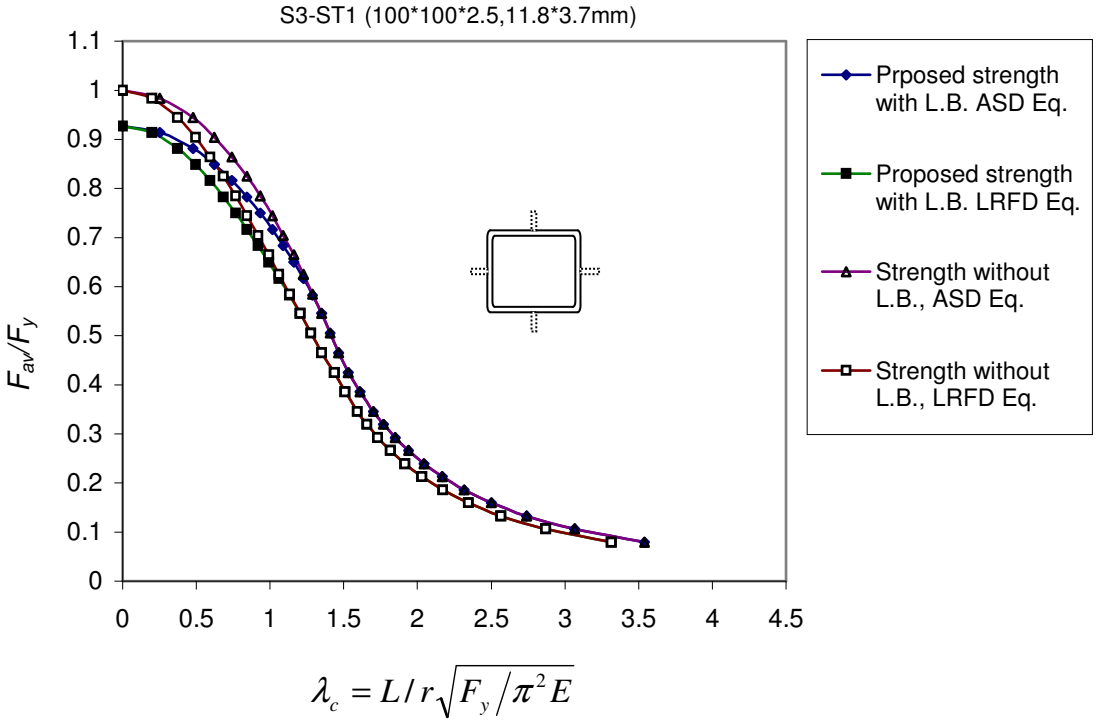

Fig.5.26 Column strength curve of section S3-ST1 (100x100x2.5, 11.8x3.7 mm)

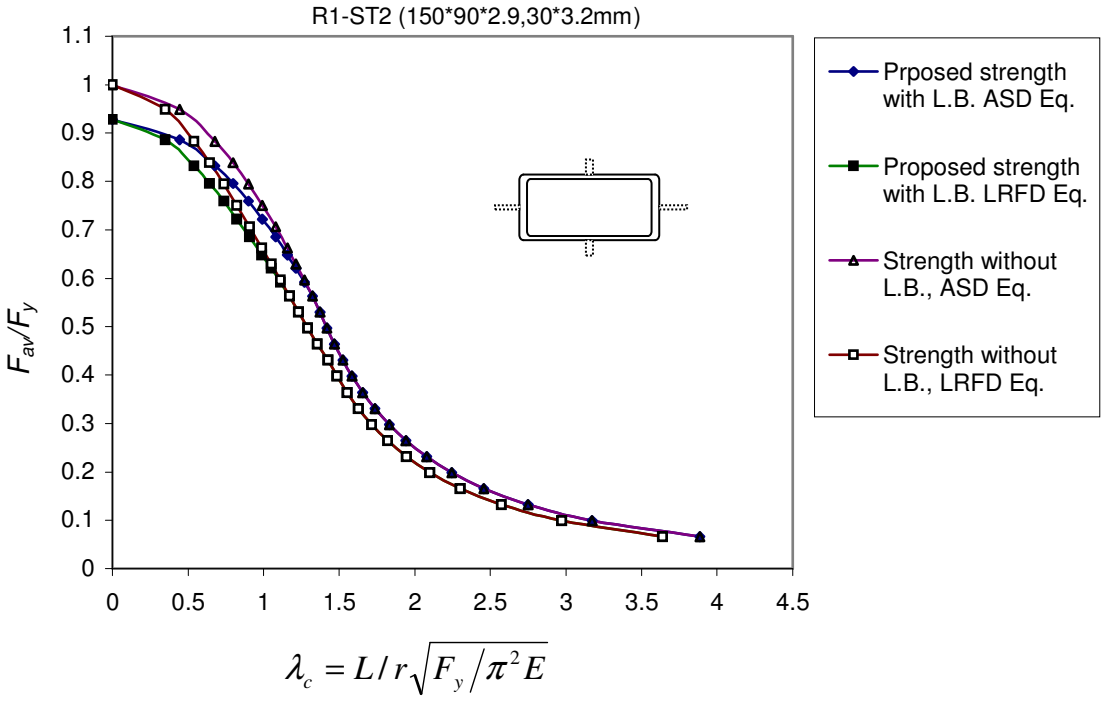

Fig.5.27 Column strength curve of section R1-ST2 (150x90x2.9, 30x3.2 mm)

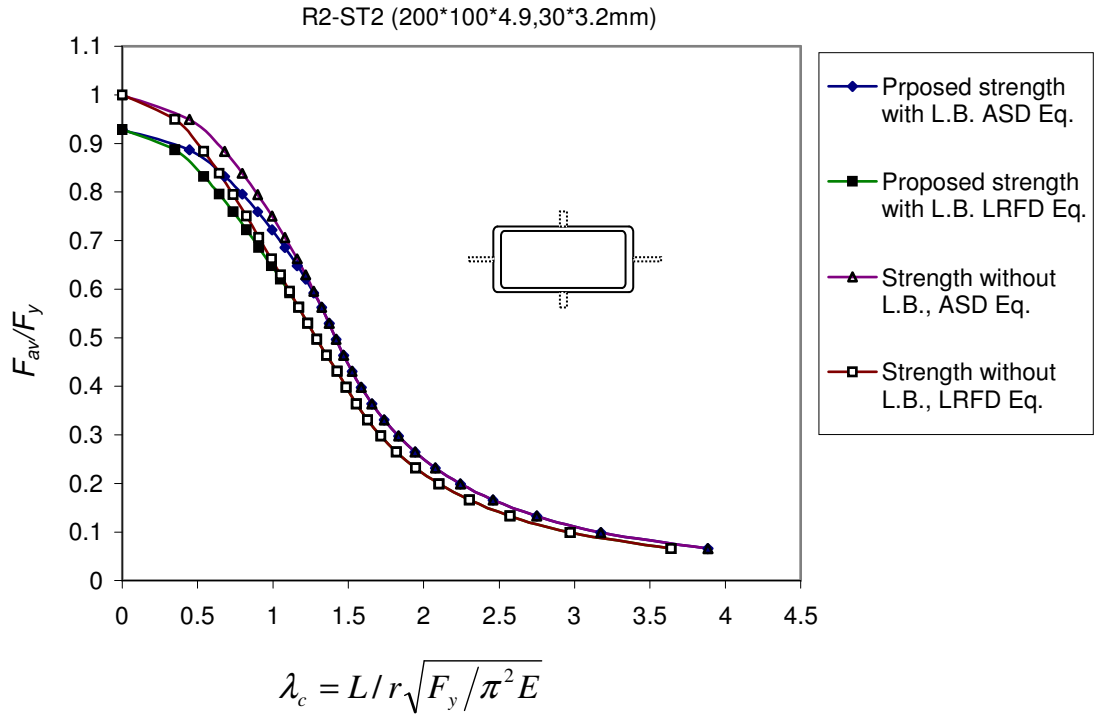

Fig.5.28 Column strength curve of section R2-ST2 (200x100x4.9, 30x3.2 mm)

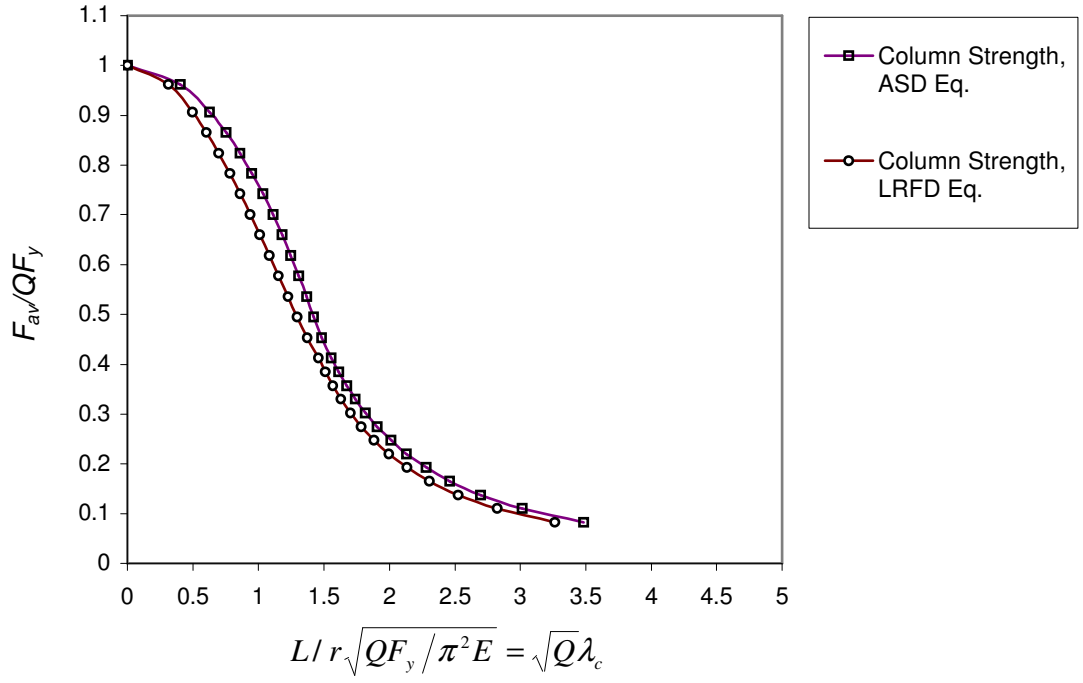

Fig.5.29 Single column strength curve for all sections

Chapter 6

SUMMARY, CONCLUSIONS AND RECOMMENDATIONS

6.1 Summary

An experimental study was conducted to investigate the behavior and postbuckling strength of plate elements in square and rectangular steel hollow sections having width-thickness ratios more than that in common rolled sections and also their effect on the strength of columns.

Two types of stub columns were tested under axial compression until failure; ordinary tubes, and tubes reinforced by longitudinal stiffeners on their sides. The variables in the study were, shape of tube sections in which square and rectangular sections were used, width-thickness ratios, and the size of the stiffeners. The stub column tubes with stiffeners were tested to investigate the effect of stiffeners on postbuckling strength of plate elements and the efficiency of the stiffeners.

Based on the test results, numerical methods were used to formulate compact effective section equations, which take into account the interaction between plate elements for unstiffened and stiffened tube sections. These equations were also compared with other formulas used in steel practice. Interaction between local and overall flexural buckling was predicted for columns having the same sections as the

tested specimens using the modified SSRC column strength equations and the interaction strength of tubular columns was obtaining using the proposed effective section formulas, and comparing results with the strength predicted by the AISC specifications, ASD and LRSD.

6.2 Conclusions

Postbuckling strength of plate elements and stiffener efficiency:

From the experimental study, the following conclusions can be drawn:

1. For the tested stub columns, Winter's formula, in general, slightly overestimates the postbuckling strength of the plate elements. The ratio between the experimental postbuckling strength to that predicted by Winter's formula varies between 83% and 105% for unstiffened tubes, and between 80% and 100% for stiffened tubes.

2. Based on the test results the following compact effective section equations are developed:

- For unstiffened square and rectangular hollow sections:

  when $\frac{b}{t} \geq 0.68\sqrt{\frac{kE}{\sigma_e}}$

  $$A_e = A\left(\frac{0.68}{(b/t)}\sqrt{\frac{kE}{\sigma_e}}\right)$$

  otherwise $A_e=A$

- For stiffened square and rectangular hollow sections:

  when $\frac{b}{t} \geq 0.415\sqrt{\frac{k_b E}{\sigma_e}}$

  $$A_e = A\left(\frac{0.122}{(b/t)}\sqrt{\frac{k_b E}{\sigma_e}} + 0.706\right)$$

  otherwise $A_e=A$

3. The discrepancies between the proposed postbuckling strength and the test results are within an acceptable range which varied between –9.5% and 14.3% for unstiffened tubes and between -13.4% and 8.3% for stiffened tubes and, consequently, the proposed effective section equations may be used for the tested sections.

4. The proposed effective section equations take into account the interaction between plate elements and yield the total effective section directly.

5. Distinct increasing in the postbuckling strength can be attained using longitudinal stiffeners in which some tested sections become entirely effective as rolled sections. The improvement in the postbuckling strength was relatively higher for sections having higher width/thickness ratios. From comparisons, stiffened tubes were capable of supporting loads between 161% and 108% of the unstiffened tubes.

6. The test results also show that the smaller stiffeners are more efficient in increasing the strength compared to their size as well as their acceptable sight on columns.

Interaction strength of tubular columns

From the predicted interaction strength of tubular columns, the following conclusions can be drawn:

1. The proposed effective section equations yield the total strength reduction factor, Q, for the sections directly.

2. The interaction between local and overall flexural buckling begins at relatively lower stress for higher values of slenderness ratio of plates. From comparisons, the proposed interaction strengths for unstiffened tubular columns are relatively closer to the predicted strength by the AISC, ASD and LRFD, for sections with relatively lower slenderness ratios of plates.

6.3 Recommendations

Based on the obtained results and conclusions, the following is recommended:

1. Further tests on stub columns and beams having square and rectangular hollow sections with wide range of sectional dimensions and material properties seem to be desirable in order to study the general behavior and postbuckling strength of the plate elements and to verify the validity of the proposed effective section equations for other ranges.

2. Tests on columns having the sectional properties of the tested tubes with and without stiffeners are recommended to investigate and verify the interaction strength with various slenderness ratios.

3. Further studies concerning the behavior of longitudinal stiffeners and the effect of imperfections due to welding and residual stress are needed. Moreover, further studies considering the stiffeners as available economic elements that can improve the load carrying capacity of columns with minimal area of steel may also be conducted.

REFERENCES

American Institute of Steel Construction (AISC) 1980. *Specifications for the Design, Fabrication, and Erection of Structural Steel for Buildings*. Chicago.

American Institute of Steel Construction (AISC) 1993. *Load and Resistance Factor Specification for Structural Steel Buildings*. Chicago.

American Iron and Steel Institute (AISI) 1980. *Specifications for the Design of Cold-Formed Steel Structural Members*. Washington.

Batista, E. Rondal, J. and Maquoi, R. 1987. Column Stability of Cold-Formed U and C Sections. Proc. of the Int. Conference on Steel and Aluminum Structures. *Steel Structures, Advances, Design and Construction*. Cardiff, UK.

Bernard, E. S. Bridge, R. Q. and Hancok, G. J. 1993. Test of Profiled Steel Decks With V-Stiffeners. *J. of Structural Engineering, ASCE,* 119(8): 2277-2292.

Bleich, F. 1952. *Buckling Strength of Metal Structures*. McGraw-Hill Book Company, New York.

Chajes, A. 1974. *Principles of Structural Stability Theory*. Prentice-Hall Inc., Englewood Cliffs, New Jersey.

Dawe, J. L. Elgabry, A. A. and Grondin, G. Y. 1985.Local Buckling of Hollow Structural Sections. *J. of Structural Engineering, ASCE*, 111(5): 1101-1112.

Desmond, T. P. Pekoz, T. and Winter, G. 1981. Intermediate Stiffeners for Thin-Walled Members. *J. of Structural Division, ASCE*, 107(4): 627-648.

DeWolf, J. T. Pekoz, T. and Winter, G. 1974. Local and Overall Buckling of Cold-Formed Members. *J. of Structural Division , ASCE*, 100(10): 2017-2036.

Galambos, T. V. 1998. *Guide to Stability Design Criteria for Metal Structures*. 5th. edition. John Wiley & Sons Inc., New York.

Gaylord, E. H. and Gaylord, C. 1972. *Design of Steel Structures*. 2nd. edition. McGraw-Hill Book Company, New York.

Hancock, G. 1981. Nonlinear Analysis of Thin Sections in Compression. *J. of Structural Division , ASCE*,107(3): 455-471.

Hancock, G. J. Davids, A. J. Key, P. W. and Rasmussen, K. J. R. 1987. Strength Test of Thin-Walled High Tensile Steel Columns. . Proc. of the Int. Conference on Steel and Aluminum Structures. *Steel Structures, Advances, Design and Construction*. Cardiff, UK.

Kalyanaraman, V. Pekoz, T. and Winter, G. 1977. Unstiffened Compression Elements. *J. of Structural Division , ASCE*, 103(9): 1833-1848.

Little, G. H. 1979. The Strength of Square Steel Box Columns-Design Curves and Their Theoretical basis. *The Structural Engineer*, 57A(2): 49-61.

McGuire, W. 1968. *Steel Structures*. Prentice-Hall Inc., Englewood Cliffs, New Jersey.

Murray, N. W. 1986. *Introduction to the Theory of Thin-Walled Structures*. Oxford University Press, Oxford.

Salmon, C. G. and Johnson, J. E. 1996. *Steel Structures Design and Behavior*. 4th. edition. Harper Collins College Publisher, New York.

Timoshenko, S. P. and Gere, J. M. 1963. *Theory of Elastic Stability*. 2nd. edition. McGraw-Hill Book Company, New York.

Usami, T. and Fukumoto, Y. 1982. Local and Overall Buckling of Welded Box Columns. *J. of Structural Division , ASCE*, 108(3): 525-542.

Usami, T.1982. Post-Buckling of Plates in Compression and Bending. *J. of Structural Division , ASCE*, 108(3): 591-609.

Walker, A. C. 1975. *Design and Analysis of Cold-Formed Section*. International Textbook Company Limited, London.

Winter, G. 1980. *Commentary on the 1968 Edition of the Specification for the Design of Cold-Formed Steel Structural Members*. American Iron and Steel Institute, Washington.

Zuyan, S. and Qilin, Z. 1991. Interaction of Local and Overall Instability of Compressed Box Columns. *J. of Structural Engineering, ASCE*, 117(11): 3337-3355.

ملخص

سلوك الصفائح الفولاذيه المعرضة للضغط المحوري وتأثيرها على مقاومة العمود

إعداد

احمد حسن احمد الوظاف

المشـرف

الأستاذ الدكتور/ ياسـر الحنيطي

لقد تم إجراء دراسه تجريبيه لإستقصاء سلوك و مقاومة الإنبعاج اللاحق للصفائح الفولاذيه المكوّنه للمقاطع المجوفة (الأنبوبية) ذات الشكل المربع والمستطيل والتي لها نسبة عرض-سماكه اكبر من المعتادة في المقاطع المسحوبه ، إضافه إلى تأثيرها على المقاومه الكلية للعمود. لقد تم اختبار نوعين من الاعمده القصيرة تحت الضغط المحوري حتى الإنهيار ، أنابيب عاديه وأنابيب مسلحة بتقاوي طوليه على الجوانب.

بالاستناد على نتائج الإختبار ، تم صياغة معادلتين تجريبيتين مختصرتين للمقطع الفعّال في كل نوع يمكن بهما توقع مقاومة الإنبعاج اللاحق ، من مميزات هذه المعادلتان انهما تأخذان في الإعتبار التفاعل بين صفائح المقطع ، إضافة الى ذلك تم توقع المقاومه الناتجه عن تفاعل الإنبعاج الموضعي للصفائح و الإنبعاج الكلي للأعمدة المكوّنه من المقاطع الأنبوبية وذلك بإستخدام معادلات مقاومة العمود المعدلة والمقدمة من SSRC .كما تمت مقارنة كل النتائج التي تم الحصول عليها بالمعادلات المعنية ذات العلاقة وكذلك مواصفات AISC .

أظهرت نتائج الإختبار أن المعادلة المستخدمة في التطبيقات الفولاذيه تعطي مقاومة أعلى نسبيا من المقاومه التي تم الحصول عليها من الإختبار، من ناحية اخرى كانت الفروقات بين المقاومة المقترحة والناتجة من الإختبار ضمن الحدود المقبولة مما يعني امكانية استخدام معادلات المقطع الفعّال المقترحة في هذه الدراسة لهذا النوع من القطاعات المدروسة.

إن استعمال التقاوي الطولية اظهر تحسنا كبيرا في مقاومة الإنبعاج اللاحق للمقاطع المدروسة الى درجة أن كثيرا منها اصبح مقطعها فعّالا بالكامل كما هو الحال في المقاطع المسحوبة ذات السماكات الكبيرة، وقد كان التحسن في المقاومة واضحا بشكل كبير في المقاطع التي تتكون من صفائح عالية النحافة ، كما أظهرت الإختبارات أن التقاوي الصغيرة اكثر كفاءة في رفع المقاومه مقارنة بحجمها الصغير.

أظهرت منحنيات المقاومه التفاعلية المتوقعة للأعمدة بوضوح أن التفاعل بين الإنبعاج الموضعي للصفائح و الإنبعاج الكلي يبدأ عند إجهادات منخفضة نسبيا وذلك عندما تكون نسبة النحافة للصفائح عاليه نسبيا، من هذه المنحنيات يمكن كذلك استنتاج تقارب المقاومه التفاعلية المتوقعة من هذه الدراسة وكذلك المتوقعة من قبل مواصفات AISC عندما تكون نسبة النحافة للصفائح منخفضة وذلك للأعمدة الأنبوبية العادية.

APPENDIX

Terminology

The following terms were frequently used in this thesis.

Bifurcation: a term relating to the load-deflection behavior of a perfectly straight and perfectly centered compression element at critical load.

Buckling load: the load at which a perfectly straight member under compression assumes a deflected position. Also called critical load.

Effective width: a reduced width of plate or flat segment of a cross section, which assuming uniform stress distribution, leads to the same behavior of a structural member as the actual section of plate and the actual nonuniform stress distribution.

Local buckling: the buckling of a compression element, which may precipitate the failure of the whole member.

Postbuckling strength: the additional load, which can be carried by a plate element or structural member after buckling.

Secant modulus, E_s: the slope of the straight line from the original point to the considered point on the stress-strain curve of material in the inelastic range.

Stability: the capacity of a compression member or element to remain in position and support load, even if forced slightly out of line or position by an added lateral force. In the elastic range, removal of the added lateral force would result in a return to the prior loaded position, unless the disturbance causes yielding to commence.

Stub column: a short compression test specimen utilizing the complete cross section, sufficiently long to provide a valid measure of the stress-strain relationship as

averaged over the cross section, but short enough so that it will not buckle as a column in the elastic or plastic range.

Tangent modulus, E_t: the slope of the stress-strain curve of material in the inelastic range, at any given stress level.

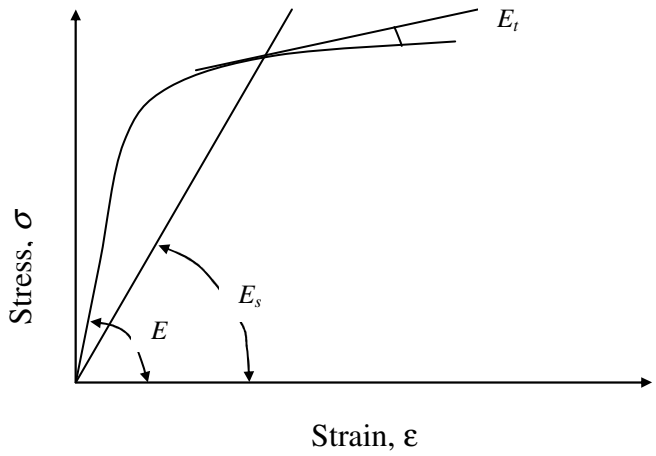

General stress-strain relationship